IDENTIFICATION AND CHARACTERIZATION OF A BACTERIAL CATALYTIC SCAFFOLD WITH SPECIFICITY FOR HOST ENDOMEMBRANE TRAFFIC

APPROVED BY SUPERVISORY COMMITTEE

Neal M. Alto, Ph.D.

Felix Yarovinsky, M.D.

Melanie Cobb, Ph.D.

Vanessa Sperandio, Ph.D.

DEDICATION

To my father Serguei Y. Seliounine (1955-2011).

ACKNOWLEDGEMENTS

I have been fortunate to be surrounded by great people throughout my scientific journey. This work would not have been possible without the support of the colleagues, friends, and family. First, I would like to extend a big thank you and my deepest appreciation to my mentor and thesis advisor, Dr. Neal Alto. His drive and passion for science sets him apart from many, but his sincerity, approachability, and knowledge make him one of a kind. I could not have wished for a better person to look up to for guidance and inspiration. So thank you, Neal, for being the best boss a grad student could have. It has been a pleasure to be a part of the Alto Lab and see it grow from the beginning.

I also want to acknowledge the Alto Lab for their support and company through it all – mornings, nights, incubation times, spinning down overnight cultures, and even sharing the tissue culture hood – I could always count on you, and I am grateful for that. I would like to especially thank Sarah Sutton for everything she does and her sense of humor, she really makes the Alto Lab the amazing Alto Lab; Bethany Weigele for lending a listening ear and her advice on many things that extend beyond just science; and Robert Orchard – one of the best scientists I've met and a great friend – for all the talks, laughs, and advice.

This work would not have been possible without the support of the great faculty and colleagues at the UT Southwestern Medical Center. I would like to acknowledge the Proteomics and Mass Spectrometry Core for their help and expertise, as well as Structural Biology Core. In particular, I would like to extend a thank you to Diana R. Tomchick for her time, patience, and knowledge she has shared, as well as her contribution to this work. I also would like to thank colleagues both at UT Southwestern Medical Center and other institutions for contributing ideas and sharing valuable reagents. Finally, I want to extend my gratitude to my committee members Vanessa Sperandio, Melanie Cobb, and Felix Yarovinsky, who have made this work better and showed me how to see and address scientific problems with a better clarity. In addition, I thank them for seeing me through.

This journey through the graduate school has been made possible and sweeter with the help of my incredible friends and family. Providing much needed distractions now and then, great laughs, or a generous portion of alcohol when the cause called for it – you were always there without hesitation, and I am sincerely grateful to you all. I couldn't have done it without you. Ganesh Kadamur, Stefan Bresson, Ryan McNamara, Jenny McCann, Alex D'Brot, and I am sure I am forgetting someone – thank you for everything. Special thank you to my friend Dhananjay Chaturvedi, I can't even describe all you've done for me and things we've been through, but you know – from riding bikes in the cold down Mockingbird Lane and to limping to the train station after the marathon. Also to my friends and family friends outside of the science world – thank you! Lastly, I want to thank my family for making me who I am and where I stand today, and for everything they had to go through with me up to this point. I hope I make you proud and you think it was worth it. Thank you.

IDENTIFICATION AND CHARACTERIZATION OF A BACTERIAL CATALYTIC SCAFFOLD WITH SPECIFICITY FOR HOST ENDOMEMBRANE TRAFFIC

by

ANDREY S. SELYUNIN

DISSERTATION

Presented to the Faculty of the Graduate School of Biomedical Sciences

The University of Texas Southwestern Medical Center at Dallas

In Partial Fulfillment of the Requirements

For the Degree of

DOCTOR OF PHILOSOPHY

The University of Texas Southwestern Medical Center at Dallas

Dallas, Texas

December, 2013

IDENTIFICATION AND CHARACTERIZATION OF A BACTERIAL CATALYTIC SCAFFOLD WITH SPECIFICITY FOR HOST ENDOMEMBRANE TRAFFIC

ANDREY S. SELYUNIN, Ph.D.

The University of Texas Southwestern Medical Center at Dallas, 2013

Supervising Professor: Neal M. Alto, Ph.D.

The fidelity and specificity of information flow within a cell is controlled by scaffolding proteins that assemble and link enzymes into signaling circuits. These circuits can be inhibited by bacterial effector proteins that post-translationally modify individual pathway components. However, there is emerging evidence that pathogens directly organize higher order signaling networks through enzyme scaffolding, and the identity of the effectors or their mechanisms of action are poorly understood. Here, we used a functional screen to identify the EHEC O157:H7 type III effector EspG as a regulator of endomembrane trafficking and we report ADP-ribosylation factor (ARF) GTPases and p21-activated kinases (PAK) as its relevant host substrates. The 2.5 Å crystal structure of EspG in complex with ARF6 shows how EspG blocks

GAP-assisted GTP hydrolysis, revealing a potent mechanism of GTPase signaling inhibition at membrane organelles. In addition, the 2.8 Å crystal structure of EspG in complex with the autoinhibitory Iα3-helix of PAK2 defines a previously unknown catalytic site in EspG and provides an allosteric mechanism of kinase activation by a bacterial effector. Unexpectedly, ARF and PAK are organized on adjacent surfaces of EspG, suggesting its dual role as a "catalytic scaffold" that effectively reprograms cellular events through the functional assembly of GTPase-kinase signaling complex. Bidirectional vesicular transport between ER and Golgi is mediated largely by ARF and Rab GTPases, which orchestrate vesicle fission and fusion, respectively. How their activities are coordinated to define the successive steps of the secretory pathway and preserve traffic directionality is not well understood, in part due to the scarcity of molecular tools that simultaneously target ARF and Rab signaling. Here, we take advantage of the unique scaffolding properties of *E.coli* Secreted Protein G (EspG) to describe the critical role of ARF1/Rab1 spatiotemporal coordination in vesicular transport at the ER-Golgi Intermediate Compartment. Structural modeling and cellular studies show that EspG induces bidirectional traffic arrest by tethering vesicles through select ARF1-GTP/effector complexes and local inactivation of Rab1. Mechanistic insights presented in this study establish the effectiveness of a small bacterial catalytic scaffold in studying complex processes and reveal an alternative mechanism of immune regulation by an important human pathogen.

TABLE OF CONTENTS

PRIOR PUBLICATIONS

Selyunin AS, Reddick LE, Weigele BA, and Alto NM. Selective protection of an ARF1-GTP signaling axis by a bacterial scaffold induces bidirectional trafficking arrest. *Cell Reports*. (In Review)

Burnaevskiy N, Fox TG, Plymire DA, Ertelt JM, Weigele BA, **Selyunin AS**, Way SS, Patrie SM, Alto NM. Proteolytic elimination of N-myristoyl modifications by the Shigella virulence factor IpaJ. *Nature*. 2013 Apr 4;496(7443):106-9. doi: 10.1038/nature12004

Selyunin AS and Alto NM. Activation of PAK by a bacterial type III effector EspG reveals alternative mechanisms of GTPase pathway regulation. *Small GTPases*. 2011 Jul;2(4):217-221.

Selyunin AS, Sutton SE, Weigele BA, Reddick LE, Orchard RC, Bresson SM, Tomchick DR, and Alto NM. The assembly of a GTPase-kinase signaling complex by a bacterial catalytic scaffold. *Nature*. 2011. 469(7328): 107-11.

LIST OF FIGURES

LIST OF TABLES

LIST OF APPENDICES

LIST OF DEFINITIONS

AID – Autoinhibitory Domain

ARF - ADP-Ribosylation Factor

CRIB - Cdc42/Rac Interactive Binding

DTT – Dithiothreitol

EDTA – Ethylenediaminetetraacetic acid

EHEC – Enterohaemorrhagic *Escherichia coli*

ER – Endoplasmic reticulum

ERGIC – ER-Golgi Intermediate Compartment

EspG – *E.coli* Secreted Protein G

FPLC – Fast protein liquid chromatography

GAP – GTPase activating protein

GBD – GTPase Binding Domain

GEF – Guanine-nucleotide exchange factor

GFP – Green fluorescent protein

GMAP-210 – Golgi Microtubule Associated Protein of 210 kDa

GSP – General Secretory Pathway

GST – Glutathione S-transferase

GTPase – Guanosine triphosphatase

IPTG – Isopropyl β-D-1-thiogalactopyranoside

KD – Kinase Domain

MBP – Maltose binding protein

Ni-NTA – nickel-nitrilotriacetic acid

PAK – p21 activated kinase

PBS – Phosphate buffered saline

PDB – Protein data bank

TBS – Tris-buffered saline

T3SS – Type III Secretion System

N-WASP - neuronal Wiskott–Aldrich Syndrome protein

WT – wild-type

CHAPTER ONE

INTRODUCTION AND LITERATURE OVERVIEW

Bacterial type III effectors hijack host signaling pathways

Bacterial pathogens must overcome a battery of immune defenses in order to successfully colonize and replicate within a host. In addition to passing through physical barriers, such as aggressive environment and mucosal surfaces, successful pathogens are able to avoid recognition and clearance mediated by both intracellular and inflammatory processes. Because these pathways are regulated form within a host cell, bacteria have evolved an extensive repertoire of mechanisms to target host signaling networks. Specifically, Gram-negative pathogens use Type III secretion system (T3SS), a needle-like apparatus that shares homology with a flagellum, to penetrate through the host membrane and deliver virulence proteins directly into the cell (Fig. 1) (Galan & Collmer, 1999; Galan & Wolf-Watz, 2006). Inside bacterial cytoplasm, these virulence proteins are inactive due to either being kept in a partially disorganized state through chaperone binding or lacking their target substrate. Upon translocation through the secretion needle in an unfolded state, they refold inside host cytoplasm and modulate cellular functions by hijacking signaling pathways(Akeda & Galan, 2005).

While many effector proteins either directly modify host enzymes or mimic their regulatory proteins, the function and the molecular mechanism of many still remain undetermined (Alto & Orth, 2012). Interestingly, analysis across bacterial species that differ in their preference for host (i.e. plant or animal), tissue tropism (e.g. lung, intestine, colon), or lifestyle (intracellular vs. extracellular) revealed presence of homologous proteins with related

functions, as well as proteins unique to individual species (Elliott et al., 2001; Li et al., 2007). These observations suggest that virulence proteins have evolved distinct properties that are specific to unique needs of a bacterium. Considering the wide variety of pathogens that use T3SS, including pathogenic *Escherichia coli, Shigella flexneri, Salmonella typhimurium, Burkholderia mallei, Yersinia pestis, Pseudomonas aeruginosa, Pseudomonas syringae*, together they represent an extensive library of molecules that bypass endogenous host regulatory circuits and can directly modulate host cell function. Therefore, bacterial type III effectors can be used as effective tools to gain insight into the interplay of multiple signaling networks within a cell and delineate the individual events underlying complex cellular processes.

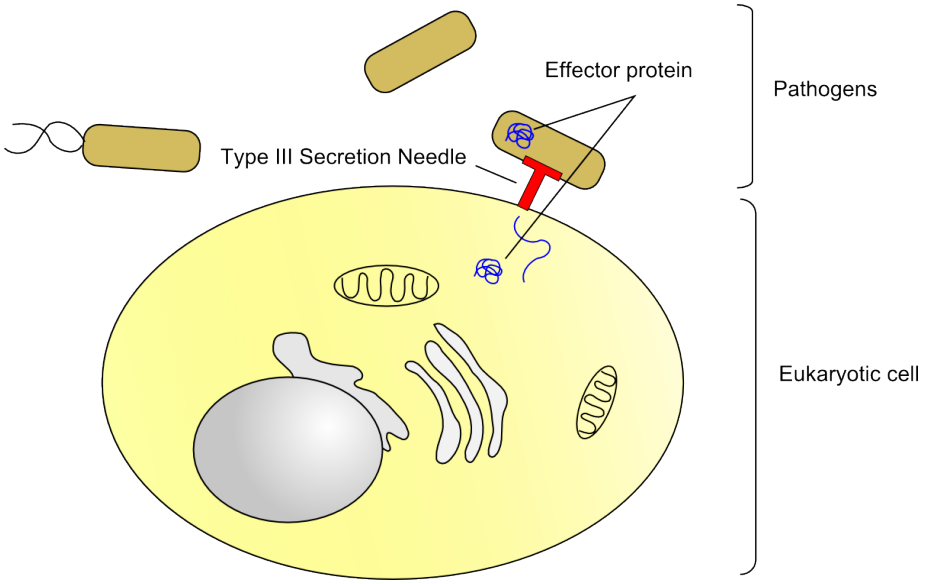

Figure 1. Bacterial Type III Secretion apparatus.
Cartoon schematic of protein translocation machinery of Gram-negative pathogens. Needle-like structure extends from bacteria and penetrates host cell membrane via a pore complex. Direct connection between bacteria and host cytoplasm allows for directed translocation of effector proteins, which are secreted through the needle in an unfolded state, and then refold inside the host.

Host endomembrane system is a frequent target of bacterial pathogens

Bacterial pathogens interact with host membranes to induce a broad range of changes in its morphology and regulation of cell function. For intracellular bacteria, they include alteration of plasma membrane dynamics to facilitate entry into host cell and modulation of endocytic pathway to avoid fusion with the lysosome and promote survival (Ham & Orth, 2012). For example, *S. typhimurium* and *S. flexneri* use effector proteins to induce actin rearrangements underneath the host cell membrane to trigger the engulfment of bacteria by membrane extensions and its consecutive uptake. In extracellular bacteria, type III secreted virulence proteins play essential roles in evading phagocytosis by immune cells. In both cases, engulfment of the bacterium by a plasma membrane-derived intracellular vacuole is normally followed by a series of membrane fusion events that terminates with the formation of phagolysosomes, which kill the bacteria inside with acidic pH and digestive enzymes.

While some pathogens have evolved strategies to escape from phagosomes or block vacuole maturation to avoid digestion by the lysosome, both intracellular and extracellular bacteria face the additional threat of recognition by bacterial sensors. Membrane associated pattern recognition receptors (PRRs), including Toll-like receptors, NOD-like receptors, RIGI-receptors, and C-type lectins, recognize bacterial and viral pathogens and induce the expression of cytokines and chemokines that amplify the inflammatory response (Takeuchi & Akira, 2010). While this system is highly effective in combating a diverse range of microbes, many bacterial pathogens have evolved effector proteins to overcome these host defenses.

Research over the past decade has primarily focused on identifying bacterial effector proteins that inhibit signal transduction cascades stimulated by the activation of PRRs (Baxt, Garza-Mayers, & Goldberg, 2013; Espinosa & Alfano, 2004). In contrast, only recently have researchers attempted to identify bacterial mechanisms that prevent cytokine and chemokine secretion by inhibiting vesicular transport through the General Secretory Pathway (GSP) (Burnaevskiy et al., 2013; Clements et al., 2011; Dong et al., 2012; Selyunin et al., 2011). (Fig. 2) While arrest of protein transport would disable a wide variety of immune signaling pathways and therefore seems highly advantageous to pathogens, this strategy presents a challenge for bacteria that rely on host resources for survival (i.e. intracellular pathogens) and thus must be carefully orchestrated.

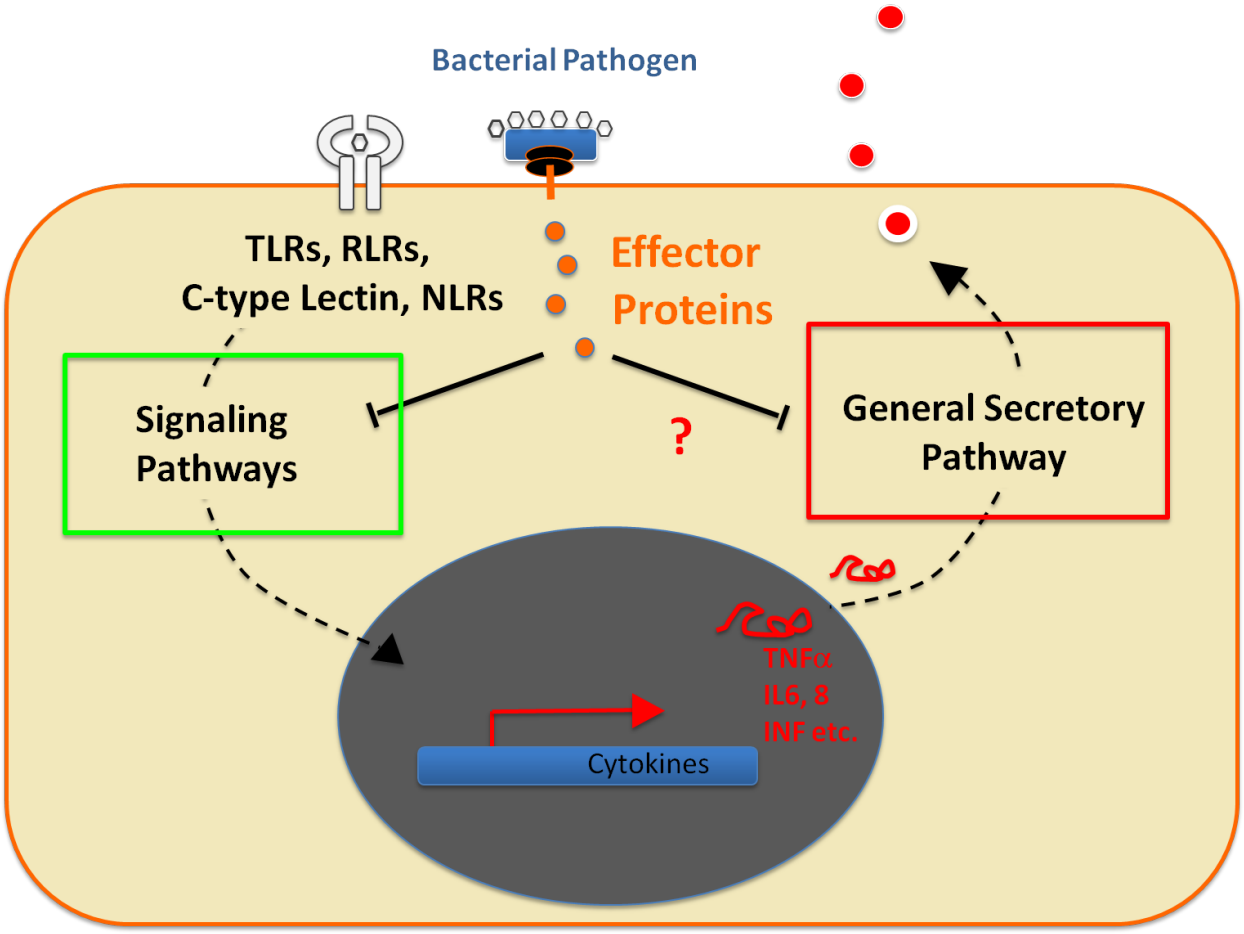

Figure 2. Bimodal approach of bacterial pathogens to combating host immune response. Innate immune receptors recognize foreign bacteria and viruses, and in turn initiate a signaling cascade that leads to trafficking and secretory events aimed at clearing the infection. Secreted bacterial virulence factors can (1) target signaling pathways to prevent activation of inflammatory cascades, or (2) inhibit protein secretion to limit the spread of immune response.

Function and regulation of the early secretory pathway

Organization and components

Endomembrane system of distinct membrane bound organelles with unique composition and function is a fundamental property of eukaryotic cells (Fig. 3). It plays a role in protein synthesis and modification, cargo sorting, and transport of proteins and lipids within a cell (Brandizzi & Barlowe, 2013). In addition, it functions as a platform for the assembly of signaling complexes and immune receptors. Detection of microbial agents results in activation of signaling cascades that lead to secretion of inflammatory cytokines and chemokines, aimed at eliminating the microbial threat (Takeuchi & Akira, 2010). Secretion of inflammatory molecules occurs through the General Secretory Pathway (GSP), a defined route from the site of protein synthesis, endoplasmic reticulum (ER), to plasma membrane.

The early secretory pathway includes ER, ER-Golgi Intermediate Compartment (ERGIC), and Golgi apparatus. ER is an extensive network associated with nuclear envelope that spans throughout the cell volume and primarily functions in protein synthesis and export. ERGIC represents a vesicle-tubular cluster in close proximity to ER exit sites, and is found in perinuclear and peripheral sites of the cell (Appenzeller-Herzog & Hauri, 2006). Golgi apparatus is the major sorting station of the cell, found in the perinuclear region. In animal cells, it displays a ribbon-like appearance during interphase of cell cycle, but is fragmented during mitosis (Sutterlin, Hsu, Mallabiabarrena, & Malhotra, 2002). Communication between these compartments is medicated by vesicular transport. COP II coated vesicles carry cargo from ER exit sites to ERGIC, which acts as a first sorting station, and then either return back to ER or continue forward toward Golgi via COP I coated vesicles (Barlowe & Miller, 2013; Brandizzi & Barlowe, 2013). At the Golgi,

cargo can be further modified and sorted for secretion or delivery to other compartments of the endomembrane networks. This bidirectional vesicular transport is critically dependent on microtubules, which act as tracks for the transport of vesicles by motor proteins. Disruption of microtubules with a depolymerizing agent, nocodazole, prevents anterograde transport of vesicles at ERGIC and results in fragmented appearance of Golgi (Cole, Sciaky, Marotta, Song, & Lippincott-Schwartz, 1996). Moreover, proteins fail to recycle back into ER and protein secretion is negatively affected.

The selectivity of directional traffic between specific membrane-bound compartments is quintessential to maintaining the functional organization of the cell and is carefully orchestrated. In particular, two key events guide the cargo delivery: 1) the budding of vesicle and coat formation, and 2) fusion of the vesicle with the target membrane. These processes are controlled primarily by ARF and Rab family of GTPases, which induce membrane curvature and coat protein recruitment, or coordinate tethering of vesicles with membranes, respectively (Donaldson & Jackson, 2011; Hutagalung & Novick, 2011). Like other members of Ras-family GTPases, ARFs and Rabs cycle between inactive, GDP- bound, and active, GTP-bound, states. With almost no intrinsic GTPase activity, they rely on GTPase Activating Proteins (GAPs) to catalyze hydrolysis of GTP to GDP, whereas Guanine-nucleotide Exchange Factors (GEFs) facilitate the exchange of GDP to GTP. Acting as molecular switches, both ARF and Rab can recruit specific downstream substrates in their active state, which in turn allows for rapid regulation of many endomembrane trafficking events (Cherfils & Zeghouf, 2013).

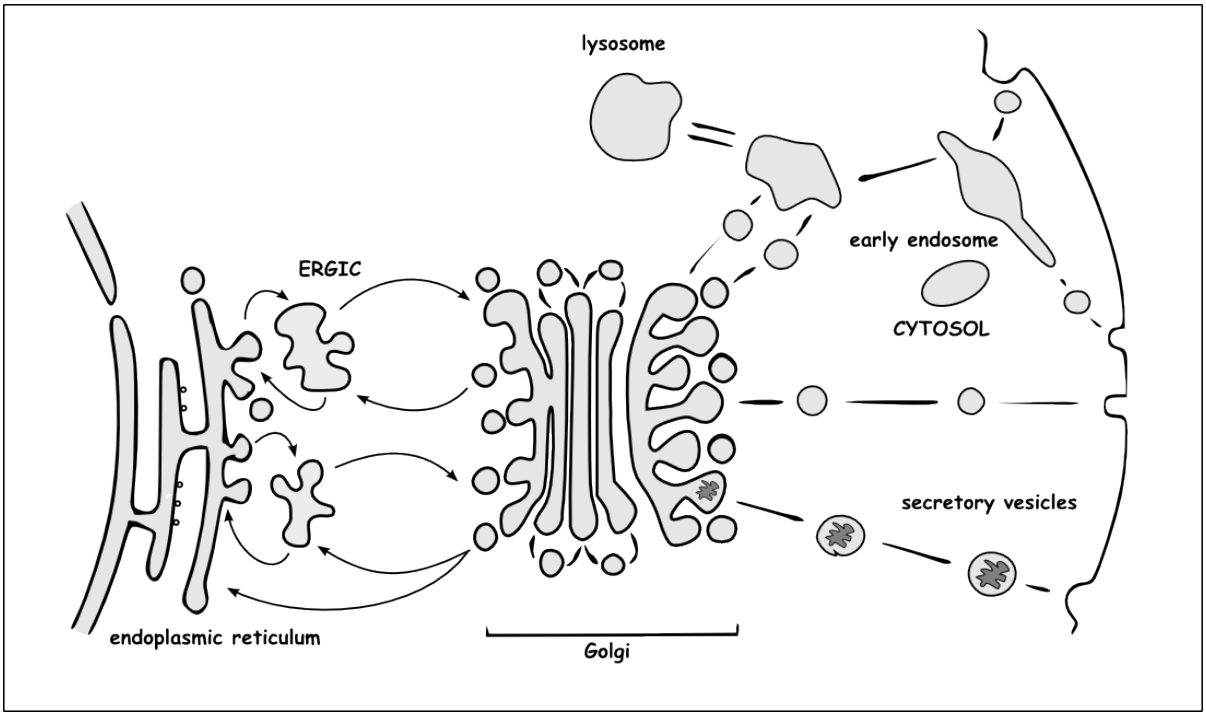

Figure 3. Eukaryotic endomembrane network.
Endomembrane network of animal cells is shown. The early General Secretory Pathway includes bidirectional transport between ER and Golgi, which is achieved via vesicular transport along microtubule tracks.

ARF-family GTPases

ARF proteins have been implicated in numerous membrane trafficking pathways, making them master regulators of endomembrane network. There are six mammalian ARF proteins, which have been categorized into three classes based on their amino acid identity. Class I ARFs (ARF1, ARF2, and ARF3) largely regulate vesicle budding in the secretory pathway and activate lipid-modifying enzymes. Class II ARFs (ARF4 and ARF5) have been linked to intra-Golgi transport, but remain poorly characterized. Finally, class III ARF6 is involved in endosomal traffic and plasma membrane organization. This work focuses primarily on the role and function of ARF1 (D'Souza-Schorey & Chavrier, 2006).

All ARF proteins are myristoylated on N-terminal glycine residue, which allows them to associate with membranes in an active state via the amphipathic helix (Fig. 4), and have similar overall structure and nearly identical effector domain regions, Switch I and Switch II, responsible for interaction with downstream substrates. In *in vitro* biochemical assays, all isoforms of ARF recruit coat proteins to Golgi membranes and activate lipid-modifying enzymes, such as PLD and PIP5K (Donaldson & Jackson, 2011). However, diversification of their function in cells suggests that localization and substrate availability drives the function of individual ARF isoforms (Donaldson & Honda, 2005). Therefore, spatiotemporal regulation of specific ARF GTPase plays a critical role in coordinating trafficking events.

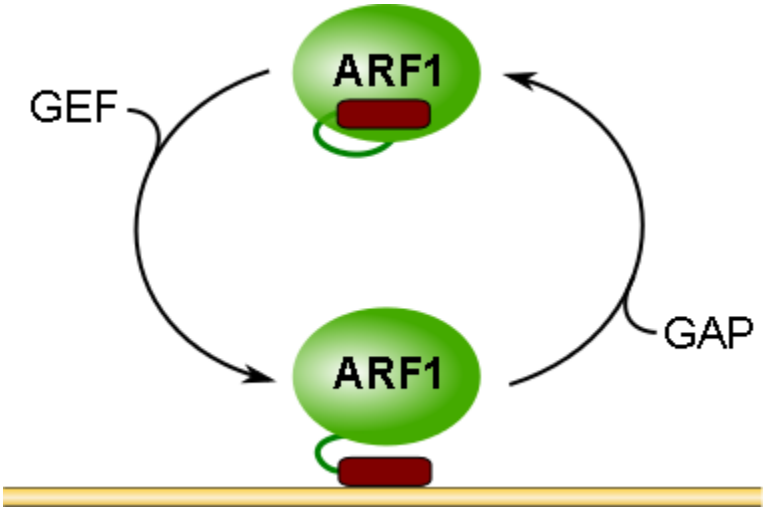

Figure 4. ARF GTPase cycle.
ARFs cycle between active (GTP-bound) and inactive (GDP-bound) states. Lacking intrinsic GTPase activity, it requires a GAP protein to cycle, whereas GEF proteins relieve the GDP and allow the exchange for GTP. Amphipathic helix with myristoylated N-terminus tail (dark red) assists with the insertion and retention of ARF on intracellular membranes.

One of the most researched member of ARF family is ARF1, in part due to its role in regulating endomembrane trafficking at the Golgi. Its most extensively studied function is recruitment of coatomer complex proteins required for the formation of Golgi vesicles, including direct interaction with COP I and AP-1 coats, and indirect recruitment of γCOP coat via binding to GGA1 adapter protein (Donaldson, Honda, & Weigert, 2005; Popoff, Adolf, Brugger, & Wieland, 2011). Although ARF1 binds downstream substrates in a GTP-dependent manner, nucleotide cycling is required for successful coat formation and vesicle budding. Additional functions of ARF1 involve activation of PLD, which generates acidic phospholipids and assists with vesicle budding and membrane fission. The relevance of PIP5K activity regulation by ARF1 is not fully understood, but could be linked to establishing identity between Golgi and plasma membrane derived membranes (Donaldson & Jackson, 2011). Moreover, ARF1 has been implicated in interactions with structural components of Golgi, including spectrin and golgin GMAP-210 (Rios, Sanchis, Tassin, Fedriani, & Bornens, 2004). The importance of ARF1 signaling in endomembrane trafficking and maintenance is particularly highlighted during inactivation of ARF1 by a fungal toxin Brefeldin A (BFA), which leads to a complete disassembly of Golgi, redistribution of Golgi enzymes into ER, and arrest of protein secretion (Klausner, Donaldson, & Lippincott-Schwartz, 1992).

Rab-family GTPases

The Rab family of GTPases is the largest family of small Ras-like GTPases with over sixty members identified in humans and eleven in yeast (Olkkonen & Stenmark, 1997). Similar

to ARF GTPases, Rabs cycle between cytosolic and membrane associated states when bound to GDP or GTP, respectively. In contrast to ARFs, however, Rab proteins undergo isoprenylation at the C-terminus, which allows it to anchor to the membrane. This isoprenyl group is bound to a GDP dissociation inhibitor (GDI) when Rab is in an inactive state and cytosolic. A GDI dissociation factor (GDF) separates GDI-Rab interaction and in turn assists with membrane targeting of Rab GTPase (Schwartz, Cao, Pylypenko, Rak, & Wandinger-Ness, 2007). Upon membrane insertion and an exchange of GDP for GTP by a GEF protein, Rab is activated and capable of interaction with downstream targets (Fig. 5).

While ARF proteins regulate vesicular trafficking by controlling coatomer recruitment, Rab GTPase mediate the tethering and fusion of vesicles to their target membranes (Stenmark, 2009). In particular, in their active state Rab proteins recruit golgins, a family of coiled-coil proteins that include p115 (Uso1 in yeast), giantin, and GM130, which help capture vesicles in close proximity to membranes and initiate fusion event via a SNARE complex (Short, Haas, & Barr, 2005). Additionally, they mediate vesicle movement through interaction with actin or microtubule associated motors, such as the kinesin (plus-end directed motors) or dynein (minus-end directed motors) (Horgan & McCaffrey, 2011).

In context of the early secretory pathway, Rab1 plays a critical role in the transport of cargo vesicle between the ER and Golgi. It was originally found that Rab1 binds p115, a coiled-coil homodimer that interacts with GM130, a golgin found primarily on cis-Golgi and linked to maintenance of Golgi architecture and vesicle docking, and giantin, a COPI vesicle factor. Moreover, p115 regulates SNARE complex assembly by directly binding some of its components, putting Rab1 at the center of vesicle fusion events. Recently, it has also been

discovered that GRIP domain found in multiple golgins is predicted to have multiple Rab-interacting sites (Sinka, Gillingham, Kondylis, & Munro, 2008). It is therefore likely that Rab signaling cascades might orchestrate complex docking processes that define the directionality and proper delivery of transport vesicles to their specific site. However, little is known about the molecular mechanisms that are involved.

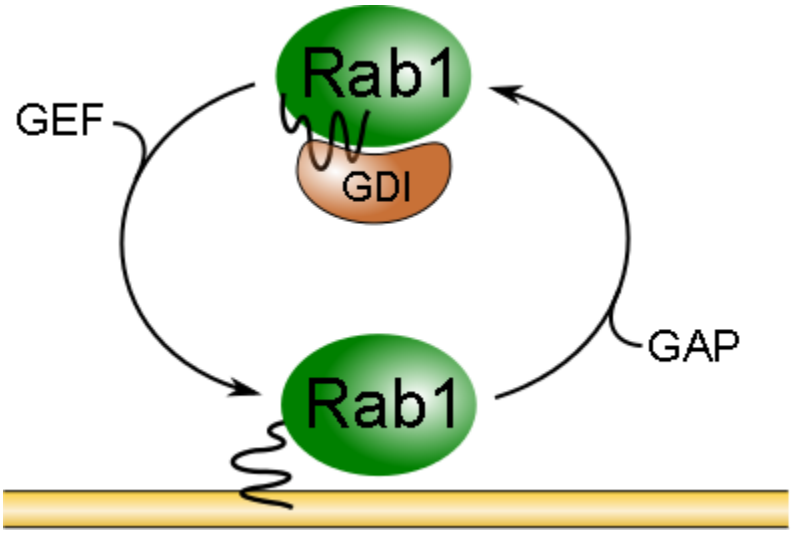

Figure 5. Nucleotide cycle of Rab1 GTPase.
Similar to other GTPases, Rab1 cycles between inactive cytosolic (GDP-bound), and active membrane-mound (GTP-bound) states. Nucleotide exchange is mediated by GEF and GAP proteins, which promote GTP and GDP states, respectively. Rab1 is prenylated on C-terminus, which allows it to associate with membranes. In an inactive state, prenyl group is bound by GDP Dissociation Inhibitor (GDI) that inhibits the exchange of GDP for GTP.

Aim of this study

Endomembrane system and the secretory pathway in particular are essential in maintaining cell function. Although many molecules and components involved in their regulation are known, the interplay between them remains poorly understood due to the complex nature of the system and the paucity of available approaches to study it. Vesicular transport between ER and Golgi is dependent on many factors, such as the function of ARF and Rab GTPases, vesicle docking through SNAREs, membrane fusion, and cytoskeletal tracks. To understand individual contribution of each factor can be addressed by disrupting it and observing the effect, which has been previously achieved with relative success. However, this strategy has a major limitation of being unable to identify or distinguish which interactions within the system drive specific trafficking events. Thus, new molecular tools capable of selectively targeting a small subset of interactions are needed.

The aim of this study is to assess the applicability of bacterial type III effector proteins as novel tools to dissect complex regulatory networks, such as endomembrane system. Considering that host membranes are common targets of bacterial pathogens, there is a potential for protein assembling new signaling hubs either indirectly, by modifying the activity of host enzymes, or directly, by bringing multiple proteins together in a manner not normally found in host cells. Indeed, bacteria can variably modulate the function of key regulatory molecules to their advantage. In addition to examples described earlier, *Salmonella* SifA effector allows for the enlargement of Salmonella Containing Vacuole by preventing the ability of Rab7 to bind Rab-interacting Lysosomal Protein (RILP) and recruit dynein-dynactin motor complex to endosomes, thus inhibiting membrane flow toward the perinuclear area of the cell (Harrison et al., 2004). On

the other hand, *Helicobacter pylori* promotes Rab7/RILP interaction to enhance the membrane transport to the vacuole in which it grows (Terebiznik et al., 2006). Given the variety of bacterial pathogens and the diversity of their lifestyles, type III effector pool provides a prime opportunity to identify novel molecules targeting signaling pathways through unique mechanisms.

In addition to identifying bacterial proteins capable of regulating host membrane traffic, this study seeks to understand host-pathogen protein interaction on the molecular level, in order to gain insight into endogenous mechanisms guiding specific trafficking events within the endomembrane systems. Effector proteins show exquisite potency and efficiency in modulating host cell function – a necessity, considering that few translocated molecules must outcompete a lieu of host regulatory proteins. Therefore, bacterial effectors may reveal alternative methods of signaling pathways regulation or expose the role of individual transient protein interactions, which can be overlooked when studying extensive and dynamic processes using traditional approaches. Altogether, this work aims to establish a directed strategy that would allow investigation of both the function of bacterial virulence factors and the molecular principles underlying the host coordination of trafficking events.

CHAPTER TWO

IDENTIFICATION OF A NOVEL BACTERIAL CATALYTIC SCAFFOLD

INTRODUCTION

General Secretory Pathway is a common secretion route that participates both in intracellular transport and secretion of proteins and other molecules into the extracellular space. It has now been widely accepted that bacteria frequently interact with the host endomembrane network via type III secreted effectors in order to replicate and survive the immune response (Ham & Orth, 2012) (Fig. 6). The nature of their interactions, however, varies and can range from post-translationally modifying host enzymes to directly mimicking regulatory proteins. In addition, different effectors can target different steps of the secretory pathway. Because the fidelity and specificity of information flow within a cell is controlled by scaffolding proteins that assemble and link enzymes into signaling circuits, it is not surprising that these circuits can be effectively inhibited by bacterial effector proteins that modify individual pathway components (Duesbery et al., 1998; Li et al., 2007; Schmidt et al., 1997; Yarbrough et al., 2009). However, there is emerging evidence that pathogens directly organize higher order signaling networks through enzyme scaffolding (Alto et al., 2007; Vingadassalom et al., 2009), yet the identity of the effectors or their mechanisms of action are poorly understood.

To identify potential bacterial virulence factors capable of hijacking the regulation of complex signaling networks, we have developed an assay to look for proteins that modulated the activity of the secretory pathway. Human growth hormone (hGH) is a single-chain polypeptide that can be expressed in tissue culture grown cells and is transported through the GSP, followed

by secretion into the media. Therefore, by assessing the amount of hGH under either normal conditions or affected by virulence factors, we can rapidly identify proteins affecting host trafficking. Although this screen initially cannot distinguish between different steps of protein secretion, this selection allows for the determination of primary candidates, whose further analysis will focus on investigating their intracellular localization and function. Importantly, this assay non-discriminatively allows for screening both intracellular and extracellular pathogens, as well as those with different species tropism, as components of the GSP are conserved among eukaryotes.

Using a functional screen together with biochemical and cell biological analysis, we identify the EHEC O157:H7 type III effector EspG as a regulator of endomembrane trafficking and report ADP-ribosylation factor (ARF) GTPases and p21-activated kinases (PAK) as its relevant host substrates. EspG induces fragmentation of the Golgi apparatus and colocalizes with Golgi remnants, consistent with its function in inhibiting protein secretion. Additionally, we have solved the high-resolution crystal structures of EspG in complex with ARF6 and in complex with a PAK2 peptide from an inhibitory element within the AID of PAK2. The 2.5 Å crystal structure of EspG in complex with ARF6 shows how EspG blocks GAP-assisted GTP hydrolysis, revealing a potent mechanism of GTPase signaling inhibition at membrane organelles. The 2.8 Å crystal structure of EspG in complex with the autoinhibitory Iα3-helix of PAK2 defines a previously unknown catalytic site in EspG and provide an allosteric mechanism of kinase activation by a bacterial effector. Unexpectedly, ARF and PAK are organized on adjacent surfaces of EspG, suggesting its dual role as a “catalytic scaffold” that effectively

reprograms cellular events through the functional assembly of GTPase-Kinase signaling network.

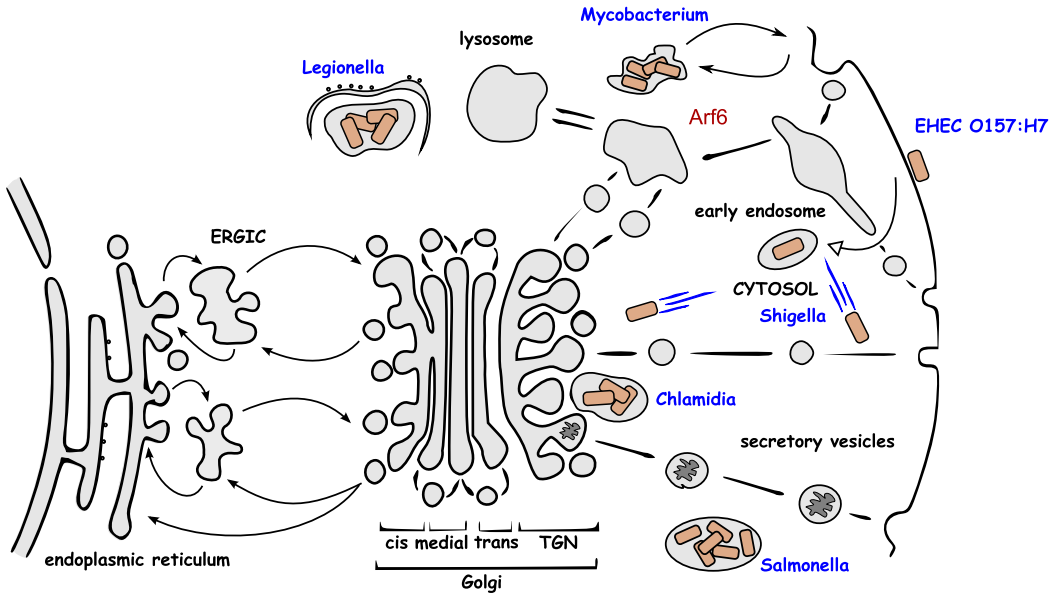

Figure 6. Endomembrane system is a frequent target of a diverse range of organisms. Cartoon representation of host eukaryotic endomembrane network, highlighting the ways bacterial pathogens have been shown to interact with host trafficking pathways.

Taken together, we now provide the first mechanistic description of EspG and specifically its role as a dual functioning GTPase inhibitor and kinase activator. These studies reveal novel facets of host enzyme regulation that have not been previously observed in eukaryotic systems. We now propose that EspG, and most likely its closely related type III effector family members, promotes cellular cross-talk between GTPase and kinase signaling networks at sites of bacterial infection.

RESULTS

Screening for bacterial inhibitors of protein secretion

To identify new signaling pathways targeted by bacterial pathogens, we used a human Growth Hormone (hGH) secretion assay (Rivera et al., 2000) to measure the ability of type III and type IV effector proteins to regulate vesicle trafficking through the General Secretory Pathway. HEK293 cells have been transfected overnight with hGH fused to a Conditional Aggregation Domain (CAD), an F36M mutant of an FKBP protein. Upon expression, hGH aggregates via CAD oligomerization and is retained in ER. Addition of cell permeable small molecule AP21998 to the media relieves aggregation and allows normal trafficking of hGH through the GSP. This allows us to synchronize the cells and monitor the levels of secreted hGH at a set time point (Fig. 7a). In order to identify virulence factors that modulate protein secretion, cells were co-transfected with CAD-hGH and GFP-tagged sequences encoding bacterial virulence factors, and hGH levels quantified by ELISA two hours after addition of AP21998 (Fig. 7a). In addition to being used to confirm the expression of transfected virulence factors, GFP signal was also used to assess the localization of proteins at host organelles.

We noted that several type III effectors encoded by the extracellular pathogen EHEC O157:H7 inhibited host trafficking events, whereas effectors secreted by *Salmonella typhimurium*, *Legionella pneumophila*, and *Bartonella henslae* displayed little inhibitory functions, consistent with their intracellular life-cycles (Fig. 7b). In particular, the EHEC type III effector EspG completely abolished exocytosis of hGH through an unknown molecular mechanism (Fig. 7b).

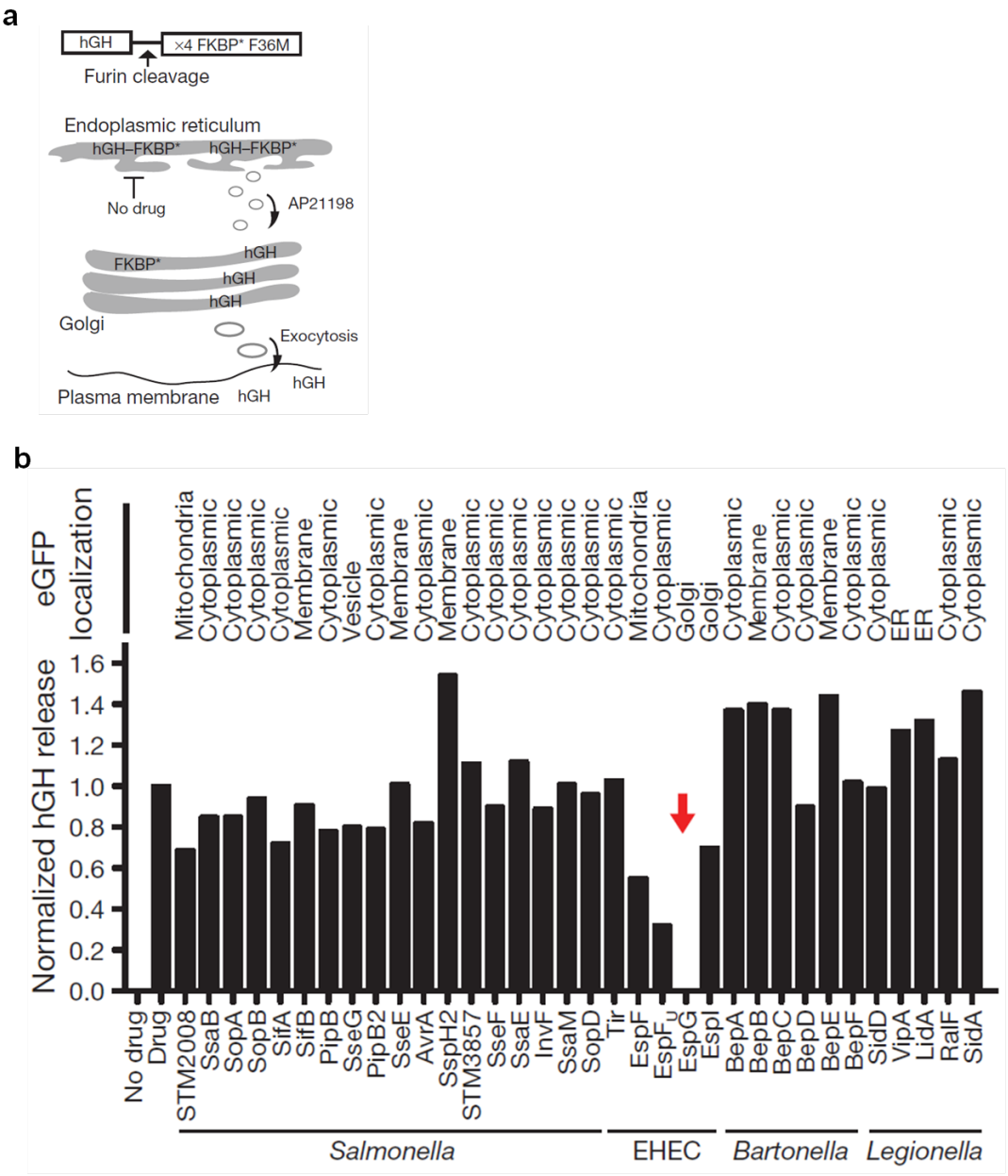

Figure 7. Inducible secretion assay screen identifies EspG as a potent inhibitor of endomembrane trafficking.

a, hGH trafficking assay showing how the hGH–FKBP* (Phe 36 Met mutant) aggregates in the endoplasmic reticulum until drug application (AP21998), whereby hGH enters the general secretory pathway and is secreted into the culture medium.

b, hGH release assay showing the effects of type III and type IV effector proteins on trafficking through the general secretory pathway. hGH was quantified by enzyme-linked immunosorbent assay and normalized to GFP control (Drug) experiments. The subcellular localization of eGFP-tagged effectors is indicated.

Identification of host targets of EspG

EspG was screened for host substrate interactions by the yeast two-hybrid (Y2H) method. From a total of 26 putative interacting clones, four sequences encoded the intact GTPase domain of ARF1 (residues 15-181) and two sequences encoded ARF6 (residues 18-175) (Fig. 8a). We also found that the GTP-loaded forms of ARF1, 5, 6, and to a lesser extent ARL1 associated with the bacterial effector, (Fig. 8b) whereas no other Ras-superfamily GTPases including H-Ras, RhoA, Rab5, or Sar1 bound EspG (data not shown). These data suggest that EspG encodes a specific mechanism to regulate select pools of ARF-family GTPases that are GTP-bound and associated with host membranes.

In addition to ARFs, we isolated six independent sequences of the p21-activated kinase (PAK) family of serine/threonine kinases (Bokoch, 2003). Every PAK clone encompassed the amino-terminal autoinhibitory domain (AID) yet lacked the kinase domain (KD) (Fig. 8c). Indeed, GST-tagged AID of PAK1 (residues 1-231) bound specifically to EspG (Fig. 8d). We further localized the EspG binding site on PAK2 to residues 121-136, a protein region that encompasses the Iα3-helix within the AID. Importantly, the sequence of Iα3 is highly conserved explaining why EspG recognizes all three PAK isoforms (see Chapter 2 for details).

ARF GTPases function within a broad range of organelle systems where they organize vesicle transport machinery, phospholipids, and signaling molecules at membrane microdomains (D'Souza-Schorey & Chavrier, 2006; Kahn, 2009), while PAK-family of serine/threonine kinases transduce Cdc42 and Rac1 GTPase signals that establish intracellular polarity (Bokoch, 2003). Some evidence also implicates PAK in regulating Golgi morphology during mitosis. Together, these findings establish two EspG substrates that are consistent with its regulatory function in

host protein trafficking identified here and in bacterial infection studies conducted *in vivo* (Borthakur et al., 2006; Guttman et al., 2007).

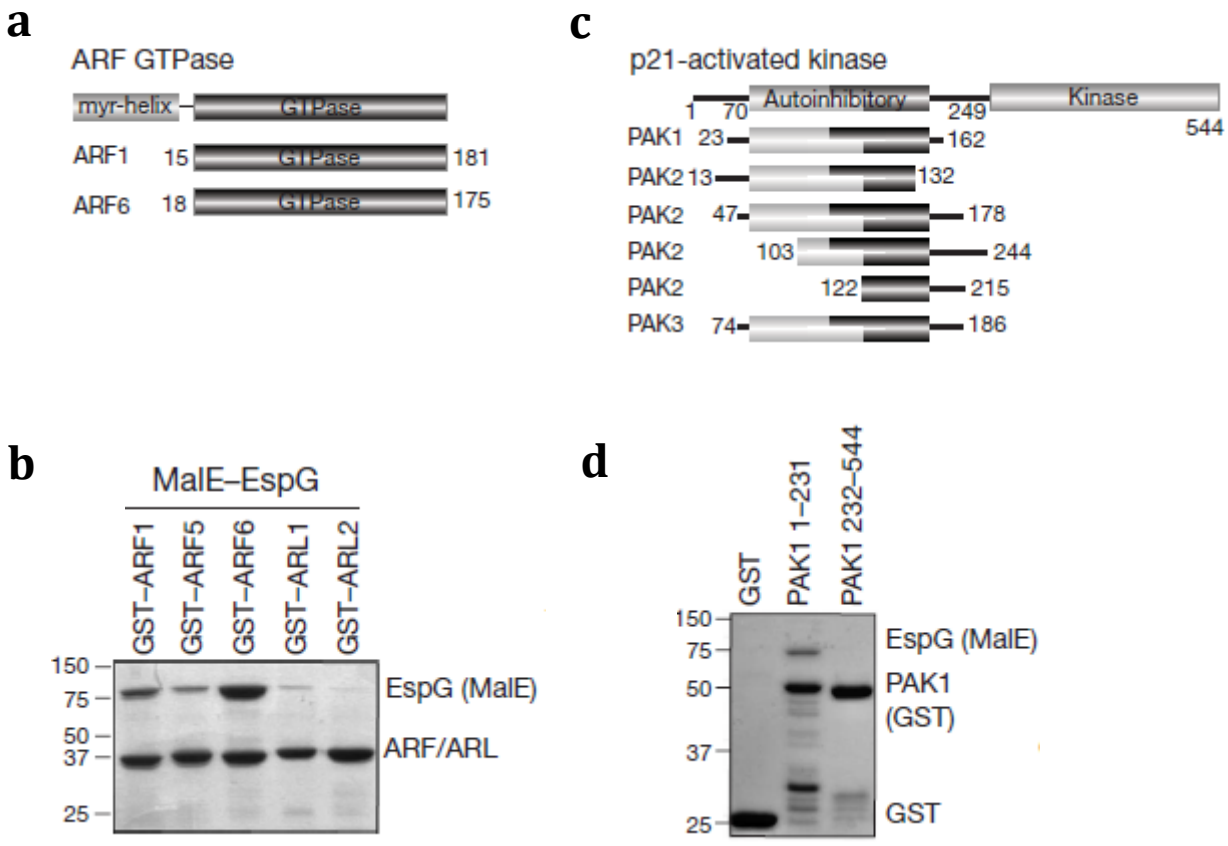

Figure 8. ARF GTPases and PAK kinase are host targets of EspG.
a, c, ARF GTPase (a) and PAK isoforms (c) that interact with EspG by yeast two-hybrid.
b, d, Glutathione pull-down of GST–ARF isoforms (b) and GST–PAK1 fragments (d) with recombinant MalE-tagged EspG.

Molecular structure of EspG/ARF complex

EspG (residues 42-398) was crystallized in complex with the GTPase domain of human ARF6 (residues 13-175). The initial structure was phased to 2.5 Å resolution by the multi-wavelength anomalous dispersion (MAD) method using selenomethionine-labeled EspG and ARF6 proteins. The crystal contained a single EspG, Arf6, and Mg^{2+}-GTP molecule per asymmetric unit (Fig. 9a). In the crystal, EspG captured the GTP-bound active conformation of ARF6 in conditions that did not include exogenous nucleotides. The coordination of the Mg^{2+}-GTP by the switch loops is nearly identical between our ARF6 structure and the previously solved active-state structure of ARF6-GTPγS (r.m.s.d. of 0.69 Å over 160 Cα atoms; PDB ID 2J56) (Fig. 9b) (Pasqualato, Menetrey, Franco, & Cherfils, 2001). The bacterial effector specifically engages the switch I loop of ARF6 as well as several residues lining the guanine-nucleotide binding pocket. Importantly, switch I is inaccessible to EspG when ARF6 is GDP-bound. An ARF-family sequence alignment also reveals that the EspG contact sites in ARF6 are invariant among ARF-family members whereas these residues are unique in other RAS-family GTPases (Fig. 9c). These data provide a structural rationale for the GTPase isoform selectivity by EspG.

The EspG-ARF6 heterodimer buries 602 $Å^2$ of total surface area. Three intermolecular interactions predominate. The first involves a collaboration of EspG loops (connecting β5-β6, β8-α6, and α12-α12') from which five residues (Pro150, Ile152, Ile184, Pro185, and Leu302) form a hydrophobic pocket to accommodate the switch I residue $Ile42^{ARF6}$. The significance of this hydrophobic interface was verified by a combinatorial mutation that included $Ile152^{EspG}$→Ser and by mutations in $Ile42^{ARF6}$, both of which resulted in EspG-ARF6 complex

disruption (Fig. 10). The second is the association of Arg306^{EspG} and Glu392^{EspG} with Thr40^{ARF6}, an interaction mediated by both electrostatic and hydrogen bonds. Indeed, charge reversal of Glu392^{EspG}→Arg and a hydrophobic substitution in Thr40^{ARF6} attenuated EspG-ARF6 complex formation (Fig. 10). Together, these hydrophobic and hydrophilic networks represent the bulk of the buried surface around switch I. The final stabilizing component of the EspG-ARF6 heterodimer is mediated by an acidic loop in EspG (Glu352 and Asp353 connecting β12-β13) and ARF6 residues that form the outer rim of the guanine-nucleotide binding pocket (Lys32, Asp125, and Thr157). In an unusual set of GTPase interactions, Glu352^{EspG} hydrogen bonds with Asp125^{ARF6} that coordinates the guanine base of GTP. In addition, Glu352^{EspG} forms a salt bridge with Lys32^{ARF6} and the main chain nitrogen of Thr157^{ARF6}. Together, these interactions appear to stabilize the GTP-bound conformation of ARF6 by immobilizing the switch I loop to the GTPase structural scaffold.

An EBI database search revealed that *Shigella* VirA (PDB ID 3EB8) is the only structural homolog to EspG, but the structural match was quite low (r.m.s.d of 3.1 Å; Z-score=5.9) and only covered the C-terminal two thirds of the protein (242 Cα atoms) (Davis et al., 2008; Germane, Ohi, Goldberg, & Spiller, 2008). While it is apparent that EspG and VirA belong to the same protein fold class, they exhibit several distinct features. EspG adopts a relatively compact structure (Fig. 11a) whereas the N-terminal domain of VirA (residues 54-124) is rotated about a hinge at Gly132 in the flexible linker between the two domains, resulting in a V-shaped architecture (Fig. 11b). The two effectors share less than 15% amino acid sequence identity and the substrate binding elements of EspG are distorted in VirA (Fig. 11c). In light of these observations, it is surprising that genetic studies place these type III effectors in a common

signaling pathway to promote EHEC and *Shigella* pathogenesis (Elliott et al., 2001). Our studies now show that members of the EspG/VirA family are only distantly related in terms of their amino acid sequence, proteins structures, and the identities of their host substrates.

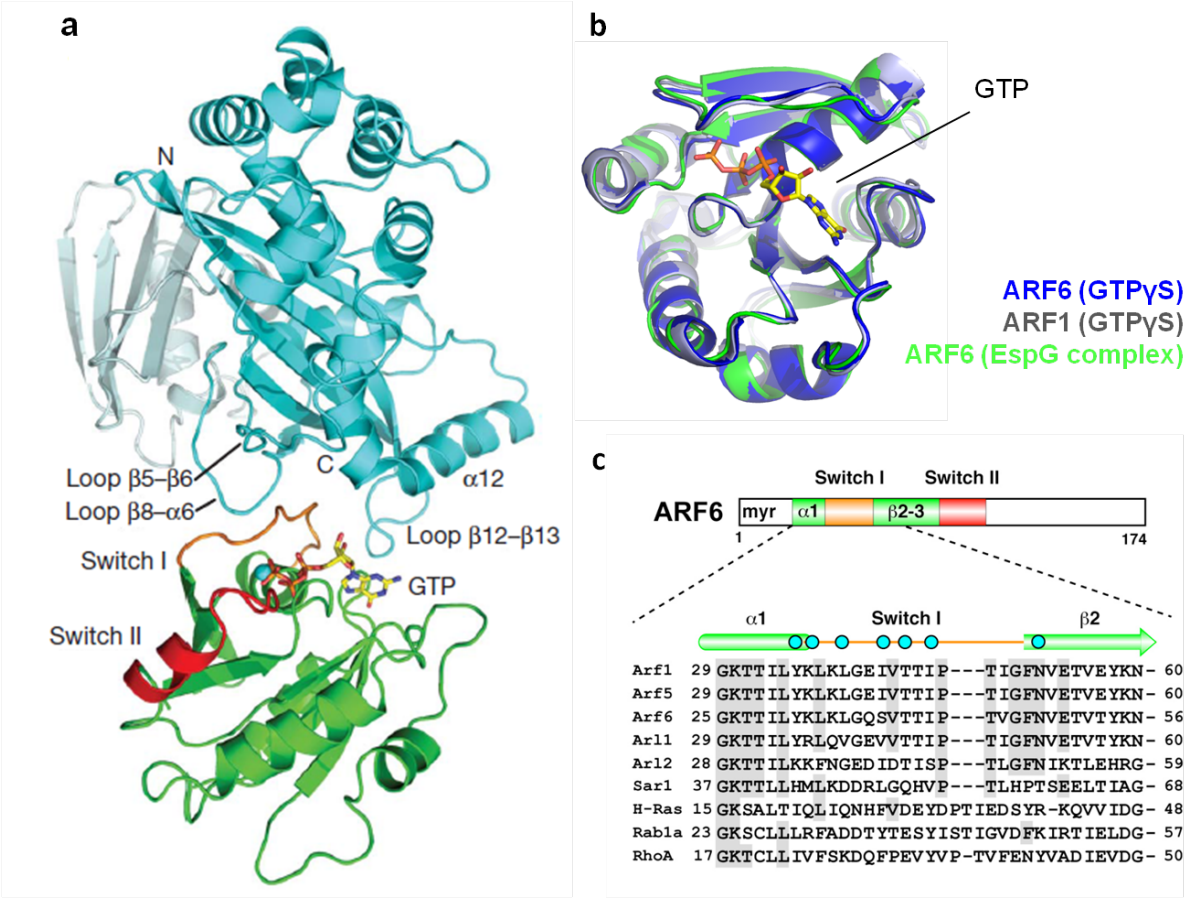

Figure 9. EspG binds ARF family GTPases.
a, Crystal structure of EspG (teal) bound to ARF6 (green).
b, Structural overlay of ARF1-GTP alone and ARF6 from EspG/ARF6 complex.
c, Sequence alignment of ARF GTPases. Residues involved in EspG binding are highlighted with teal circles.

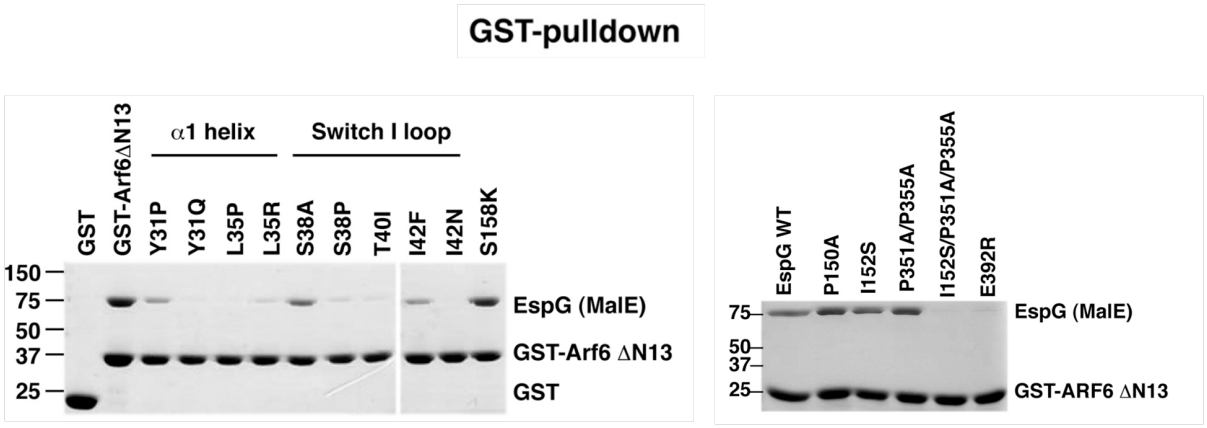

Figure 10. Identification of key residues involved in EspG/ARF interaction.
Pull-down experiments testing the involvement of residues identified in a crystal structure as being important in protein recognition. ARF6 mutants, left. EspG mutants, right.

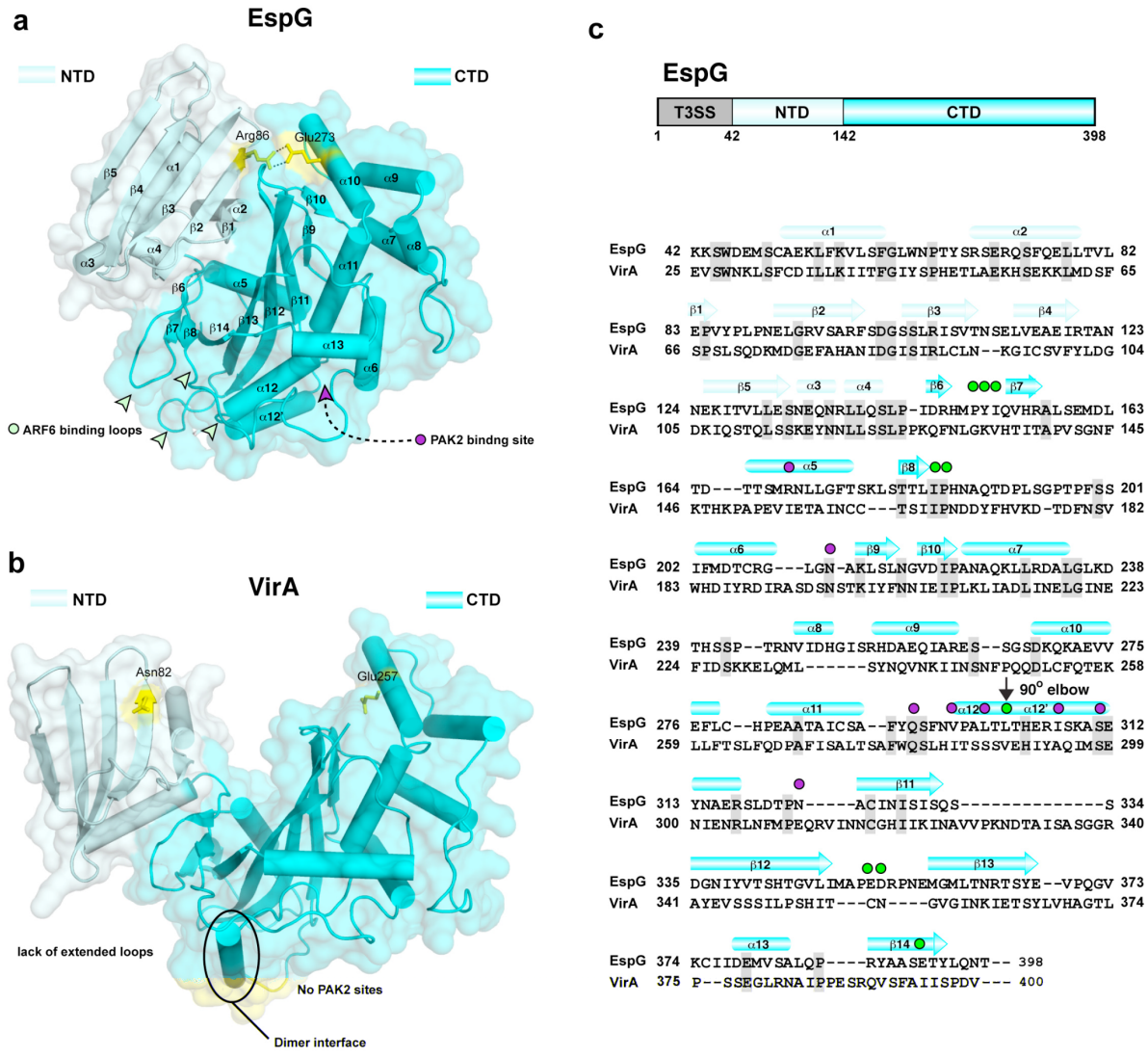

Figure 11. Structural analysis of EspG and Shigella VirA.

a-b, Structural comparison between EspG (a) and VirA (b, PDB ID: 3EB8). Structures are colored light blue and cyan and the secondary structural elements are labeled. Corresponding residues in the N- and C-terminal domains are shown in yellow and illustrate the structural translations that occur between EspG and VirA. The sites of ARF6 and EspG are marked with arrows and the PAK2 binding site is indicated. The dimerization site in VirA is circled.

c, Domain diagram of EspG and a composite sequence alignment of EspG and VirA based on primary sequence (CLUSTAL-W alignment) and modified to match secondary structural elements. The secondary structure of EspG is shown with α-helices displayed as bars and β-sheets as arrows. ARF6 (green) and PAK2 (magenta) contact residues are shown with circles.

Molecular structure of EspG/PAK complex

EspG (residues 42-398) was crystallized in complex with the essential binding peptide of PAK2 (residues 121-136). The EspG-PAK2 structure was then phased to 2.8 Å resolution by the molecular replacement method using the EspG monomer of the EspG-Arf6 structure as an initial search model. The refined structure contained four EspG monomers and four PAK2 peptides in the crystal asymmetric unit (Fig. 12a). The structures of all five EspG molecules (from the two crystal lattices) were nearly identical with a root mean square deviation (r.m.s.d) ranging from 0.612 Å to 0.639 Å over 349 Cα atoms.

EspG recognizes an N-terminal helical turn of the Iα3-helix whereas the remainder of the peptide adopts an extended strand conformation that lies orthogonal to the EspG six-stranded β-sheet. The complex buries 684 $Å^2$ of surface area and is primarily supported by a large hydrophobic interface and hydrogen bonding between Asn323 of EspG to the main chain of Val126 and Lys128 of PAK2 (Fig. 12b). This structural interface was confirmed by a series of *in vitro* binding studies and kinase assays using PAK2 and EspG mutant proteins (Fig. 12c, d).

We were surprised to find that both PAK2 and ARF6 are closely associated on neighboring surfaces of EspG but their binding sites do not overlap (see Fig. 16a). Remarkably, EspG contributes four residues from the inner face of the α12 helix (Val297, Leu300, Ile307, and Ser311) toward PAK2 binding and two residues (Leu302 and Arg306) from the outer face of the α12 helix toward ARF6 binding. However, PAK2 had no affect on EspG binding to ARF6 and similarly, ARF6 did not affect EspG affinity for PAK binding (data not shown).

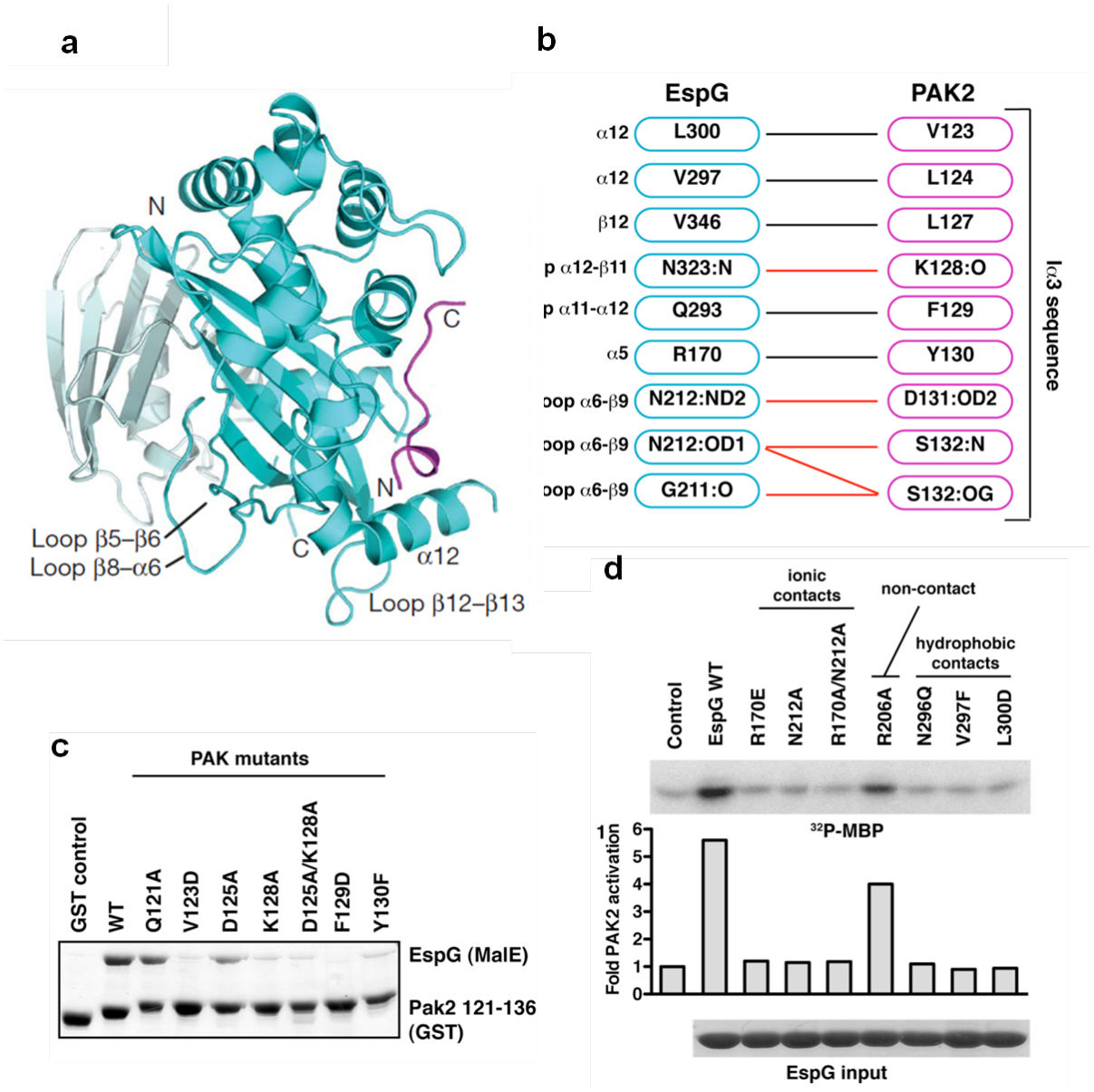

Figure 12. The EspG-PAK2 complex interface.
a, Crystal structure of EspG bound to the Ia3 fragment of PAK.
b, Specific interaction between EspG (left) and PAK2 Iα3-derived peptide (right). The location of each residue within the complex is listed alongside of each amino acid. Hydrophilic contacts including hydrogen bond or electrostatic interactions are shown by red lines and hydrophobic contact within less than 5 Å are shown by a black line.

c, Mutagenesis of PAK2 residues 121-136 to confirm the binding interface with EspG. GST-pulldown experiments of GST-PAK2 121-136 or mutants PAK2 proteins (as indicated) binding to MalE-tagged EspG. Several PAK2 interface residues were substituted by residues with opposite chemical features including charge or size, all of which had an effect on EspG binding.

d, PAK2 kinase assays showing the effect of EspG mutations on the ability of EspG to stimulate PAK kinase activity. Mutations were introduced into EspG residues that directly interact with PAK2 (as indicated). GFP-tagged PAK2 was immunoprecipitated from HEK293A cells, and incubated with EspG mutants for 5 minutes in kinase reaction buffer (see methods). Phosphorylation of MBP substrate by PAK2 is shown in the upper gel. The fold increase of substrate phosphorylation compared to the negative control lane is shown in the graph. All of the EspG interface mutants inhibited PAK activation.

EspG disrupts Golgi morphology

We found that eGFP-tagged EspG localized to the cis-Golgi apparatus where it induced severe fragmentation of the organelle (Fig.13a). The Golgi disruption phenotype was observed when estimated 50 pM recombinant EspG protein was microinjected into cells to mimic the protein concentration delivered by *E. coli* through the type III secretion apparatus (Winnen et al., 2008). In addition, EspG disrupted the recycling endosome compartment in both transfection and microinjection experiments (Fig. 13b). Thus, EspG represents a new class of bacterial signaling effectors that functionally regulate trafficking from membrane organelles.

The biochemical interaction studies between ARFs, PAKs, and EspG agree with the molecular mechanisms revealed by our X-ray crystal structures. The combined molecular analysis thus predicts that EspG signaling (*i*) relies on the guanine-nucleotide cycling of ARF GTPases, (*ii*) is dependent on the spatial and temporal function of the vesicle budding machinery, and (*iii*) is manifested by the multifunctional nature of the EspG protein surface and its ability to nucleate a novel GTPase-kinase signaling complex. To test the applicability of these models and their relevance toward *in vivo* signaling processes, we turned to established cell biological methods for dissecting EspG function within host cells.

Microinjection of as little as 10 nM EspG protein induced severe morphological alterations at the Golgi apparatus. The Golgi was fragmented and tubulovesicular remnants were dispersed throughout the cytoplasm as determined by GM130 immuno-staining. Previous genetic studies have implicated EspG (Shaw et al., 2005; Tomson et al., 2005) and related *Shigella* family members (Yoshida et al., 2006) in microtubule depolymerization, however we found no

evidence to support this notion (Fig. 13c), consistent with previous reports (Davis et al., 2008; Germane et al., 2008).

We next sought to determine if the Golgi defects induced by EspG are consistent with the GTPase and kinase signaling models elucidated by our structural analyses. EspG displays rapid inhibitory kinetics as the Golgi fragmented within 20 minutes of protein microinjection. These kinetics compared favorably to the fungal toxin Brefeldin A (BFA), an uncompetitive inhibitor of GDP/GTP cycling on ARF1 GTPase (Chardin & McCormick, 1999) (Fig. 13d). By comparison, injection of N-GAT GGA had no inhibitory affects on the Golgi within the time frame of these experiments. These data suggest that the structural architecture of EspG binding to ARF GTPases is uniquely inhibitory since occupying GTP-ARF1 at its normal signaling site by exogenous N-GAT GGA is insufficient to produce the Golgi disruption phenotype. Consistent with this interpretation, neither the Golgi architecture (Fig. 14a) nor the GSP trafficking pathway (Fig. 14b) were affected by mutant EspG proteins that disrupted the ARF binding interface. Moreover, pre-absorption of the non-cycling mutant Arf6ΔN13 onto EspG protein prior to cell microinjection significantly delayed the Golgi inhibitory kinetics of EspG (Fig. 13d). Thus, the cell biological functions of EspG at the Golgi are consistent with the structural-based hypotheses described here..

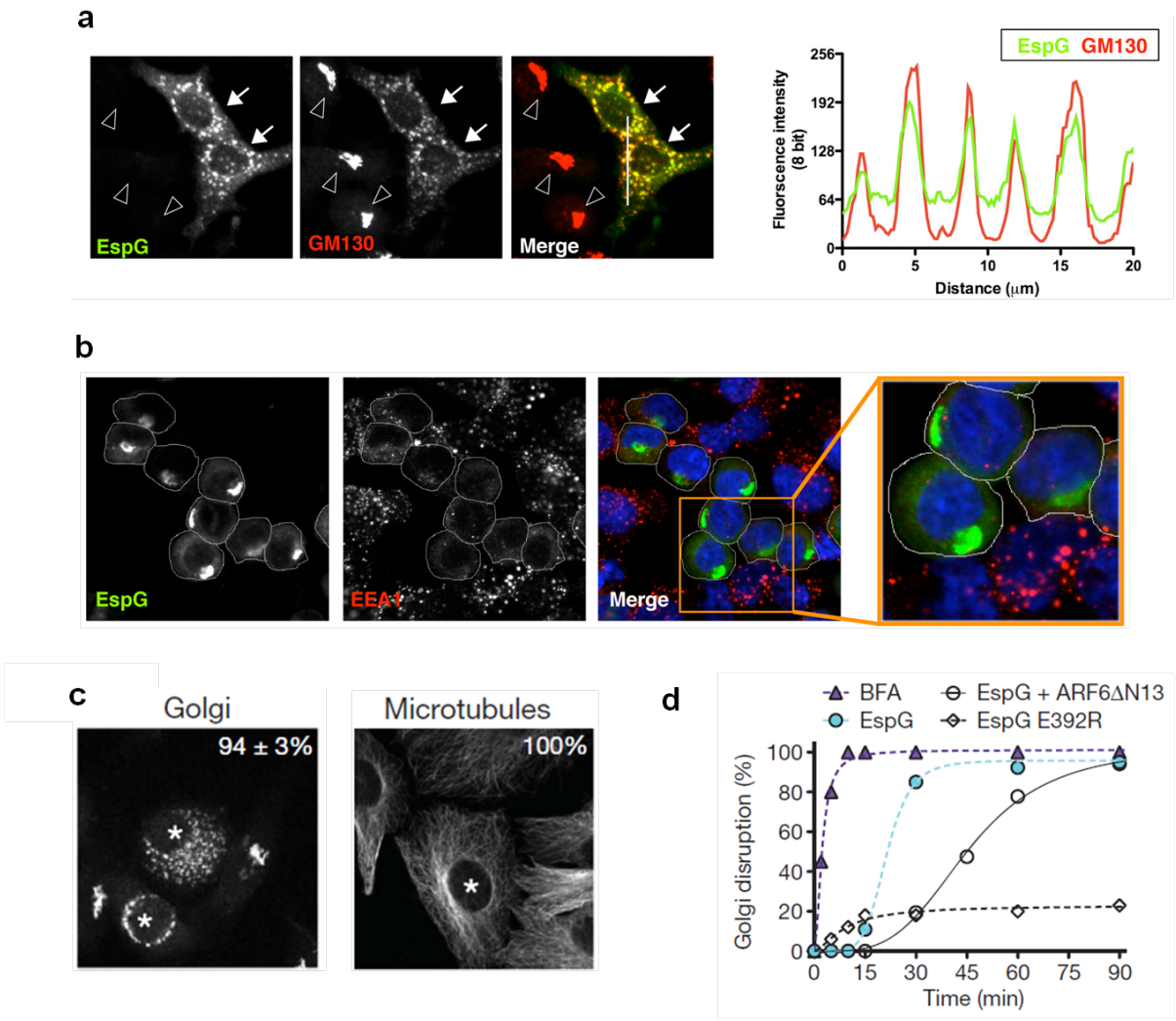

Figure 13. Cellular effects of EspG and Golgi fragmentation.
a, EGFP-tagged EspG was transfected into HeLa cells and stained for Golgi marker GM130. EspG transfected cells are marked with closed arrows. EspG co-localized with GM130 and these proteins displayed over 95% overlap (graph). Three untransfected cells show normal cis-Golgi morphology (open arrowheads).
b, HEK293A cells were transfected EGFP-EspG and stained for EEA-1, a protein constituent of the recycling endosomes. EspG transfected cells in the population are outlined. The merged image is shown and expanded to show the clear endosome disruption phenotype induced by EspG compared to normal endosome morphology observed in untransfected cells.
c, Golgi and microtubule phenotypes induced by EspG protein microinjection (asterisk). The percentage of microinjected cells exhibiting each phenotype is indicated (n>3, from ~40 cells per experiment)
d, Time course of the Golgi disruption phenotype presented as the percentage of microinjected cells with altered Golgi morphology.

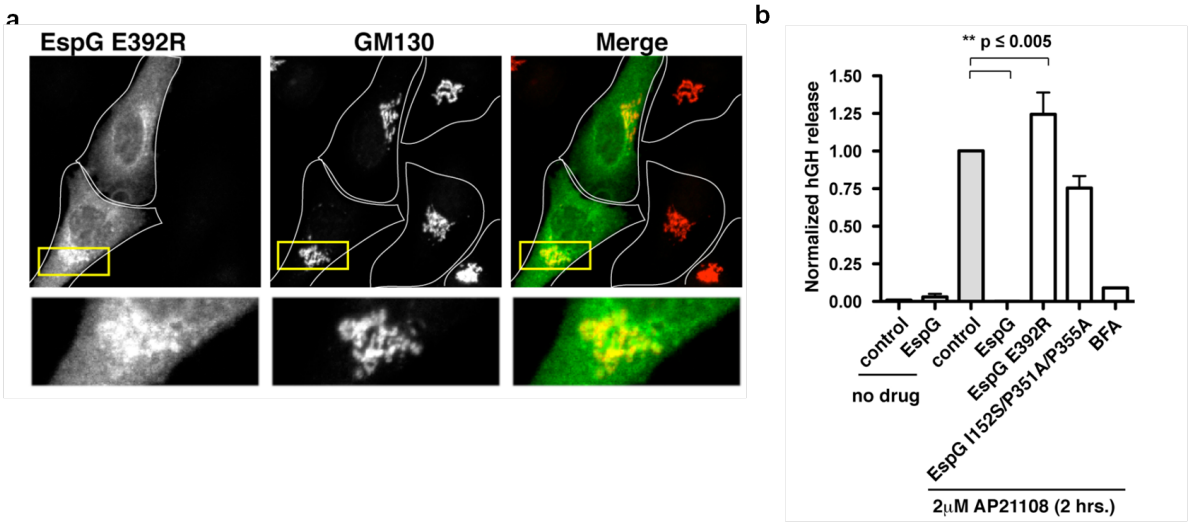

Figure 14. ARF-binding deficient EspG does not disrupt endomembrane traffic.
a, Fluorescent microscopy showing that EGFP-EspG mutants defective in ARF and PAK binding are distributed throughout the cell cytoplasm and do not disrupt the Golgi architecture. Quantification showing % cells exhibiting the Golgi disruption phenotype is presented. Over 50 cells in at least 3 independent experiments were quantified. SEM is shown.
b, Quantification of secreted hGH before (no drug) or after drug addition (AP21108) (see methods) in the presence of the indicated proteins or BFA. hGH release was normalized to control plasmid transfected cells that had not affect on hGH trafficking. Both EspG transfected (but not mutants) and BFA treated cells blocked hGH trafficking through the General Secretory Pathway (GSP).

EspG nucleates GTPase/Kinase signaling complex

The two EspG structures in complex with ARF6 and PAK reported here are nearly identical with a root mean square deviation (r.m.s.d) of 0.612 Å over 349 Cα atoms. As shown in Fig. 15a, ARF6 and PAK2 occupy distinct, non-overlapping binding sites on adjacent surfaces of EspG. Consistent with this view, EspG nucleates a trimeric complex between the kinase and GTPase in solution (Fig. 15b). This complex could also be reconstituted on Golgi mimetic liposomes (Fig. 15c). ARF1·GTP recruited EspG to the artificial membrane surface (Fig. 15c, lanes 2 and 4), which in turn localized PAK2 to these sites (Fig. 15c, lane 6). Importantly, PAK2 localization was strictly dependent on formation of the EspG/ARF1·GTP complex (Fig. 15c, lane 7-8) and ARF1 tethering to the membrane (Fig. 15c, lane 9-10).

As predicted by these findings, EspG co-localized with ARF1 at the Golgi (Fig. 15d) and we further speculated that PAK would also be regulated at these sites. To test this hypothesis, an *in vivo* 'activity' probe was engineered by fusing the PAK2 Iα3-helix sequence (residues 121-136) to the C-terminus of mCherry fluorophore. The PAK2-probe recognized cellular EspG and was targeted to the Golgi in 78±5% of EspG transfected cells (Fig. 15d). By comparison, mutant EspG N212A that lacked PAK binding properties (see Chapter 3) localized to the Golgi but did not recruit PAK2 to these sites (Fig. 15d). All together, our studies support the function of EspG as an enzyme scaffold that links GTPase inhibition with kinase signal transduction pathways at membrane organelles (Fig. 15e).

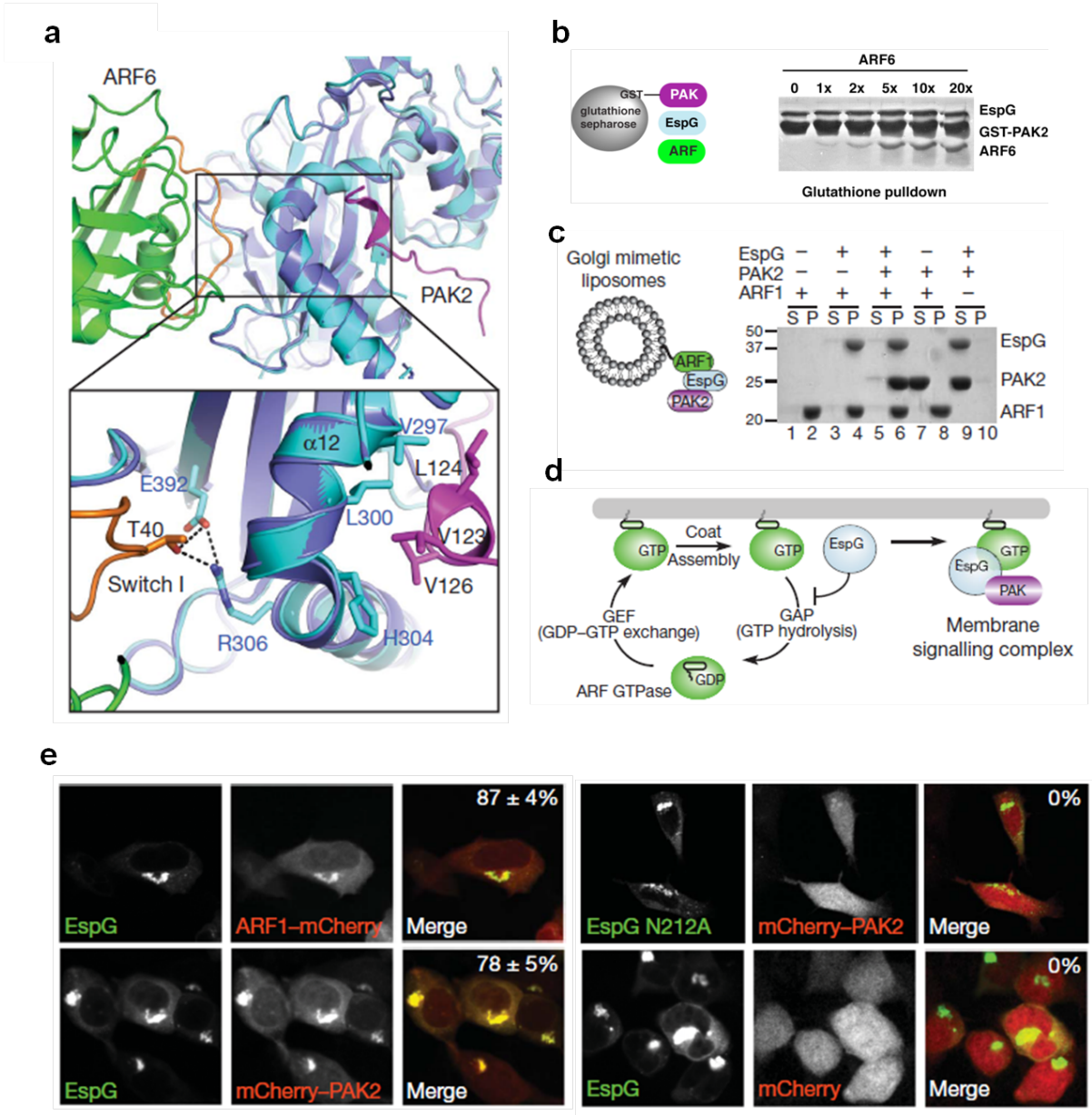

Figure 15. EspG nucleates a GTPase/Kinase signaling complex.
a, Structural overlay of EspG–ARF6GTP and EspG–PAK2Ia3 highlighting the close association between ARF and PAK on the surface of EspG. Colors are as in Figs 2a and 3a except that EspG from the PAK2 structure is colored purple.
b, EspG nucleates a trimeric complex between ARF6 and PAK2 *in vitro*. GST-tagged PAK2 (residues 65-136) were loaded on glutathione sepharose beads at a concentration of 2 μM. EspG (0.5 μM) was added in the presence of increasing concentrations of ARF6-GTP from 0 to 20x molar excess over EspG. ARF6 did not compete with EspG showing that EspG nucleates a trimeric complex between PAK2-EspG-ARF6.

c, Golgi-mimetic-liposome-binding assays showing that EspG nucleates a trimeric complex between ARF1 and PAK2 on membrane surfaces. After centrifugation, proteins remaining in the supernatant (S) or those associated with liposomes in the pellet (P) are indicated.

d, Model of the dual function of EspG as an inhibitor of membrane trafficking and as a catalytic scaffold that assembles a GTPase–kinase signaling complex at cellular membranes. GEF, guanine nucleotide exchange factor.

e, HEK239A cells co-transfected with the indicated constructs showing that eGFP–EspG co-localizes with ARF1–mCherry and recruits a PAK activity probe (mCherry–PAK2121–136) to Golgi membranes. The percentage of cells exhibiting co-localized EspG with mCherry-tagged proteins (n53) is shown in the upper right of the merged micrographs.

DISCUSSION

The structure-confirmed interactions of EspG with of ARF family GTPases and PAK kinase are in complete agreement with its cellular functions in membrane trafficking (Figure 7G). Given the overall importance of ARFs and PAKs in maintaining epithelial homeostasis, our studies define a fundamentally new mechanism of bacterial virulence employed by EHEC O157:H7. Indeed, ARF GTPases are master regulators of apico-basolateral trafficking and maintain epithelial cell polarity by sorting protein constituents to their appropriate membranes (D'Souza-Schorey & Chavrier, 2006). Moreover, PAK kinases also set up cell polarity programs (Bokoch, 2003), particularly relevant to the wounded epithelium. Therefore, the ability of EspG to engage diverse signaling systems simultaneously, provides EHEC with a powerful tool to exploit these cell biological processes. We also expect numerous type III effector proteins to work in concert with EspG during the complex pathogenic insult. Our laboratory and others have identified effector proteins that hijack membrane trafficking organelles at points both upstream (J. Kim et al., 2007) and downstream (Alto et al., 2007) of the EspG function reported here. Nevertheless, this study provides the first molecular insights into how the EspG/VirA family members recognize eukaryotic signaling enzymes.

One of the most surprising finding from this study is that EspG and its *Shigella* homolog VirA are structurally diverse and are likely to recognize unique host substrates. It is also intriguing that the ARF and PAK binding interfaces on EspG do not overlap, yet are closely associated on adjacent surfaces. Together, these observations suggest that bacteria can extensively modify protein structures to evolve multiple host signaling outputs within the constraints of a single protein domain. If this observation is applied to other bacterial effectors

and toxins, it is possible that we have vastly underestimated the potential signaling functions employed by human pathogens. In fact, it is conceivable that both EspG and VirA bind additional host substrates through the amino terminal domain whose function is currently unassigned. Given these possibilities, we are much closer to reconciling the biochemical activities of these effectors with genetic studies that often reveal multiple functions within the host cell. Therefore, elucidating the structural mechanisms of effector-enzyme complexes will be required to pave the way for future systems biology approaches between bacteria and their host.

EXPERIMENTAL PROCEDURES

Plasmids

The *espG* gene from EHEC O157:H7 was PCR cloned in-frame into pEGFP-C2 (Clontech) and pcDNA3.1-mCherry. For bacterial expression, 38 and 41 amino-acid N-terminal deletions (39–398 and 42–398) of EspG were PCR subcloned into pGEX-4T1 (GST-tag) (Amersham), pProEX-HTb (6xHis tag) (Novagen) and pET28b-MalE (6xHis tag, MalE-tag) vectors. EspG mutants were generated with QuickChange site-directed mutagenesis (Stratagene) following manufacturer's instructions. N-terminal deletions of ARF GTPases (ARF1Δ17, ARF5Δ17 and ARF6Δ13) and ARL proteins (ARL1Δ17 and ARL2Δ16) were PCR subcloned into pGEX-4T1 and pProEX-HTb vectors. Human PAK1 construct was obtained from Dr Gary Bockoch (TSRI, La Jolla, California), and rabbit PAK2 and PAK3 were obtained from Dr Melanie Cobb (UTSW). PCR cloning was used to generate variable-length constructs of PAK isoforms in pGEX-4T1 vector. All constructs were verified by DNA sequencing.

Yeast two-hybrid system

The yeast expression vector pLexA encoded a gene with an NH2-terminal LexA-binding domain and residues 1–398 of EHEC EspG. Day 9.5 and 10.5 mouse embryo cDNA library (250 μg) in VP16 were screened using the yeast two-hybrid system.

Protein purification for in vitro assays

Recombinant proteins were produced in BL21-DE3 *E. coli* strains. Protein expression was induced with 0.4 mM IPTG for 16 h at 18 °C. Bacterial pellets were lysed in either His buffer (100 mM HEPES, pH 7.5, 300 mM NaCl) or GST buffer (TBS; 50 mM Tris pH 7.5, 150 mM NaCl, 2 mM DTT) supplemented with protease cocktail (Roche). Proteins were purified with nickel agarose (Qiagen) or glutathione Sepharose (Amersham Biosciences) following manufacturer's instructions. Eluted proteins were buffer exchanged into TBS using concentration centrifugal columns (Millipore), glycerol was added to 15% and the proteins were then stored at −80 °C.

In vitro GST pull-downs

Protein interactions were examined through GST pull-down assays. Unless otherwise stated, 15 μg of recombinant GST proteins immobilized to glutathione Sepharose were incubated with 20 μg of 6xHis- and/or MalE-tagged proteins for 1 h at 4 °C. Samples were washed three times in TBS supplemented with 0.5% Triton X-100. Proteins were eluted from beads with Laemelli sample buffer and were separated by SDS–polyacrylamide gel electrophoresis and

stained with Coomassie blue. For nucleotide loading, ARF1Δ17 and ARF6Δ13 were incubated in nucleotide loading buffer (40 mM HEPES, 150 mM NaCl, 2 mM EDTA, 10% glycerol) with 10 μM of either GDP or GTP for 30 min at 37 °C, and then $MgCl_2$ was added to 10 mM and the reaction was transferred to ice after 15 min at room temperature (25 °C).

Cell microinjection, transfections and immunofluorescence microscopy

Normal rat kidney cells were microinjected with EspG proteins using a semi-automatic InjectMan NI2 micromanipulator (Eppendorf). A needle concentration of 10 nM was calculated to inject between 5,000 and 20,000 copies because we microinjected ~5% cell volume, giving a final estimated cellular concentration of 50 pM in a cell volume of 5,000 μm^3. HeLa and HEK293A cells were transfected using calcium phosphate. At 16–18 h post-transfection, cells were fixed with 3.7% formaldehyde and stained with antibodies for immunofluorescence. In co-transfection experiments, equal amounts of DNA were used for each sample. Brefeldin A treatment was performed by adding 5 μg ml^{-1} of Brefeldin A to the medium before fixation with formaldehyde. As a negative control, ethanol was added to the medium. All immunofluorescence images were acquired with a Zeiss LSM 5 Pascal confocal microscope. Golgi, endosomes and microtubules were detected using anti-GM130 (transduction labs), anti-EEA1 (transduction labs) and anti-α-tubulin (Sigma) antibodies, respectively.

hGH trafficking assay

For hGH trafficking assay, HeLa cells (50% confluence) were transfected with 1 μg of 4xFKBP-hGH (Ariad Pharmaceutical, Inc.;http://www.ariad.com/regulationkits; source of

material, David Bernstein) and either 0.5 μg eGFP–EspG or pEGFP control plasmid with Fugene6 (Roche). Sixteen hours later, the medium was replaced with medium containing AP21998 (final concentration, 2 μM) or vehicle control. AP21998 was incubated with the cells for 2 h before the supernatant was collected. The supernatant was then diluted 100-fold and compared against a hGH standard curve (12.5–400 pg ml^{-1}) for the quantification of hGH released using an hGH enzyme-linked immunosorbent assay (Roche). For no drug controls, 100% ethanol (2 μl) was incubated with the cells for 2 h.

Liposome pull-downs and GAP assays

Liposome preparation: Lipids were purchased in powder form from Avanti Polar Lipids. Golgi mimetic liposomes were created by combining 20 mol% DOGS-NTA with DOPC, DOPE, DOPA, DOPS, PI, PI_4P and $PI_{4,5}P_2$ in the molar ratios reported previously[29]. Total lipid (5 mM) was solubilized in chloroform, dried under an anhydrous nitrogen stream and further dried in a vacuum desiccator for approximately 5 h. Dried lipids were hydrated with liposome-binding buffer (20 mM Tris-HCl, pH 7.6, 50 mM NaCl, 10 mM $MgCl_2$) and vigorously vortexed between five freeze–thaw cycles (liquid nitrogen and 80 °C to ensure appropriate phase transition and dispersion of the various lipids), after which liposomes were generated by means of ultrasonication in a bath sonicator (Laboratory Supplies Company). Liposomes were collected from the supernatant after centrifugation (2,500*g* for 5 min) and used in subsequent assays.

Liposome pull-down assays: Liposomes were prepared as described above. ARF1 GTP loading was carried out by incubating purified 6xHis-tagged ARF1ΔN17 in nucleotide exchange buffer (20 mM Tris-HCl, pH 7.6, 50 mM NaCl, 5 mM EDTA, 10% glycerol, 1 mM DTT) with

100 μM GTP. After incubation at 37 °C for 30 min, 10 mM $MgCl_2$ was added to stabilize ARF1(GTP). The requisite volume of ARF1(GTP), GST PAK (residues 121–136) or EspG was added to bring the protein concentration to 3 μM in a 100-μl volume. Liposomes were added for a final lipid concentration of 10 μM and reactions proceeded at room temperature for 30 min. Samples were subjected to centrifugation at 100,000*g* in a Beckman TLA100.3 rotor and a Beckman TL100 ultracentrifuge at 4 °C for 1 h. Supernatant and pellet were separated and analyzed on a 12.5% polyacrylamide gel and visualized with Coomassie blue.

Crystallization and structure determination

Protein expression and purification: A stable protein fragment of EspG residues 42–398 was identified by limited proteolysis and mass spectrometry. cDNA-encoding EHEC O157:H7 EspG residues 42–398 and human ARF6 residues 14–175 were synthesized by PCR and ligated into the pPRO-EX-HTb expression vector. The resulting plasmids were then transformed into the *E. coli* strain BL21-DE3. Protein expression was induced by 1 mM IPTG overnight at 16 °C and proteins were purified on Ni-NTA agarose, concentrated to 10 mg ml^{-1} in TBS buffer with 5% glycerol, snap-frozen in liquid nitrogen and stored at −80 °C. The Se-Met variant of EspG and ARF6 was expressed in methionine auxotrophic *E. coli* strain B834-DE3 and grown in minimal medium supplemented with natural amino acids and Se-Met. Expression and purification were unchanged. EspG–ARF6 complex was formed overnight at room temperature in the presence of 1:100 TEV protease to cleave the 6xHis tag. The complex was purified by successive anion exchange (Q-HP) and gel filtration (Superdex 200 GL) chromatography and concentrated to 7 mg ml^{-1} in 25 mM Tris, pH 7.5, and 50 mM NaCl. For the PAK2 crystal trials, EspG protein was expressed and purified identically to that described. However, after the anion

exchange, EspG was incubated with a fivefold molar excess of PAK2 peptide (residues 121–136). The complex was purified by gel filtration as described.

See Appendix A for structure determination details. Combination models were generated by structural alignment of homologous or identical proteins from separate independent structures where applicable, using PYMOL.

CHAPTER THREE

REGULATION OF PAK KINASE ACTIVITY BY EspG

INTRODUCTION

The Pak-family of serine/threonine kinases transduce Cdc42 and Rac1 GTPase signals downstream of receptor activation (Bokoch, 2003). While little is known about how bacteria may usurp PAK signaling, its critical role in cell migration, wound healing and epithelial polarization makes it an ideal target (Bokoch, 2003). The PAK protein is composed of two primary domains, the Kinase Domain (KD) and Autoinhibitory Domain (AID). The KD is the functional output, phosphorylating a myriad of substrates particularly associated with actin and microtubule dynamics. The AID performs two essential functions: (*i*) it inhibits kinase activity and (*ii*) it serves as the receptor for stimulatory input by GTPases. The core inhibitory elements of the AID include a three-helix bundle (known as the Inhibitory Switch; IS) that folds onto the substrate binding-site of the KD and a 'kinase inhibitory' loop (known as the KI loop) that is directly inserted into the enzyme catalytic cleft (Lei et al., 2000). The AID receives stimulatory input from GTPases at the Cdc42 and Rac Interacting Binding (CRIB) domain that partially overlaps with the IS and KI loop inhibitory elements. Key structures have suggested that Cdc42 binding to CRIB releases the AID from the KD, thus activating the kinase (Lei et al., 2000). Our identification of PAK as bacterial type III effector substrate has potentially broad implications on the signaling mechanism of this important eukaryotic kinase family.

A related protein that is regulated by interaction of the inhibitory CRIB domain with the active domain and directly targeted by a bacterial protein (EspFu) is N-WASP. In free WASP,

autoinhibitory domain folds onto the hydrophobic α5-helix of the activity bearing VCA domain, preventing its recruitment of Arp2/3 actin nucleation complex (Figure 1A). Binding of Cdc42 to CRIB disrupts the GBD/α5-helix interface by destabilizing GBD and making it unfold, which exposes VCA residues for interaction with Arp2/3.(Padrick & Rosen, 2010) Interestingly, studies of WASP have shown that isolated GBD and VCA domains are largely unfolded in solution, thus suggesting a potential role for the inhibitory interaction in stabilizing the protein.(Abdul-Manan et al., 1999; A. S. Kim, Kakalis, Abdul-Manan, Liu, & Rosen, 2000) Analogous to WASP, the isolated GBD of PAK appears unstable in solution, but stable when folded onto KD in an autoinhibited homodimer. These observations make the unstable nature of GBD one of the characteristic features of CRIB proteins, and implicate CRIB-domains in being able to not only regulate the activation state of the protein, but also control its stability and dynamics.

In our recent study we have identified EspG as an activator of Class I p21-family kinases and showed that it binds to the Iα3-helix of the autoinhibitory domain.(Selyunin et al., 2011) All Class I PAKs share the CRIB domain and dissociate into active monomers upon binding of Cdc42/Rac. Dissociation of inactive homodimer is necessary for the removal of the autoinhibitory loop (AI) that is linked to autoinhibitory domain and runs through the catalytic site of PAK KD.(Lei et al., 2000) The KD is fully active on its own, but can be inhibited by titrating in GBD, again showing the importance of interaction between inhibitory and active domains in modulating protein activity. Therefore, we set to determine if bacterial virulence factors not only exploit the basic principles of a unique endogenous mechanism to activate their downstream host targets, but define new regulatory sites through which this activation is achieved.

Here, we discuss new findings for how the bacterial virulence factor EspG from EHEC O157:H7 exploits a CRIB-independent activation mechanism of the Rho GTPase effector PAK. We also compare this mechanism to that of EHEC EspFu, a bacterial virulence factor that directly activates N-WASP. While both virulence factors break the inhibitory interaction between the autoinhibitory and activity-bearing domains of PAK or WASP, the underlying mechanics are very distinct from endogenous Cdc42/Rac GTPase regulation. The ability of bacterial proteins to identify novel regulatory principles of host signaling enzymes highlights the multi-level nature of protein activation, and makes them effective tools to study mammalian Rho GTPase signaling pathways.

RESULTS

Analysis of EspG binding site on PAK

After identifying the KD of PAK family kinases as a principal target of EspG through Y2H screen, we sought to determine the binding residues of PAK to gain insight into the potential role of EspG. Using binding assays and serially truncated constructs of KD, we found residues PAK2 residues 121-136 necessary and sufficient to bind EspG. These residues corresponded to the Ia3 helix of the AID, in contrast to the CRIB domain that is normally associated with PAK agonist binding (Fig. 16a).

Because the AID is sensitive to both stimulatory control by GTPases (Bokoch, 2003) and inhibitory control by small molecule compounds (Deacon et al., 2008) we tested if EspG regulated PAK enzyme activity *in vitro*. Incubation of purified PAK2 with recombinant EspG protein resulted in a 7.6±2.5 fold (n=10) activation of the kinase (Fig. 16b). This kinase

activation profile is comparable to stimulation by GTPγS-loaded Cdc42 (7.8±3.4 fold; n=3), a natural PAK agonist (Fig. 16b). In control experiments, EHEC type III effectors Map and EspFu/TccP displayed no PAK stimulatory activity, further demonstrating the signaling specificity of EspG (Fig. 16c). It is worth noting that Ia3 helix is largely conserved among PAK isoforms, suggesting that EspG may differentially regulate the activity of all PAK family members (Fig. 16d).

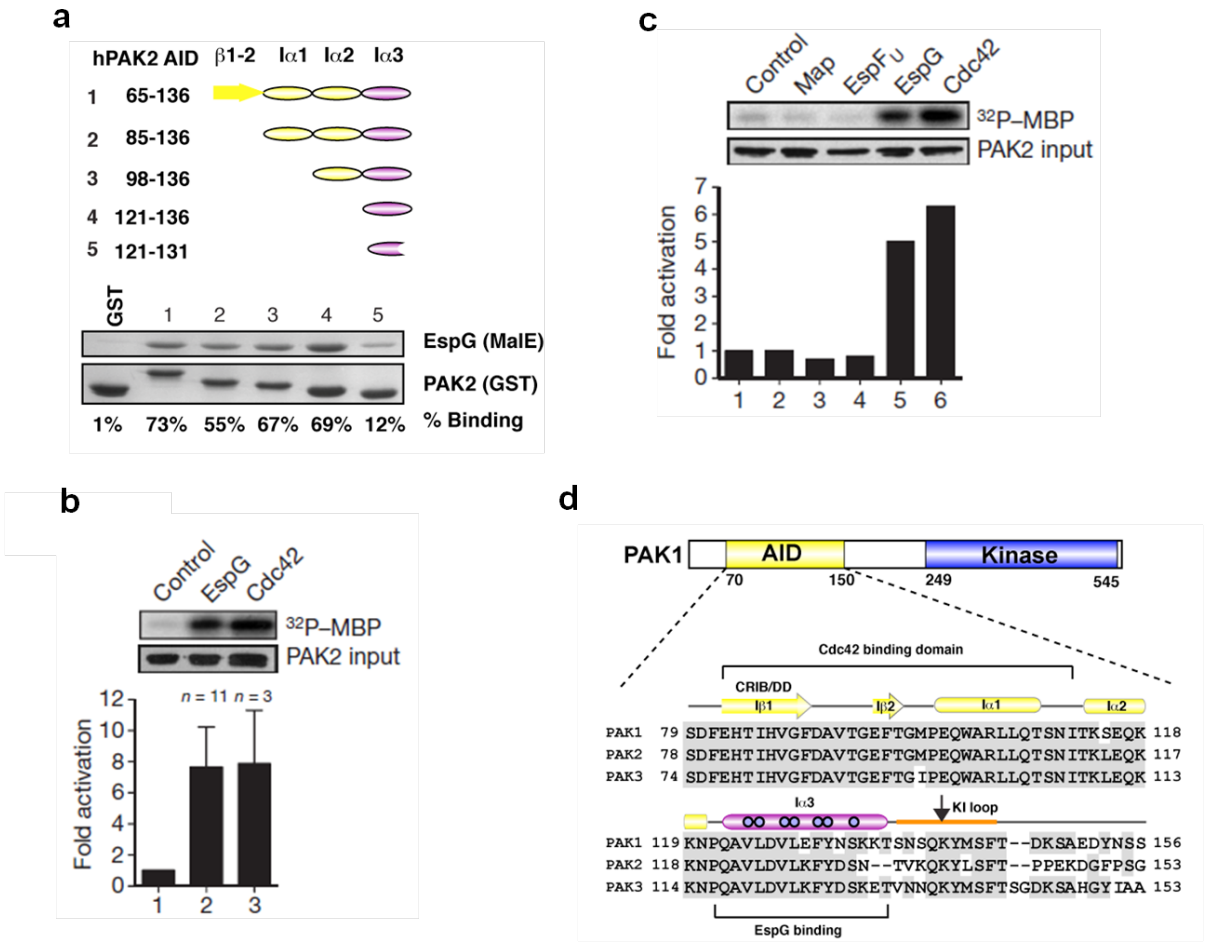

Figure 16. EspG activates PAK kinase.

a, EspG specifically recognizes residues 121-136 that encompasses the Iα3-helix of PAK2. All of the yeast two-hybrid clones encompassed overlapping regions of the AID. Therefore the AID domain of PAK2 was truncated at defined secondary structural elements and tagged at the N-terminus with GST. GST-tagged PAK2 fragments were mixed with MalE-tagged EspG and purified on Glutathione-agarose and run down SDS-PAGE gel (Coomassie Brilliant Blue stain is used to visualize proteins). The percent EspG bound to each PAK2 fragment was calculated from the signal ratio of EspG to PAK as determined by densitometry.

b, c, PAK2 kinase assays comparing 2 mM EspG with equimolar GTPγS-loaded Cdc42 (b) and the indicated EHEC type III effectors (c).

d, Domain diagram of PAK1 and sequence alignment of the AID domain of PAK-family kinases. α-helices are shown as bars, β-strands as arrows. The Iα3 helix is shown in purple and the residues that interact with EspG are highlighted with slate circles. The Cdc42 biding region is indicated and does not overlap with the EspG binding site. The kinase inhibitory loop (KI) loop is shown in orange.

EspG induces PAK activity through a unique mechanism

Previous studies have subdivided the AID of PAK into both structural and functional elements that are partially overlapping and are critical for Cdc42-mediated kinase activation (Lei et al., 2000). Most pertinent to our study however is that EspG interacts with residues corresponding to the Iα3-helix, a secondary structural element of the autoinhibitory three-helix bundle (Iα1-3). Examination of the PAK1 homodimer reveals that Iα3 is deeply buried between the KD and AID interface where it serves three autoinhibitory functions: (*i*) it provides the primary folding interface between the substrate binding site in KD and the AID, and (*ii*) it directly positions the KI loop across the kinase catalytic cleft, and (*iii*) it support PAK homodimerization by maintaining AID three helix bundle structure (Fig. 17a). Thus, the identification of Iα3 as the primary site of bacterial intervention by EspG provides a structural rationale for PAK activation.

To explain the mechanism behind kinase activation, we first examined the details of the EspG and PAK2 interface. A total surface area of 684 $Å^2$ is buried in the EspG-PAK2 protein:protein complex. The EspG α12-helix cradles a single helical turn at the N-terminus of the PAK2 peptide and the remainder of the peptide adopts an extended strand conformation and lies orthogonal to the strands of the six-stranded β-sheet (Fig. 17a, b). While van der Waals contacts predominate in the complex, several hydrogen bonds contribute to the signaling specificity of EspG (particularly surrounding Asn323) (Fig. 17c). In support of these structural observations, mutagenesis of Val297 and Leu300 in the α12-helix as well as key interface side chains Arg170 and Asn212, abolished PAK2 kinase activation by EspG (Fig. 17c). Altogether, our findings suggest that EspG does not overlap with the Cdc42 binding site of PAK GBD, but

instead recognizes and unwinds the Iα3-helix, which is directly connected to the AI loop (Fig. 17a).

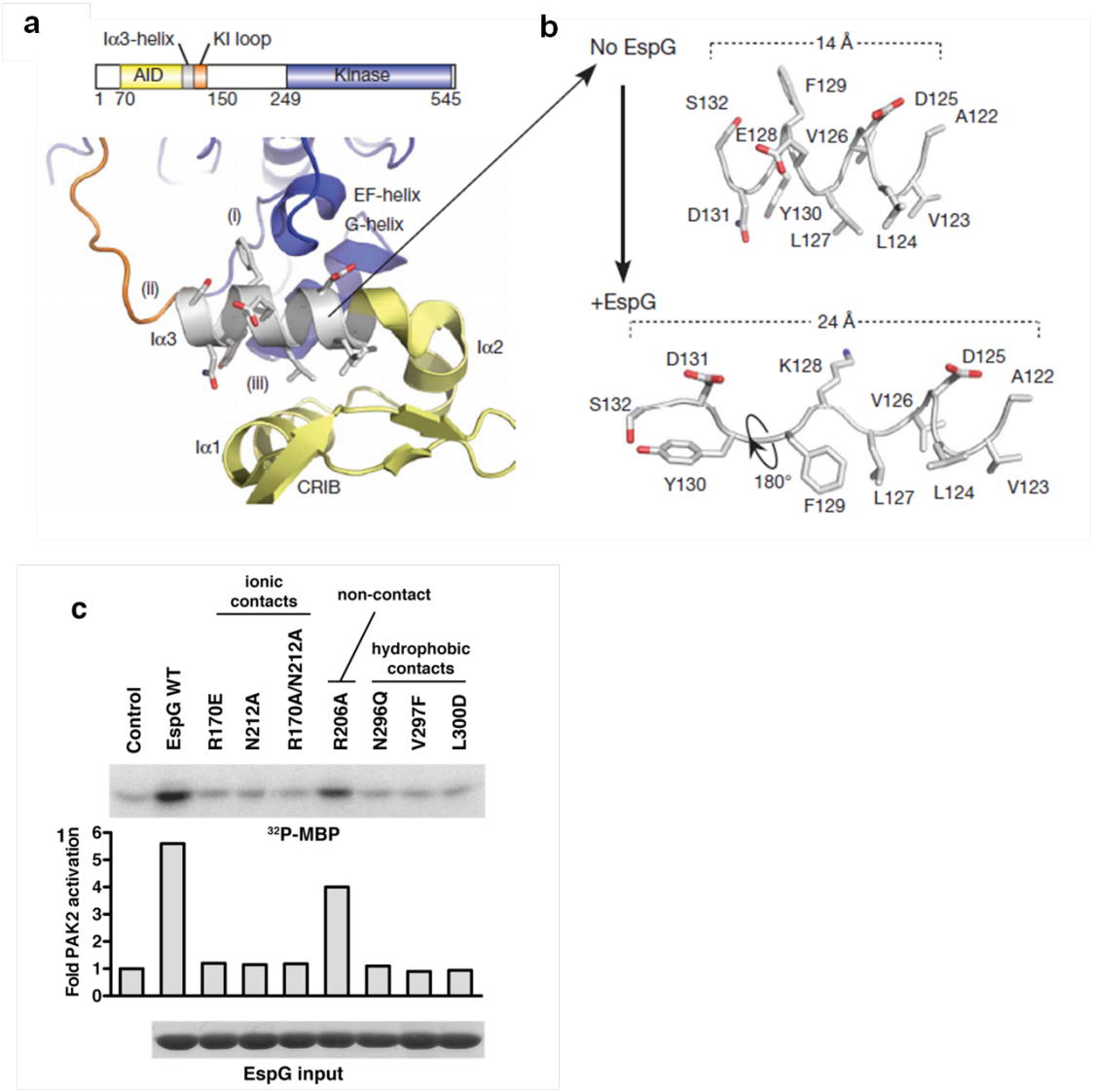

Figure 17. EspG activates PAK by unwinding the autoinhibitory Iα3 helix.
a, Close-up view of autoinhibited PAK1 homodimer (Protein Data Bank ID, 1F3M) focused on chain B (kinase domain, blue) and chain D (autoinhibitory domain, yellow). The Ia3-helix inhibitory functions are labeled (i)–(iii) corresponding with those outlined in the results section.
b, The Ia3-helix extracted from the PAK1 structure (numbering corresponds to PAK2 for ease of comparison) is shown at the upper right. The corresponding PAK2 Ia3-helix extracted from the EspG structure (lower right) is oriented by the amino-terminal helical residues 123–127.
c, PAK2 kinase assays showing the effect of EspG mutations on the ability of EspG to stimulate PAK kinase activity.

Susceptibility of PAK activation by EspG to a specific kinase inhibitor

IPA-3 is an allosteric non-ATP competitive small molecule inhibitor specific for PAK family kinases (Deacon et al., 2008; Viaud & Peterson, 2009). It is believed to inhibit PAK activation by binding to PAK AID and preventing its interaction with and unfolding by Cdc42. Interestingly, IPA-3 appears to bind covalently to AID and kinase inhibition is reversible under reducing conditions. However, preactivated (unfolded) PAK is resistant to IPA-3, suggesting that conformational orientation of AID is important either for interaction of PAK with IPA-3, or for its mechanism of inhibition. Because EspG binds to a site on AID distinct from that used by Cdc42, we hypothesized that activation of PAK2 by EspG would be insensitive to IPA-3 treatment.

We found that despite recognizing different sites within AID, both Cdc42 and EspG mediated kinase activation were subject to inhibition by IPA-3 (Fig. 18a). Significantly, IPA-3 inhibited both auto- and substrate phosphorylation of PAK when activated by EspG. This observation suggested that IPA-3 prevented unfolding of autoinhibited PAK dimer in a manner independent of Cdc42 and EspG binding site activation. We then tested if IPA-3 could prevent binding of EspG to PAK. Unexpectedly, neither EspG nor Cdc42 binding to AID was affected by IPA-3 addition, although PAK inhibition was still observed (Fig. 18b).

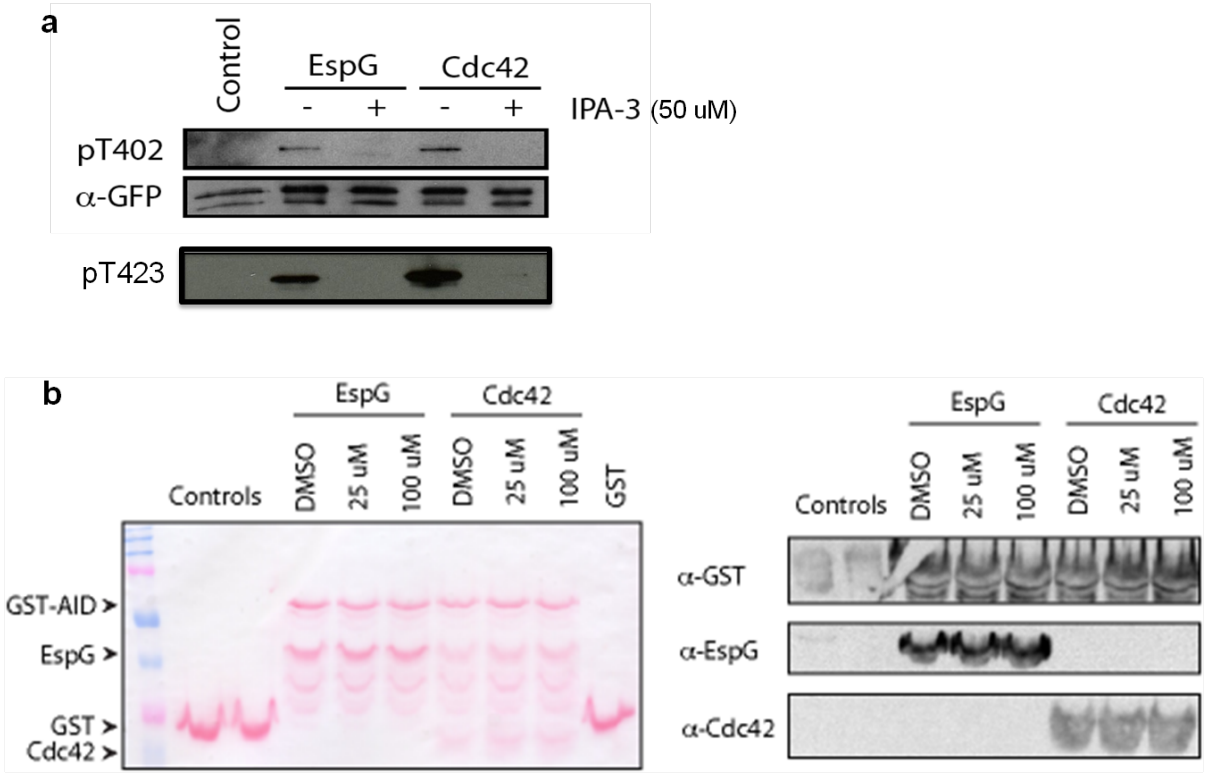

Figure 18. Effects of IPA-3 on EspG activity toward PAK kinase.
a, IPA-3 inhibits PAK activation by EspG. T402 and T423 are autophosphorylated when PAK is active.
b, Pulldown experiment showing that IPA-3 does not interfere with EspG?Cdc42 binding to PAK AID. Left, Ponceau stain for total proteins. Right, West blot with specific antibodies to confirm binding of EspG/Cdc42.

These observations imply that IPA-3 interferes with kinase activation step common to both EspG and Cdc42 dependent mechanisms, instead of preventing binding of the activator to AID. Indeed, we found IPA-3 capable of inhibiting KD domain kinase activity with dynamics comparable to the rates of Cdc42 and EspG inhibition (Fig. 19). Therefore, it appears that IPA-3 targets an inherent step underlying PAK activity that does not necessarily involve AID unfolding and separation from KD. This is consistent with EspG induced activation of PAK being sensitive to IPA-3 to the same extent as Cdc42 despite different biding sites and, consequently, distinct mechanisms.

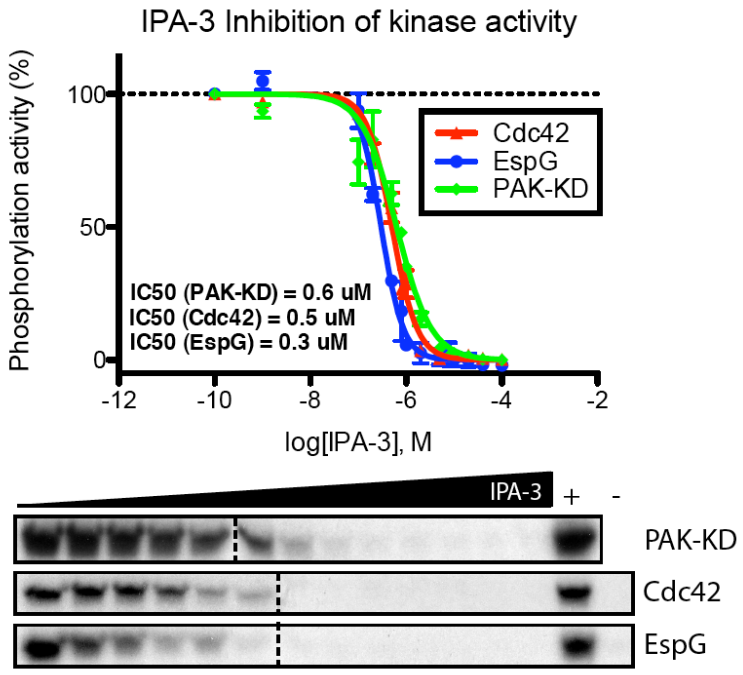

Figure 19. IC-50 assay testing the sensitivity of active PAK to inhibition by IPA-3.
Full-length PAK was preincubated with IPA-3 at different concentrations and then activated by either Cdc42 or EspG. For comparison, KD alone was used.

Novel conformation-dependent mechanism of PAK activation

The most striking feature of the EspG-PAK2 structure is that the Iα3-helix is unfolded over the surface of EspG compared to the corresponding Iα3-helix observed in autoinhibited PAK1 (Fig. 20a) (Lei et al., 2000). In this way, our structure may thus capture a transition-state in the kinase activation mechanism. We now predict that $Arg170^{EspG}$ and $Asn212^{EspG}$ initially recognizes the Iα3-helix since these residues interact with the only surface accessible Iα3 residues ($Tyr130^{PAK2}$ and $Asp131^{PAK2}$) in the autoinhibited PAK conformation. Upon kinase interaction, EspG reorganizes all of the Iα3 side chains that normally contact the substrate-binding site in KD and maintain the AID three-helix structure (Fig. 20b). We specifically recognize the 180° translation of $Phe129^{PAK2}$ relative to $Val123^{PAK2}$ in the amino terminal helix as a key molecular event that activates the kinase (see Fig. 17b). Indeed, Phe129 makes extensive hydrophobic contacts with the large lobe of the kinase and Val123 mediates structural interactions within the AID three-helix bundle.

To experimentally confirm that PAK activity can be controlled by local changes in the environment around Iα3, we modified the hydrophobic residues $Val123^{PAK2}$ and $Phe129^{Pak2}$ to charged residues with the hypothesis that these mutations would disrupt the autoinhibitory interface. Both PAK2 Val123→Asp and Phe129→Asp resulted in a constitutively active kinase with over 60-fold enhancement of substrate phosphorylation (Fig. 20c). Based on these structural and biochemical studies, EspG activates the kinase by sterically interfering with the KD/AID interface, extracting of the KI loop from the catalytic cleft, and destabilizing the AID three helix bundle (Fig. 20d). These actions are directed by EspG unfolding the Iα3 helix.

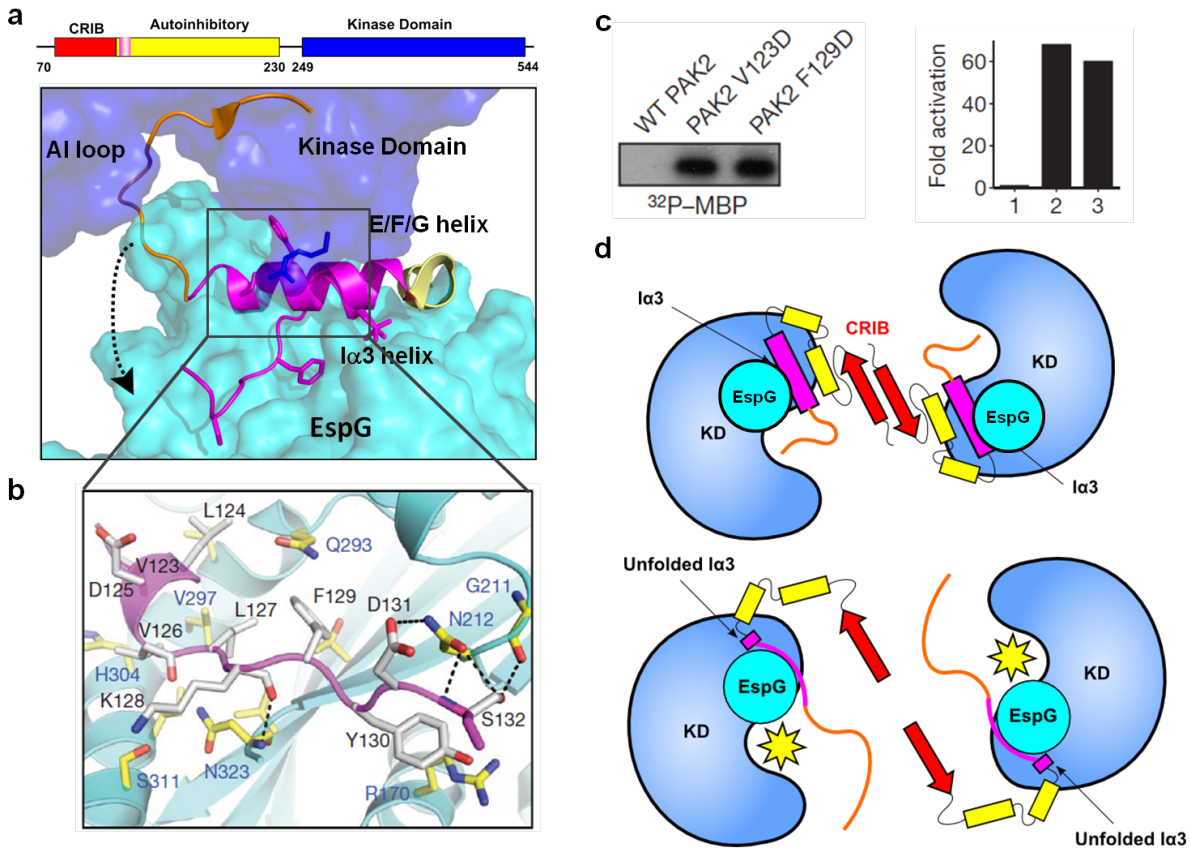

Figure 20. Novel mechanism of PAK activation exploited by EspG.
a, Structural model of PAK, highlighting Ia3 helix in an autoinhibited conformation and when bound to EspG.
b, Detailed interactions between EspGandPAK2Ia3. Key binding residues from EspG(blue labels) and PAK2 (black labels) are shown
c, PAK2 kinase assays comparing autoinhibited wild-type (WT) PAK2 with PAK2 mutants Val 123 Asp and Phe 129 Asp.
d, Cartoon diagram illustrating the mechanism of dimer dissociation and PAK activation by EspG.

Interestingly, the EspG activation scheme described here is reminiscent to that previously proposed for Cdc42 (Lei et al., 2000). However, the bacterial and eukaryotic agonists recognize distinct, non-overlapping binding sites within the AID structure. We then directly compared this mechanism to an endogenous activation by Cdc42. We have created an *in vitro* autoinhibited kinase complex by titrating AID into KD solution until no kinase activity was detected. Under these conditions, we then assessed if addition of either purified EspG or Cdc42 would restore kinase activity. Surprisingly, while kinase activity was indeed observed when inhibited complex was incubated with Cdc42, PAK-KD remained inactive in presence of EspG (Fig. 21). To exclude the possibility of unbound AID sequestering EspG molecules, we used 10- and 50-fold molar excess of EspG, but still could not detect an increase in kinase activity (data not shown). The mechanism of PAK activation by EspG thus appears dependent on direct nexus between AID and KD, rather than their interaction. Therefore, while Cdc42 activates PAK by relieving *in-trans* auto inhibition, EspG may induce an in-trans conformational change as an alternative strategy to achieve full kinase activity, but this remains to be investigated further.

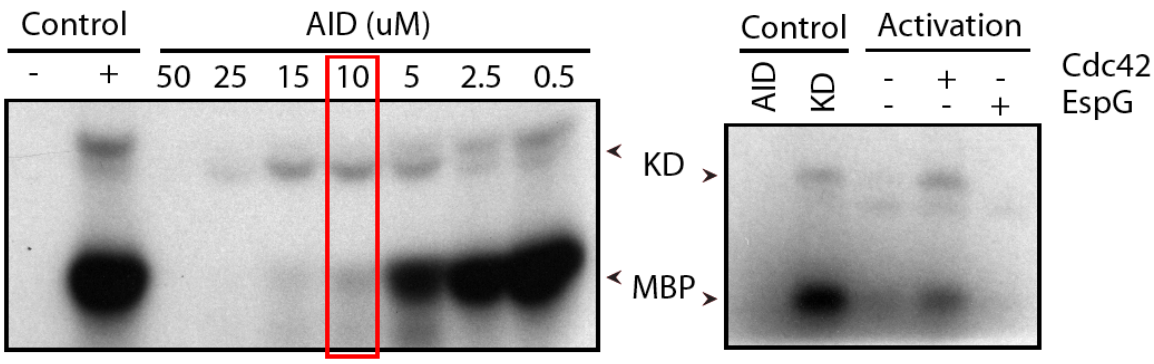

Figure 21. Conformational dependence of PAK activation by EspG.
Inhibited PAK complex was induced by incubating purified KD with molar excess of AID. Ten-fold excess results in a robust inhibition of KD activity, left panel. Inhibited complex was activated by either EspG or Cdc42 under conditions of 10-fold excess of AID. Cdc42 shows significant increase of KD activity, whereas EspG fails to remove inhibition; right panel.

DISCUSSION

Potency in the hijacking of cellular machinery is one of the hallmarks of bacterial virulence factors. The complexity of eukaryotic signaling networks includes spatial and temporal regulation of activating molecules, co-factors, and substrate availability. While multiple checkpoints ensure precise and accurate response, they put pressure on bacteria to overcome endogenous inhibitory mechanisms. Post-translational modification of host regulatory molecules by secreted bacterial effectors usually results in a constitutively active or inhibited enzyme, producing an all-or-nothing effect (Aktories, Schmidt, & Just, 2000; Visvikis, Maddugoda, & Lemichez, 2010).

By itself, this would make it extremely difficult for a pathogen to fine tune an entire network of signaling events. On the other hand, however, this makes a good platform for bacterial effectors that can then target specific downstream proteins of the Rho GTPase pathways for activation. The precision of targeting is particularly striking, considering that both WASP and PAK can be activated by Cdc42/Rac through conserved binding to CRIB, whereas EspFu and EspG exclusively activate their respective targets. By reducing "background" host signaling, the effect of virulence factors is thus amplified, allowing pathogens to be remarkably efficient despite limited repertoire of secreted effectors. This supports the concept that multiple bacterial proteins function in concert, with some affecting the global regulatory hubs while others initiating specific pathways, and suggests that more secreted effectors are likely to be discovered that exploit conserved host mechanisms of activation through novel regulatory sites.

Studying the molecular mechanisms of bacterial effectors that activate downstream targets is particularly interesting for our understanding of multi-level regulation of GTPase

signaling. Multiple factors can be involved in a signaling pathway within a cell, making it extremely difficult to observe and study under *in vitro* conditions. Bacterial proteins have evolved the ability to maximize the signaling potential due to limited availability, and bring into focus new ways in which signaling may potentially be controlled *in vivo*. For example, EspFu contains multiple domains that mimic the amphipathic helix of VCA in tandem, and was found to display much higher actin-nucleation ability than endogenous activator, Cdc42 (Sallee et al., 2008). This has lead to the discovery that oligomerized WASP has a higher affinity for Arp2/3, introducing dimerization factors into the signaling equation of WASP activation (Padrick et al., 2008; Sallee et al., 2008). Similarly, understanding of how scaffolding properties of EspG come into play during its activation of PAKs may provide insight into additional levels of kinase regulation. Bacterial virulence factors can function as distinct, but equivalent activators of GTPase targets, in as much as they utilize similar global mechanism of relieving inhibition, but display a stronger activity and precise specificity for their substrate through novel regulatory sites.

EXPERIMENTAL PROCEDURES

Plasmids

For bacterial expression, EspG (39-398) was PCR subcloned into pProEX-HTb (6xHis tag) (Novagen) vector. Human PAK1 construct was obtained from Dr. Gary Bockoch (TSRI, La Jolla, Ca), and rabbit PAK2 and PAK3 were obtained from Dr. Melanie Cobb (UTSW). PCR cloning was used to generate variable length constructs of PAK isoforms in pGEX-4T1 vector. All constructs were verified by DNA sequencing.

Protein Production

Recombinant proteins were produced in BL-21/DE3 *E. coli* strain following standard methods. Bacterial pellets were lysed in either His buffer (100mM HEPES, pH 7.5, 300mM NaCl) or GST buffer (TBS; 50mM Tris pH 7.5, 150mM NaCl, 2mM DTT) supplemented with protease cocktail (Roche). Proteins were purified with Nickel agarose (Qiagen) or glutathione sepharose (Amersham Biosciences) following manufacturer's instructions. Proteins were buffer exchanged into TBS via Concentration Centrifugal Columns (Millipore), glycerol added to 15%, and then stored at -80°C.

In vitro GST-pulldown

Basic protein interactions were examined through GST-pulldown assays. 10 μg of recombinant GST proteins immobilized to glutathione sepharose were incubated with 20 μg of 6xHis proteins for 1 hour at 4ºC. Proteins were separated by SDS-PAGE and stained with Coomassie Blue or specific antibodies where applicable. To determine if IPA-3 interfered with EspG or Cdc42 binding to PAK AID, GST-AID was incubated with indicated amounts of IPA-3 for 30 minutes at RT prior to the addition of EspG/Cdc42. IPA-3 was prepared fresh and diluted in DMSO. In all reactions, final concentration of DMSO was 1%.

Kinase Assays

To obtain full-length Pak2 kinase, 10-cm dishes with 293A cells were transfected with 5 μg rabbit PAK2 DNA in pEGFP-C2 vector and expressed for 48 hours post transfection. Cells were lysed in lysis buffer (20mM Tris, pH 7.5, 150 mM NaCl, 5mM EDTA, 0.5% Triton X-100)

and whole cell lysates combined. PAK2 kinase was purified by immunoprecipitation with 1:1000 polyclonal α-GFP antibody (Clontech) and 25 µl protein A/G slurry for 1 hour at 4°C. Beads were washed twice with lysis buffer and twice with kinase buffer (40mM HEPES, pH 7.5, 10mM $MgCl_2$). 5 µg of Myelin Basic Protein (MBP) and appropriate amount of protein of interest were added to the beads for a 30 µl total volume. Reaction was incubated on ice for 30 min to allow binding. The kinase activity was initiated by an addition of 10 mM ATP and 5 uCi ATPγP^{32}. After 5 minutes at RT, the reaction was stopped with 30 µl 2x SDS buffer. Contents were separated on SDS-PAGE, transferred to nitrocellulose membrane, and either analyzed by Western blot (1:5000 monoclonal anti-GFP) or exposed by autoradiography. Bands were cut out and radioactive signal measured on a scintillation counter.

IPA-3 inhibition sensitivity assay

GFP-PAK2 was purified from HEL293 cell lysates and was preincubated with MBP and IPA-3 or DMSO in Kinase buffer for 20 min at 4°C. Cdc42-GTPγS or EspG (2uM) were then added, and the reaction was pre-equilibrated 10 min at 30°C. Reactions were started by the addition of ATP with [^{32}P] ATP and were incubated 15 min. Finally, reactions were analyzed by SDS-PAGE and autoradiography, and quantified using scintillation counter.

In-vitro autoinhibited complex formation:

Purified PAK2 KD and AID domains were mixed in a kinase buffer with molar ratios or amounts indicated. Proteins were allowed to mix at 4C for 1 hr. Kinase activity was determined by measuring autoradiography from MBP substrate and autophosphorylation of PAK2 KD.

Cdc42 and EspG were added in at least 1.5 molar excess relative to AID amount, in order to ensure sufficient binding.

CHAPTER FOUR

REGULATION OF ARF1 SIGNALING BY EspG

INTRODUCTION

ARF GTPases were initially isolated over 25 years ago as co-factors required for the ADP-ribosylation activity of *Vibrio cholera* toxin (CTA) (Kahn & Gilman, 1984). More recently, ARF1 was shown to be directly activated by the Legionella type IV effector, RalF (Nagai, Kagan, Zhu, Kahn, & Roy, 2002), further suggesting that bacteria to impose their control over ARF GTPase signaling systems. In the eukaryotic cell, ARF-family members (ARF1-6) function within a broad range of organelle systems where they organize vesicle transport machinery, phospholipids, and signaling molecules at membrane microdomains (D'Souza-Schorey & Chavrier, 2006). To perform these essential functions, ARFs cycle between a GDP-bound inactive and GTP-bound active state. In addition, these GTPases are lipid modified at their amino terminus, providing a mechanism to localize GTPase signaling to specific membrane sites. Thus, the regulation of ARF GTPases by bacterial pathogens may provide a potent mechanism to disrupt surface trafficking in host cells.

We have identified ARF GTPases as relevant host targets of a type III EHEC effector EspG. Microinjection of EspG induces rapid disassembly of Golgi apparatus and changes in the morphology of endosomes, consistent with affecting the functions of ARF1 and ARF6 GTPases, respectively. Because EspG localizes to Golgi remnants, it is likely that ARF1 is the primary target of EspG. However, it is not known how binding of EspG to ARF1 regulates its activity and is connected to the mechanism of Golgi disruption. Moreover, because EspG binds to GTP-

ARF1, it is unclear if EspG competes with endogenous downstream targets of ARF1, or whether it acts through an allosteric mechanism.

Here, we show that EspG prevents vesicle transport by directly inhibiting ARF guanine-nucleotide turnover on host membranes. By binding over the nucleotide pocket of ARF1, EspG prevents GAP-mediated hydrolysis of GTP, essentially locking ARF1 in an active conformation. Importantly, EspG interacts with ARF1 in a unique manner that does not compete for binding with its effectors. Our findings thus implicate EspG in allosteric regulation of ARF1 signaling. Specifically, EspG establishes an active ARF1 signaling complex on Golgi membranes and prevents its nucleotide cycling.

RESULTS

EspG binds to active GTP-bound conformation of ARF

The EspG/ARF6 complex revealed ARF GTPase to be in a GTP bound state. Further structural analyses revealed that switch I is inaccessible to EspG when ARF6 adopts the GDP-bound conformation (Fig. 22a), suggesting that EspG can only recognize active ARF1. Indeed, EspG selectively bound the GTP-loaded forms of ARF1 and ARF6, but did not interact with GDP-ARFs (Fig. 22b). Moreover, EspG interacted with ARF6-GTP in its full-length myristoylated form that was isolated from membrane fractions (Fig. 22c). Thus, EspG preferentially targets the active ARF·GTP signaling molecule.

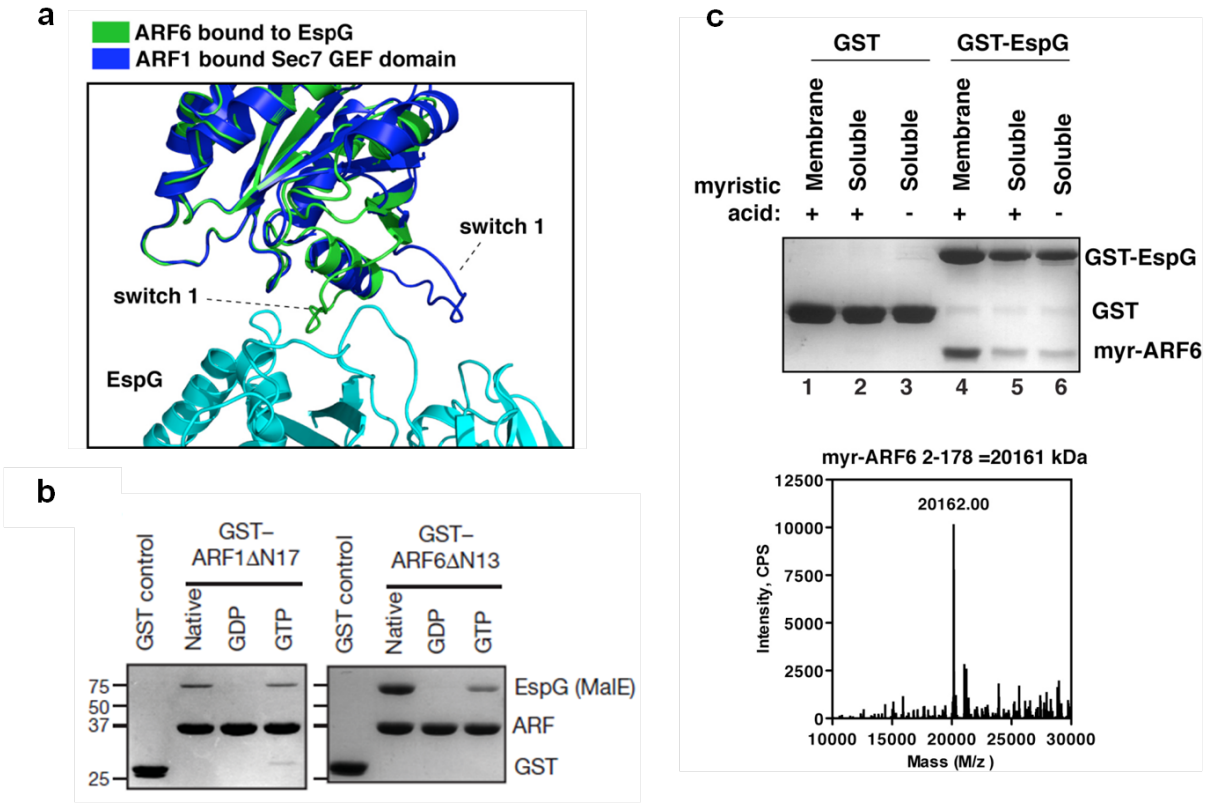

Figure 22. EspG specifically interacts with active GTP-bound ARF GTPase.
a, Structural overlay of ARF6-GTP (bound to EspG) to ARF1 bound to Sec7 GEF domain (PDB ID: 1R8S). Importantly the switch I loop is displaced in the GEF complex compared to its position in the EspG complex indicating that EspG does not induce an ARF conformation similar to human GEFs. These structures further support the hypothesis that EspG does not function as a GEF.
b, EspG selectively binds the GTP-loaded ARF1 and ARF6 (GST tagged) in glutathione pull-down assays. The native lane represents ARF GTPases purified from bacteria without removing or loading specific nucleotides.
c, GST-pulldown experiment showing binding of GST control (lanes 1-3) or GST-tagged EspG (lanes 4-6) to myristoylated ARF6 isolated from either membrane (lanes 1 and 4) or soluble fractions. EspG preferentially associated with membrane bound ARF6. To confirm its myristoylation state, the lower band in lane 4 was excised and subject to mass spectrometry. Myr-ARF6 predicted MW was 20161 and the isolated ARF6 was within 1 Da of this value due to the single charge on this species, thus confirming its myristoylated state.

Interestingly, neither structural changes nor post-translational modifications have been found on ARF6. However, severe Golgi fragmentation and changes in the endosome staining observed during microinjection of cells with EspG suggest that EspG mechanism somehow involves the regulation of ARF1 activity and is not simply its effector. COPI coatomer, vesicle complex adaptors, and signaling enzymes primarily associate with switch 2 and the β2/3 interswitch of ARF·GTP (Hanzal-Bayer, Renault, Roversi, Wittinghofer, & Hillig, 2002; Isabet et al., 2009; O'Neal, Jobling, Holmes, & Hol, 2005; Shiba et al., 2003; Zhao et al., 1997) (Fig. 23). Given the frequent occurrence of this binding mode, we were surprised to find that EspG is rotated away from these common binding elements and is positioned directly over the guanine-nucleotide binding pocket. Although several EspG residues approach GTP of ARF GTPase in an EspG/ARF6 complex to within ~6 Å, we found no evidence to support its function as a GEF or GAP (unpublished observations).

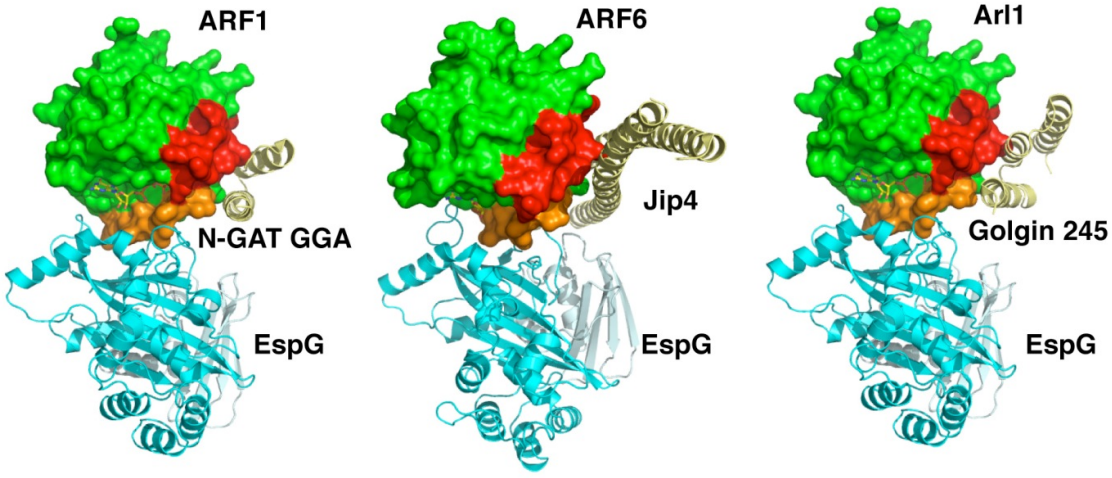

Figure 23. EspG binds to a unique site on ARF GTPases.
Structural overlay of EspG (cyan) onto ARF1 (PDB: 1J2J), ARF6 (PDB: 2W83), or ARL1 GTPases (PDB:1UPT) (space filling in green) in complex with their effectors GGA, Jip4, and Golgin-245, respectively (yellow). Switch I and II loops of GTPases are colored orange and red respectively.

EspG prevents GAP-mediated inactivation of ARF

GTP hydrolysis and exchange on ARF is required for proper membrane transport functions. Because EspG neither modified ARF GTPase nor appeared to exhibit GEF/GAP properties, we hypothesized that EspG allosterically regulated its activity. Specifically, we noticed that EspG forms a lid over the guanine-nucleotide biding pocket that may restrict regulatory access to GTP. Superimposing the transition-state model of ARF6 in complex with its GAP (ASAP3) onto the EspG-ARF6 structure shows that EspG would sterically hinders catalytic access (the Arginine finger) to the γ-phosphate in GTP (Fig. 24a). Indeed, EspG completely abolished the GAP stimulated GTPase hydrolysis on lipid anchored ARF1 (Fig. 24b, diamonds) compared to the control ARF-GAP reaction (Fig. 24b, blue triangles). The inhibition of GAP by EspG relied on a direct interaction between EspG and ARF since the binding deficient mutant EspG E392R had no affect on GAP stimulated hydrolysis (Fig. 24b, open circles). Because GTP hydrolysis is essential for ARF signaling, these activities of EspG would have profound effects on vesicle trafficking and organelle architecture in host cells.

Our observations thus show that EspG inhibits Golgi trafficking by blocking its guanine nucleotide cycle (D'Souza-Schorey & Chavrier, 2006; Zhao et al., 1997). Several lines of evidence support this idea. First, EspG disrupted the Golgi with rapid inhibitory kinetics (Fig. 14d, cyan circles) and a phenotype nearly identical to the fungal toxin Brefeldin A (BFA) (see Chapter 5), a potent ARF1 GTPase inhibitor that also blocks the guanine nucleotide cycle (Chardin & McCormick, 1999). Second, microinjection of ARF protein lacking N-terminal helix (ARFΔN13) to sequester EspG caused a significant delay in Golgi disruption induced by EspG (Fig. 14d, open circles). Third, EspG E392R, a mutant that does not interact with ARFs, had no

effect on Golgi morphology or trafficking function (Fig. 15). Finally, EspG co-localized with the ARF1 effector β-Cop (Zhao et al., 1997) on Golgi membranes, consistent with ARF1 being in an active state when bound to EspG (Fig. 24c). These combined structure and cellular studies provide a mechanism for bacterial regulation of membrane trafficking: EspG prevents vesicle transport by directly inhibiting ARF guanine-nucleotide turnover on host membranes.

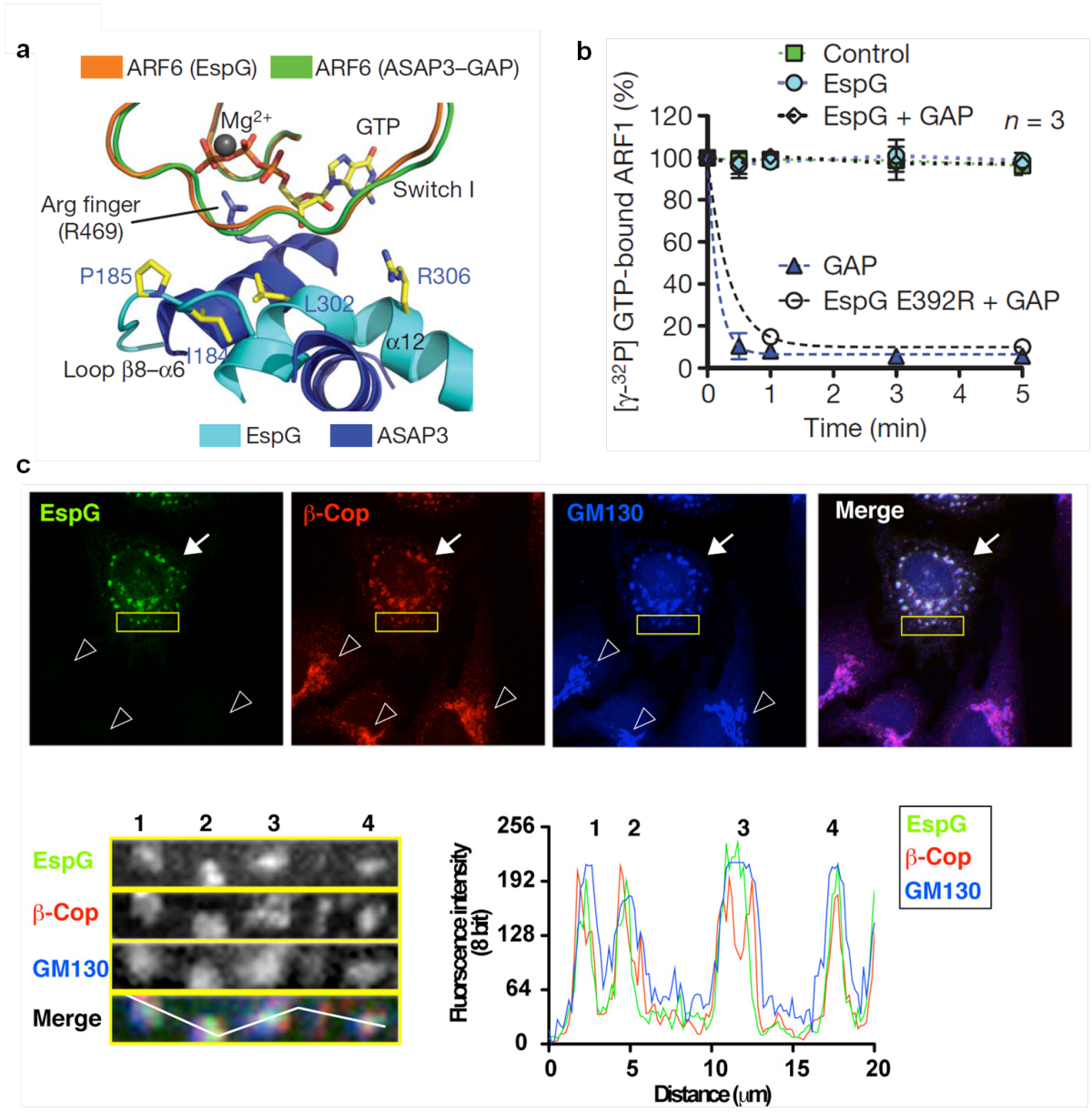

Figure 24. EspG induces active ARF1 signaling complex on membranes.
a, Structural overlay of EspG–ARF6GTP and ASAP3(GAP)–ARF6GDP?AlFX (Protein Data Bank ID, 3LVQ) showing how EspG sterically hinders ARF binding to ASAP3–GAP. The catalytic Arg finger of ASAP3 is labeled.
b, GTP hydrolysis assay showing that EspG inhibits GAP-assisted GTP hydrolysis on ARF1. The rate of c32P[GTP] hydrolysis was measured as the percentage of c32P[GTP] remaining on ARF1 over time. Intrinsic ARF1
GTPase activity (control, green), GAP-stimulated activity (GAP, blue triangle), and EspG inhibition of GAP activity (EspG1GAP, open diamond) or mutant EspG Glu 392 Arg (open circle) are shown.

c, HEK293A cells were transfected EGFP-EspG and stained for EEA-1, a protein constituent of the recycling endosomes. EspG transfected cells in the population are outlined. The merged image is shown and expanded to show the clear endosome disruption phenotype induced by EspG compared to normal endosome morphology observed in untransfected cells.

EspG does not interfere with binding of downstream ARF substrates

To further expand our understanding of how EspG binding may affect ARF1 signaling, we modeled EspG into a vesicle budding reaction (Fig. 25, top) by superimposing EspG-ARF6 onto ARF1 and its complex with the N-GAT domain of GGA (Golgi localizing, γ-adaptin ear homology domain, ARF interacting protein) (Fig. 25, left). Importantly, GGA is an adaptor molecule that links ARF GTPases to both clathrin and membrane receptors at the Golgi (Collins, Watson, & Owen, 2003; Puertollano, Randazzo, Presley, Hartnell, & Bonifacino, 2001; Shiba et al., 2003). It is clear from our structural model that ARF1-GTP can accommodate both the N-GAT domain and bacterial EspG through non-overlapping binding surfaces. Indeed, EspG and GGA simultaneously bound to ARF1-GTP as determined by liposome pulldown assays using purified recombinant proteins (Fig. 25, inset).

Further structural analysis revealed that the binding interface of EspG is quite different from any reported structures of ARF-family GTPases in complex with their natural effector substrates (Isabet et al., 2009) (Hanzal-Bayer et al., 2002)] or with the bacterial toxin CTA (O'Neal et al., 2005). Consequently, EspG can be modeled into these complexes with no steric hindrances (See Fig. 23). All together, our studies are consistent with a GTPase inhibitory model in which EspG integrates into the vesicle transport reaction where it halts the guanine-nucleotide cycle of ARF as the budding machinery is being assembled on host membranes. Inhibition of vesicle coat formation and budding is consistent with observed fragmentation of Golgi and the arrest of protein secretion associated with EspG.

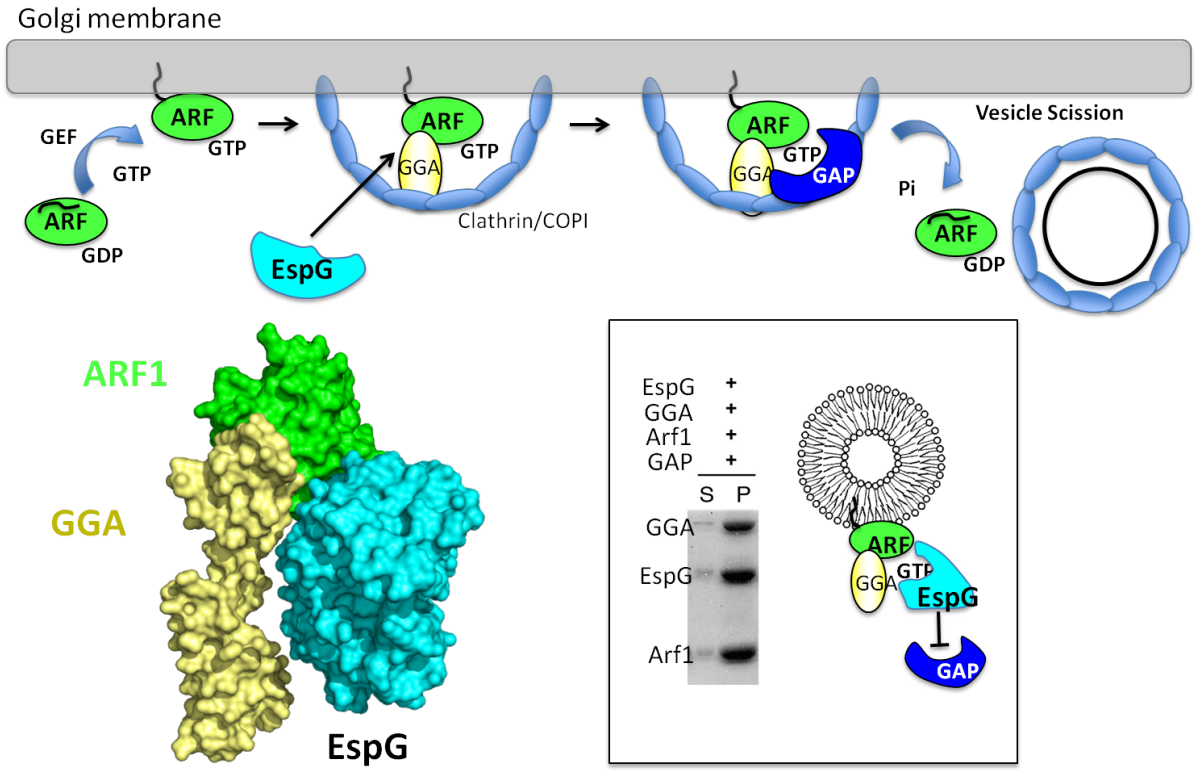

Figure 25. EspG blocks cycling, but not downstream substrate interaction of ARF1.
Coat recruitment and vesicle budding require nucleotide cycling of ARF GTPase, top. Structural modeling predicts that EspG does not interfere with ARF1 substrate binding, left panel. Liposome pulldown experiment highlights the ability of ARF1 to recruit its downstream targets to membrane even when bound by EspG, inset.

DISCUSSION

Our EspG-ARF6 complex reveals a sophisticated signaling mechanism employed by a bacterial type III effector. Once integrated into the vesicle-budding machinery, EspG would restrict regulatory access to GTP by capping the guanine nucleotide-binding pocket. We also envision that the hydrophobic and acidic loops of EspG would physically lock ARF in its GTP-bound state. Because hydrolysis of nucleotides are strictly required for cargo selection and vesicle budding induced by ARFs, our structure is consistent with an EspG inhibitory function. Consistent with this view, molecular modeling shows that EspG attacks ARF-family GTPases in a spatially and temporally coordinated manner in which each round of vesicle budding would produce an EspG-ARF-effector inhibitory complex.

It is intriguing to speculate that EspG functionally opposes the release of ARF GTPases from membrane domains. The strong, ARF-dependent localization of EspG to Golgi remnants is consistent with such an inhibitory function. It is also clear that by specifically targeting the transient pools of GTP-ARF found at cell membranes, EHEC ensures that the small amount of type III secreted EspG is not exhausted on unproductive binding to the large pools of cytosolic ARF-GDP. This notion was confirmed by the observation that low levels of EspG could disrupt Golgi architecture in the microinjection experiments. Finally, EspG may nucleate multiple signaling systems at the membrane by coupling ARF-GTP to the activation of PAK kinases. We do not currently know what functional output that such a signaling system would entail, but it would likely disrupt the cell polarity cues in the intestinal epithelium by hijacking two signal transduction systems critical for these processes.

EXPERIMENTAL PROCEDURES

Plasmids

The *espg* gene from EHEC O157:H7 was PCR cloned in-frame into pEGFP-C2 (Clontech) and pcDNA3.1-mCherry. For bacterial expression, 38 and 41 amino acid amino-terminal deletions (39-398 and 42-398) of EspG were PCR subcloned into pGEX-4T1 (GST-tag) (Amersham), pProEX-HTb (6xHis tag) (Novagen), and pET28b-MalE (6xHis tag, MalE-tag) vectors. EspG mutants were generated with QuickChange™ Site-Directed Mutagenesis (Stratagene) following manufacturer's instructions. Amino-terminal deletions of ARF GTPases (Arf1Δ17, Arf5Δ17, and Arf6Δ13) and Arl proteins (Arl1Δ17 and Arl2Δ16) were PCR subcloned into pGEX-4T1 and pProEX-HTb vectors.

Protein Production.

Recombinant proteins were produced in BL-21/DE3 *E. coli* strain following standard methods. Bacterial pellets were lysed in either His buffer (100mM HEPES, pH 7.5, 300mM NaCl) or GST buffer (TBS; 50mM Tris pH 7.5, 150mM NaCl, 2mM DTT) supplemented with protease cocktail (Roche). Proteins were purified with Nickel agarose (Qiagen) or glutathione sepharose (Amersham Biosciences) following manufacturer's instructions. Proteins were buffer exchanged into TBS via Concentration Centrifugal Columns (Millipore), glycerol added to 15%, and then stored at -80°C.

In vitro GST pull-downs

Protein interactions were examined through GST pull-down assays. Unless otherwise

stated, 15 μg of recombinant GST proteins immobilized to glutathione Sepharose were incubated with 20 μg of 6xHis- and/or MalE-tagged proteins for 1 h at 4 °C. Samples were washed three times in TBS supplemented with 0.5% Triton X-100. Proteins were eluted from beads with Laemelli sample buffer and were separated by SDS–polyacrylamide gel electrophoresis and stained with Coomassie blue. For nucleotide loading, ARF1Δ17 and ARF6Δ13 were incubated in nucleotide loading buffer (40 mM HEPES, 150 mM NaCl, 2 mM EDTA, 10% glycerol) with 10 μM of either GDP or GTP for 30 min at 37 °C, and then $MgCl_2$ was added to 10 mM and the reaction was transferred to ice after 15 min at room temperature (25 °C).

Cell microinjection, transfections and immunofluorescence microscopy

HeLa cells were microinjected with EspG proteins using a semi-automatic InjectMan NI2 micromanipulator (Eppendorf). A needle concentration of 1 uM was used unless specified otherwise. HeLa and HEK293A cells were transfected using calcium phosphate. At 16–18 h post-transfection, cells were fixed with 3.7% formaldehyde and stained with antibodies for immunofluorescence. In co-transfection experiments, equal amounts of DNA were used for each sample. All immunofluorescence images were acquired with a Zeiss LSM 5 Pascal confocal microscope. Golgi, endosomes and microtubules were detected using specific antibodies or translationally fused fluorescent signal.

ARF GTP hydrolysis assays

ARF1 was incubated in nucleotide exchange buffer with 250 nM γ^{32}P[GTP](MP Biomedical) for 30 min at 37 °C, after which 10 mM $MgCl_2$ was added to stabilize

ARF1(γ^{32}P[GTP]). ARF1(γ^{32}P[GTP]) was incubated with 10 μM Golgi mimetic liposomes 5 min before the addition of fivefold molar excess rat ARFGAP1 (ref. 30), EspG and EspG(E392R). In the case of hydrolytic protection assays, EspG or EspG(E392R) was added 5 min before the addition of rat ARFGAP1. Aliquots (5 μl) of the 50-μl reaction were removed at times indicated, added to 5 ml ice-cold binding buffer (TBS + 10 mM $MgCl_2$) and vacuum-filtered through nitrocellulose membranes. Membranes were washed three times with ice-cold binding buffer and subjected to scintillation counting. Data analysis was carried out in GRAPHPAD PRISM 5.0b.

CHAPTER FIVE

SCAFFOLDING PROPERTIES OF EspG DEFINE THE MOLECULAR MECHANISM OF BIDIRECTIONAL TRAFFICKING ARREST

INTRODUCTION

Cargo transport through the GSP follows a concerted route that includes the ER, ER-Golgi intermediate compartment (ERGIC), and the Golgi apparatus. The packaging and delivery of transport vesicles between these compartments depends on microtubules and golgins, which control trafficking infrastructure and structural organization, and the function of ARF- and Rab-family GTPases, which play essential roles in regulating coat protein recruitment and budding, as well as tethering and fusion with target membranes, respectively (Donaldson & Jackson, 2011; Hutagalung & Novick, 2011). Like other members of the Ras superfamily, ARFs and Rabs cycle between active GTP-bound and inactive GDP-bound conformations. Exchange of GDP for GTP is mediated by guanine-nucleotide exchange factors (GEFs), whereas GTPase activating proteins (GAPs) stimulate hydrolysis of GTP to GDP (Cherfils & Zeghouf, 2013). In their active state, specific interactions of ARF and Rab GTPases with their downstream substrates define the molecular sequence of events that coordinate specific membrane trafficking events. Because the rapid turnover of GTPase signaling networks is essential for receptor localization and cytokine secretion, microbial regulation of host GTPases and their downstream interactions may be a powerful mechanism of immune evasion.

My work has led to the discovery that the Enterohaemorrhagic *E.coli* (EHEC) type III bacterial effector protein EspG directly interacts with the GTP-active form of ARF1 and inhibits GAP-stimulated GTP hydrolysis (Selyunin et al., 2011). In addition, EspG was found to

stimulate p21-activated kinase (PAK) through a non-overlapping protein surface adjacent to the ARF1 binding site (Selyunin et al., 2011). In subsequent studies, Shao and colleagues showed that EspG functions as a Rab1-specific GAP through an endogenous TBC-like mechanism of action, despite having a unique structural fold (Dong et al., 2012). Interestingly, similar to ARF1/PAK binding, EspG can simultaneously interact with ARF1 and Rab1. Together, these findings revealed a strong mechanistic connection underlying simultaneous recognition of multiple host proteins by EspG and for the first time suggested that scaffolding properties of a bacterial effector protein may allow selective control over signaling pathways at the Golgi apparatus. However, the significance of GTPase coupling through scaffolding properties has never been directly tested and the molecular mechanism of membrane trafficking regulation by EspG remains elusive. Considering the critical role of the GSP in innate immune function, we sought to delineate the biochemical significance behind simultaneous targeting of ARF1 and Rab1 signaling by EspG.

Here, I describe a model whereby EspG arrests vesicular transport by stabilizing the ARF1-GTP tethering complex with simultaneous local inhibition of Rab1 signaling. By preventing GAP mediated cycling of ARF1-GTP, EspG promotes recruitment of ARF1-dependent tethering factors that restrict vesicle movement, whereas the Rab1-GAP activity of EspG further inhibits intracellular trafficking by preventing vesicle fusion. Importantly, I show that scaffolding properties that afford simultaneous activity of EspG toward ARF1 and Rab1 GTPases are required for full potency during arrest of host intracellular trafficking. Considering the wide variety of bacterial pathogens and their lifestyles, regulatory coupling of multiple host enzymes by individual secreted bacterial proteins could thus present a strategy for establishing a

specific niche within complex signaling networks, and be used as an effective tool to study coordinated activity of multiple host signaling pathways, such as immune function.

RESULTS

EspG disrupts Golgi through a unique GTPase regulatory mechanism

The framework for understanding regulation of the GSP by ARF and Rab GTPases has been established by studying cellular phenotypes resulting from their inactivation. In particular, our knowledge of ARF1 function in ER and Golgi trafficking has been aided by the discovery of Brefeldin A (BFA), a fungal toxin that inhibits vesicle budding and transport by stabilizing an ARF1-GDP/GEF complex and preventing its transition into an active state (Klausner et al., 1992; Mossessova, Corpina, & Goldberg, 2003). Although biological toxins that specifically inhibit Rab1 function have not been described, its roles have been studied using inhibition by GAPs and dominant negative constructs (Haas et al., 2007). Importantly, inactivation of ARF1 or Rab1 signaling induces severe trafficking defects due to an arrest of ER export of proteins, manifested by accumulation of Golgi enzymes in the ER (Haas et al., 2007; Lippincott-Schwartz, Yuan, Bonifacino, & Klausner, 1989). However, the gross phenotypic changes associated with inactivation of an entire GTPase pathway using these methods make it difficult to understand the details of numerous protein interactions that regulate Golgi function. In addition, because this approach targets individual pathways, it is not effective at elucidating the potential coordination of ARF1 and Rab1 signaling systems.

Detailed examination of a single bacterial effector molecule in the context microbial infection has so far proven difficult, since type III secretion systems can deliver multiple effector

proteins at any one time (Galan & Collmer, 1999). To overcome the problems associated with this complex system, we used microinjection of purified recombinant protein to introduce bacterial protein into cells, which allowed us to focus exclusively on the effects of EspG under physiologically relevant concentrations. When microinjected into cells, EspG induces fragmentation of the perinuclear Golgi ribbon and swelling of the ER-Golgi Intermediate Compartment (ERGIC), a complex system of tubulovesicular membrane clusters found near ER exit sites (Fig. 26a). Considering that EspG arrests ARF1 GTP-cycling (Selyunin et al., 2011) and displays Rab1-GAP activity (Dong et al., 2012), we set out to determine if EspG functions by blocking ER export analogously to BFA and overexpression of eukaryotic Rab1-GAPs, or whether there exist important mechanistic differences between EspG and these independent GTPase inhibitors.

To accurately address the effects of EspG on ER export, an assay was needed that could be used to experimentally control ER-to-Golgi traffic while minimizing off-target effects, such as those associated with classic temperature shift assays (Presley et al., 1997). We therefore developed a technique that tracks the movement of fluorescently labeled resident *trans*-Golgi enzyme b-1,4-galactosyltransferase (GalT) through the secretory network. The fragment responsible for ER-export and Golgi retention of this enzyme (residues 1-81) was translationally fused to the conditional aggregation domain (CAD) of a ligand-reversible crosslinking protein FKBP F36M (Rivera et al., 2000), producing a marker we termed Golgi-CAD (Fig. 27a). When transfected into cells, Golgi-CAD aggregates in the ER preventing its export (Fig. 27b, left). Addition of the small molecule AP21998 to the cell culture medium relieves aggregation and initiates normal trafficking of Golgi-CAD from ER to the Golgi apparatus (Fig. 27b, right).

To establish that the secretory pathway behaves normally under these conditions, Golgi-CAD was first allowed to accumulate in the ER, and then cells were treated with BFA for 30 minutes. AP21998 was added and Golgi-CAD localization was assessed after 2 hours. As expected, BFA potently inhibited ER export of Golgi CAD. To then determine if EspG functions similarly, cells expressing Golgi-CAD were microinjected with EspG protein 1 hour prior to AP21998 addition. Surprisingly, Golgi-CAD was able to successfully exit the ER in EspG injected cells, however its movement was arrested near vesicular clusters positive for p58, a marker associated with ERGIC (Fig. 27c). These data indicate that EspG does not directly mimic the inhibitory mechanisms of BFA, as shown here, or overexpression of Rab1-GAP as demonstrated previously (Haas et al., 2007). This notion was confirmed by additional studies on the medial Golgi enzyme N-acetylglucosaminyltransferase I (NAGT I) (Fig. 26b).

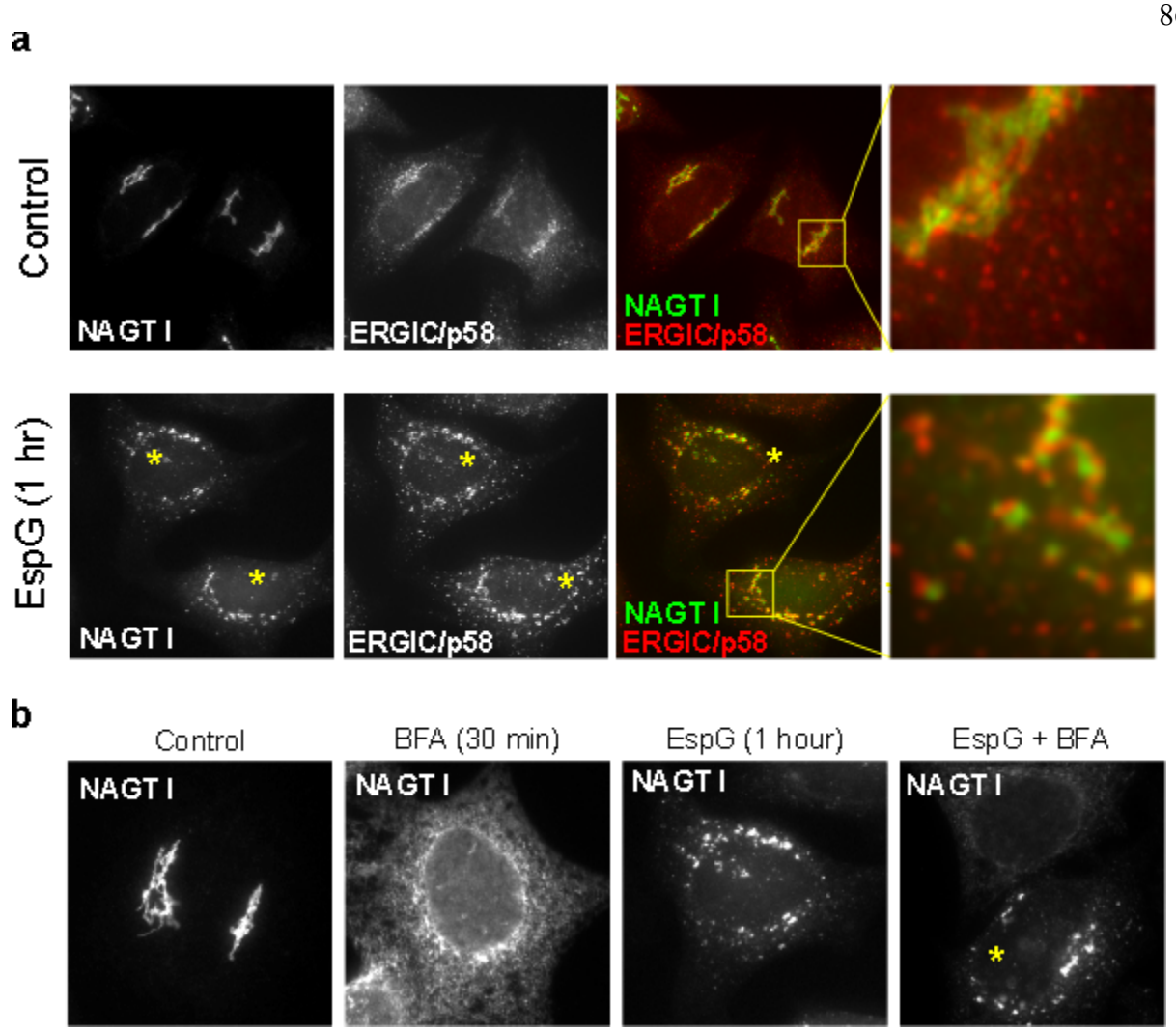

Figure 26. EspG fragments Golgi into perinuclear structures near p58 clusters.
a, EspG induces fragmentation of Golgi ribbon into clusters within close proximity to ERGIC associated membranes. Injected cells are marked with asterisks.
b, BFA treatment leads to rapid accumulation of Golgi enzymes in ER. Despite also targeting ARF1 cycling, EspG arrests Golgi enzymes near p58 clusters instead. Moreover, microinjection of EspG (asterisk) protects Golgi enzymes from redistribution into ER even after consecutive treatment with BFA.

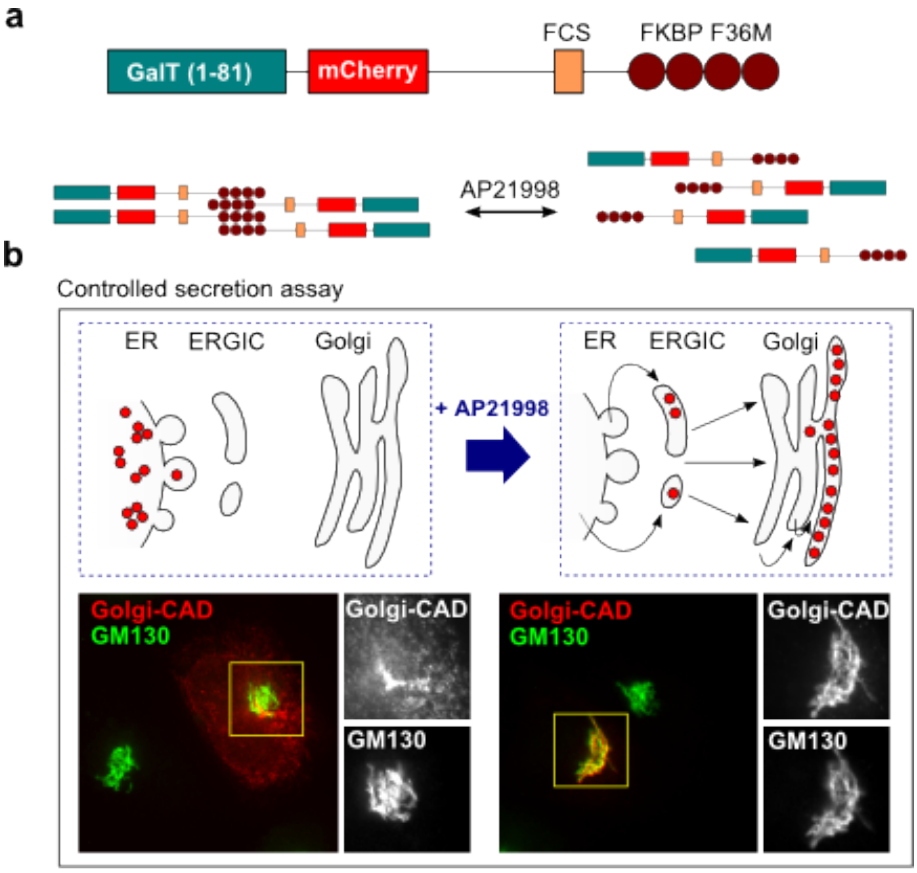
a
GalT (1-81)
mCherry
FCS
FKBP F36M
AP21998
b
Controlled secretion assay
ER
ERGIC
Golgi
+ AP21998
Golgi-CAD
GM130
c
BFA
+ AP21998
Fix
30 min
2 hrs
BFA (30 min)
Golgi-CAD
ERGIC/p58
EspG
1 hr
EspG

Figure 27. EspG does not interfere with protein export from ER.
a, Schematic representation of Golgi-CAD construct design. Aggregation of Golgi-CAD is mediated by FKBP F36M domains and can be reversed by addition of AP21998 molecule.
b, Development and confirmation of the inducible ER-to-Golgi trafficking assay to study protein transport through early secretory pathway. Trans-Golgi associated marker (Golgi-CAD) is trapped in ER upon transfection (left), but is trafficked to Golgi after addition of small molecule AP21998 (right).
c, Fluorescent micrographs showing final localization of Golgi-CAD two hours after addition of AP21998. Golgi-CAD escapes ER, but is arrested near p58-positive clusters in cells microinjected with EspG (asterisks). No ER export occurs in cells treated with BFA.

EspG induces trafficking arrest phenotypes similar to microtubule disruption

Because EspG neither inhibited ER-export nor induced accumulation of Golgi enzymes in the ER, we sought to define additional host factors that could complement its GTPase regulatory activities. In particular, EspG has been implicated in connection with host microtubules (Matsuzawa, Kuwae, Yoshida, Sasakawa, & Abe, 2004), which both serve as tracks for vesicular transport by motor proteins and for perinuclear Golgi ribbon formation (Cole et al., 1996), To examine the extent of this potential connection, we compared the distribution of a panel of cellular markers in cells treated with either EspG or nocodazole, a small molecule inhibitor of microtubule polymerization. Nocodazole induced the redistribution of cis- (GM130), medial- (NAGT I), and trans-Golgi (TGN46) markers in a manner remarkably similar to EspG (Fig. 28a**)**. More importantly, during Golgi-CAD trafficking assay neither nocodazole nor EspG treatment blocked ER export, but instead arrested Golgi-CAD trafficking at the ERGIC, resulting in enlarged p58-positive clusters (Fig. 28b). Surprisingly, however, no distinguishable defects in the microtubule network could be found in cells microinjected with EspG, despite fragmented Golgi **(**Fig. 28c**)**. Thus, EspG appears to mimic the cellular effects of nocodazole through a mechanism independent of microtubule depolymerization.

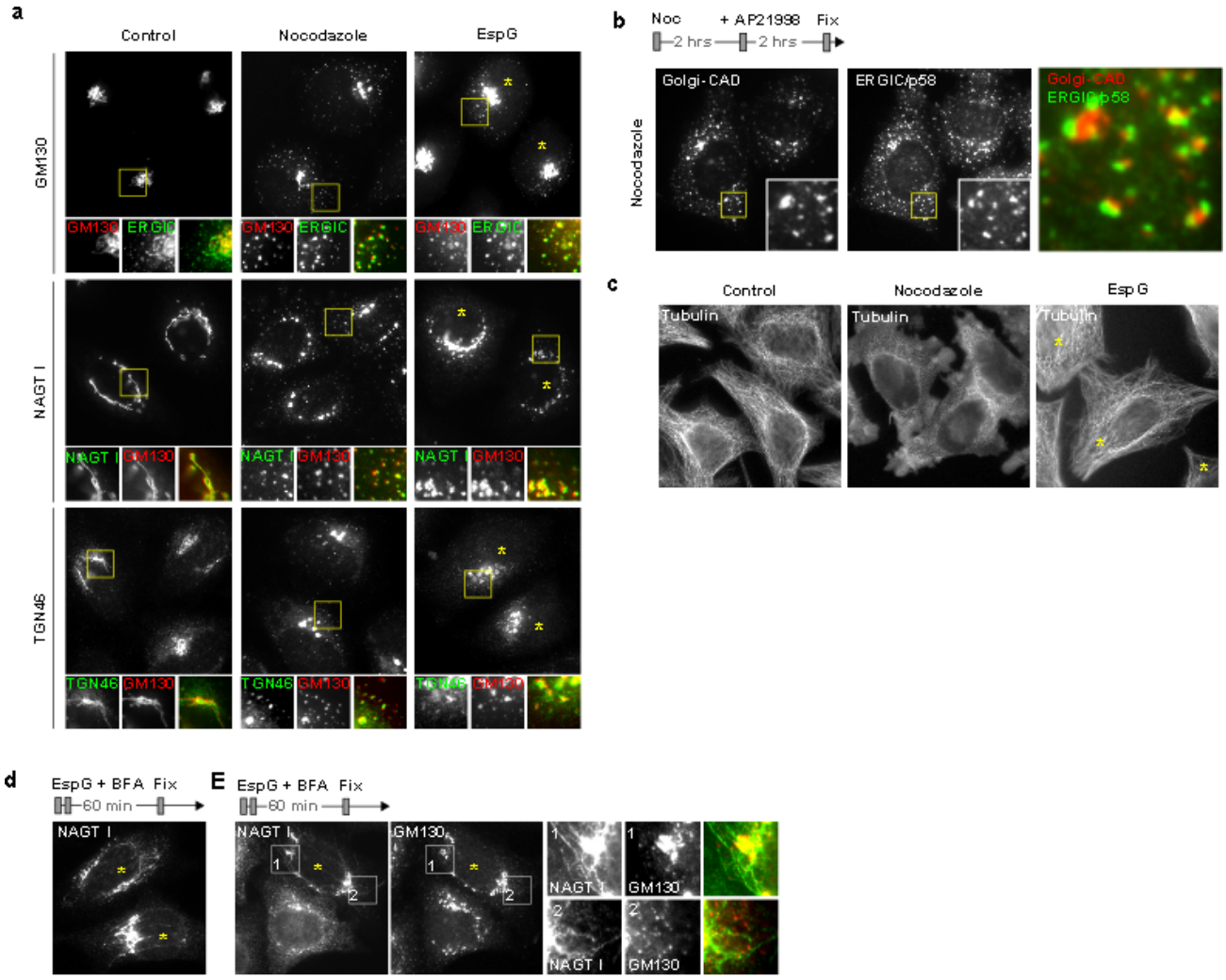

Figure 28. EspG functionally mimics disruption of microtubule dependent processes.
a, Fluorescent micrographs showing Golgi morphology relative to positioning of cis (GM130), medial (NAGT I), and trans-Golgi (TGN46) markers in cells treated with nocodazole or microinjected with EspG.
b, Nocodazole prevents Golgi-CAD transport at p58-positive clusters during inducible trafficking assay in a manner analogous to EspG.
c, EspG shows no apparent defect in microtubule network, despite similar presentation of Golgi phenotypes. Microinjected cells are marked with an asterisk.
d, BFA-induced Golgi tubules persist in EspG injected cells and fail to fuse with ER, suggesting inhibition of membrane transport along microtubules. Microinjected cells are marked with an asterisk.
e, Persistent BFA-induced Golgi tubules emerge from and connect Cis-Golgi in cells transfected with EspG (asterisks).

To further establish the link between EspG function and microtubule dependent processes, we examined retrograde membrane transport from Golgi to the ER, a process critically dependent on the microtubule cytoskeleton. This step of retrograde transport can be readily studied in cells treated with BFA, which induces the formation of long Golgi membrane-tubules along microtubule tracks that rapidly fuse with ER membranes (Sciaky et al., 1997). Normally, Golgi tubulation and fusion is complete within 5-10 minutes of BFA addition. We took advantage of this phenotype to determine if EspG arrests microtubule dependent retrograde trafficking of Golgi tubules. Cells were stimulated with BFA (to induce tubulation) and simultaneously microinjected with EspG. Remarkably, Golgi tubules that normally disappear within minutes of BFA treatment were instead completely arrested in the presence of EspG, and persisted even after 1 hour of observation (Fig. 28d). Importantly, further cellular observations confirmed that these tubules extended from the cis-Golgi (Fig. 28e). Because it is unlikely that EspG family of proteins directly binds (Germane et al., 2008) or depolymerizes microtubules (shown in Figure 2C), we hypothesized that its mechanism is dependent on simultaneous interaction with ARF and Rab family GTPases, which have been linked to microtubule-based functions (Horgan & McCaffrey, 2011)**.**

Structural separation of the ARF1 and Rab1 regulatory functions of EspG.

Although both structural and biochemical interaction data support the simultaneous binding of ARF1 and Rab1 to EspG (Dong et al., 2012), the relative contribution of each interaction to Golgi fragmentation and/or coordination with microtubule processes is unknown. To dissect their functional roles, we first generated EspG mutants that lacked either ARF1

binding or Rab1-GAP activity (Fig. 29a). After detailed analysis of available crystallographic data and systematic mutagenesis, we identified an EspG mutant I152S/P351A/P355A (EspG IPP), which was unable to bind ARF1 (Fig. 29b), but retained potent GAP activity toward Rab1 (Fig. 29c). Additionally, mutations in catalytic residues Arg-208 and Gln-293, which are required for EspG to function as a Rab1-GAP (Dong et al., 2012), had no defect in ARF1-GTP binding (Fig. 29b, c).

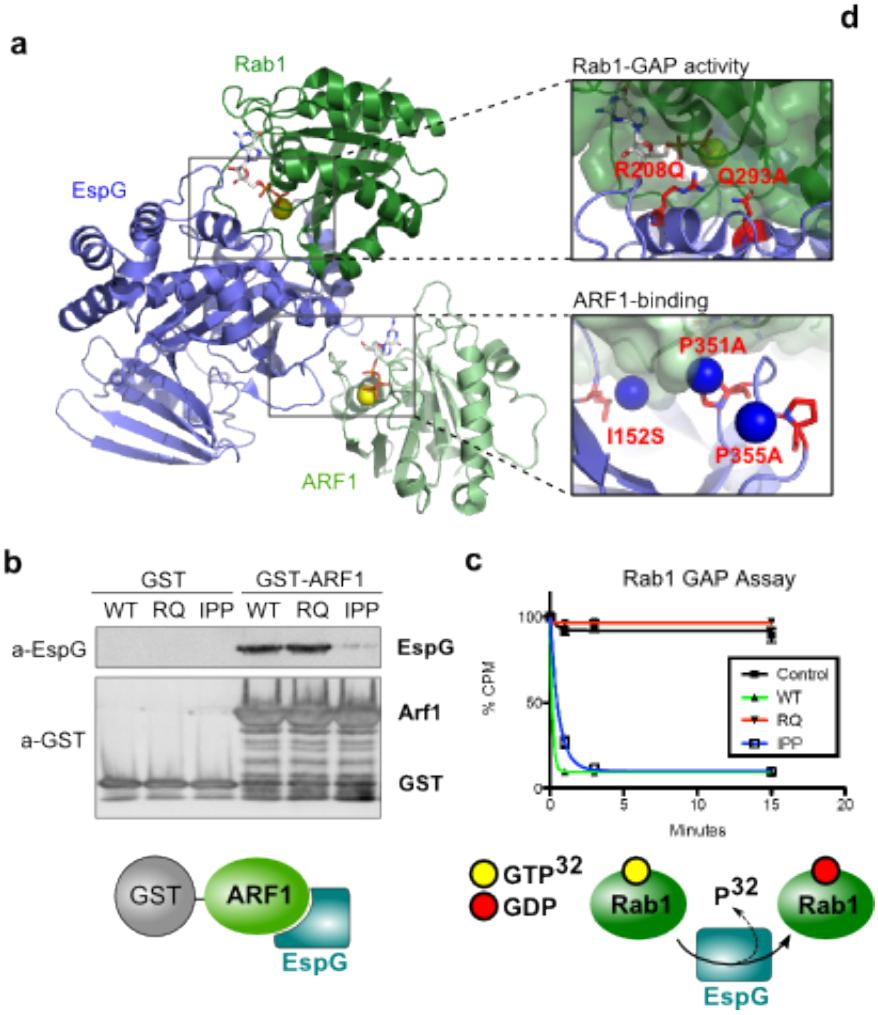

Figure 29. Separating the roles of ARF1 and Rab1 in EspG mechanism.
a, Identification of predicted ARF1 and Rab1-specific functional mutants based on structural data of EspG bound to ARF and Rab GTPases (3PCR, 4FMC, 4FME). Mutations are shown in red, blue spheres denote water molecules.
b, Pull-down experiments testing the ability of EspG mutants to bind ARF1.
c, Rab1-GAP assay testing the GAP activity of EspG constructs.
d, Golgi disassembly by EspG deficient for either ARF1 binding or Rab1-GAP activity as determined by Golgi ribbon fragmentation and enlarged p58 clusters. Representative micrographs are shown for lowest and highest concentrations tested. Microinjected cells are marked with an asterisk.
e, Quantification of disrupted Golgi and p58 clusters phenotype. Needle concentrations are shown.

Having created mutants specific for individual GTPases, we next compared their ability to produce changes in Golgi ribbon morphology and alter the appearance of p58-positive clusters to WT EspG protein. Even at low cellular concentrations of protein, EspG WT induced Golgi disassembly and enlarged ERGIC in virtually every cell (Fig. 30a, b). In contrast, the ARF1-binding deficient mutant, EspG IPP, did not disrupt Golgi architecture at any protein concentrations tested, despite its ability to function as a Rab1 GAP (Fig. 30a, Fig. 31). The cellular Rab1-GAP function of EspG may therefore require association with ARF GTPase in order to manifest the Golgi disruption phenotype. In agreement with this coordination of activities, the EspG RQ mutant, deficient for Rab1-GAP properties, induced Golgi fragmentation at significantly less potency than EspG WT (Fig. 30a, b). However, increasing the concentration of microinjected EspG RQ resulted in subsequent increase in the number of cells with fragmented Golgi (Fig. 30b), suggesting that higher levels of ARF1 binding could compensate for the absence of its Rab1-GAP activity. These data indicate that cooperation between ARF1 and Rab1 signaling is required for full potency of EspG, and establish EspG interaction with ARF1 as a key regulatory point in the EspG mechanism.

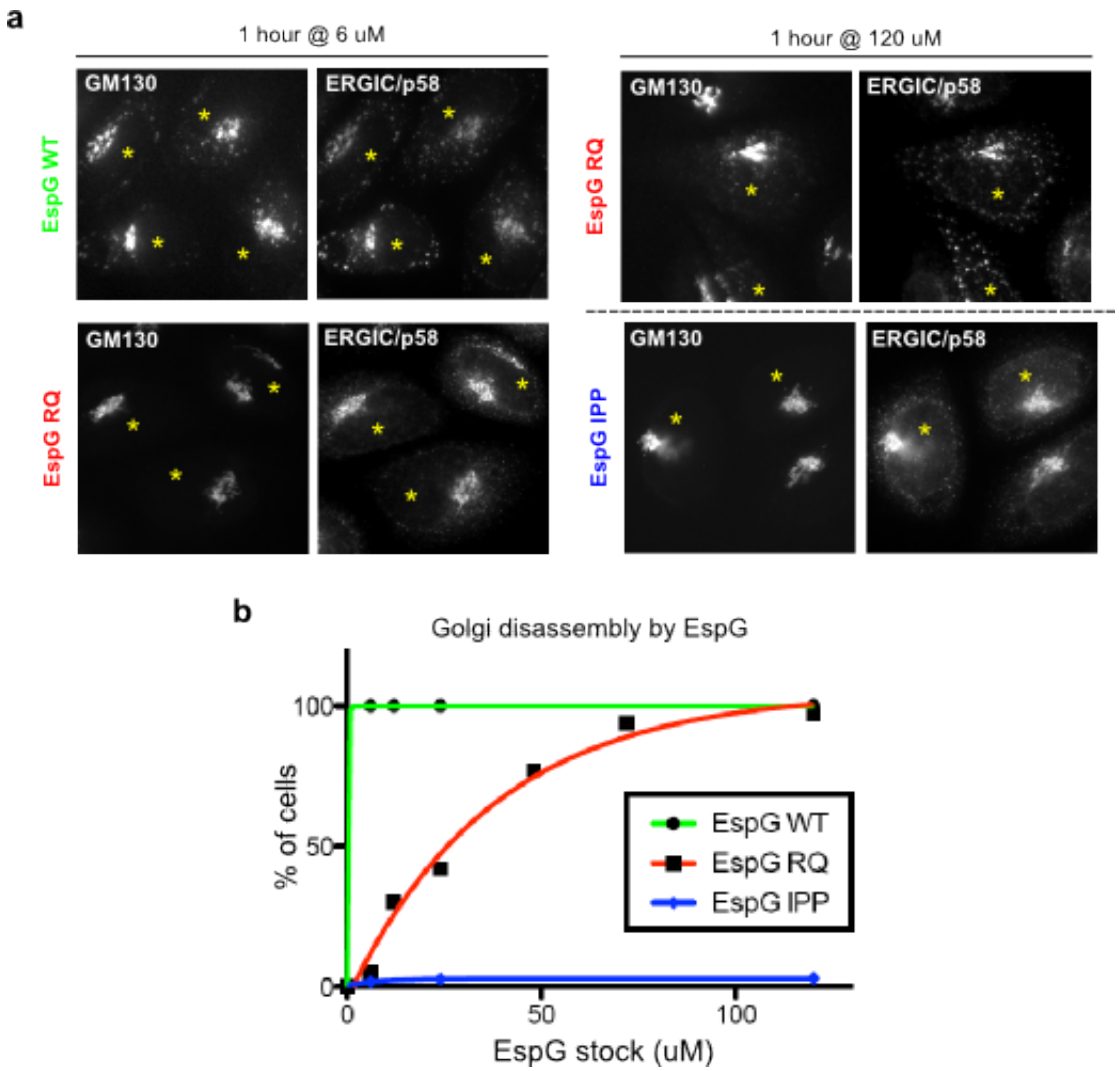

Figure 30. Individual contributions of ARF1 and Rab1 to Golgi disassembly by EspG.
a, Golgi disassembly by EspG deficient for either ARF1 binding or Rab1-GAP activity as determined by Golgi ribbon fragmentation and enlarged p58 clusters. Representative micrographs are shown for lowest and highest concentrations tested. Microinjected cells are marked with an asterisk.
b, Quantification of disrupted Golgi and p58 clusters phenotype. Needle concentrations are shown.

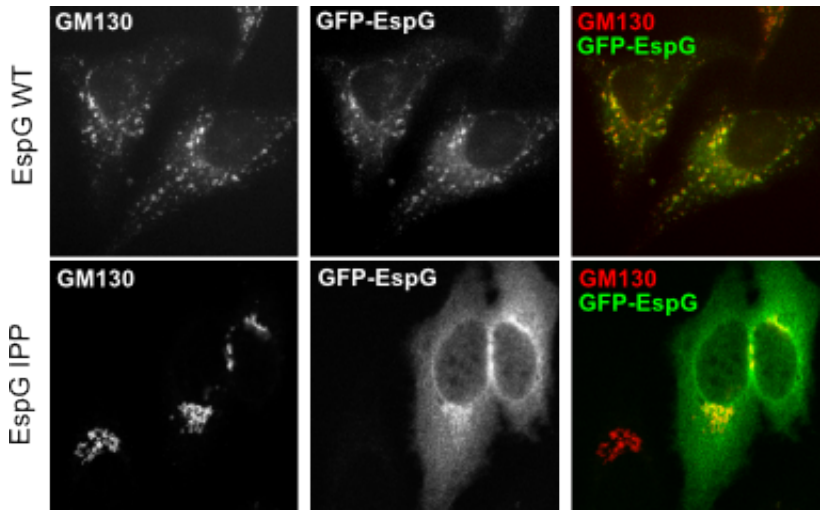

Figure 31. ARF1 binding is required for Golgi disassembly by EspG.
Fluorescent micrographs showing Golgi morphology after overnight transfection with either WT or ARF1-binding deficient EspG (IPP).

EspG functions through ARF1 signaling

In previous structural studies we found that EspG occludes ARFGAP access to the GTP binding pocket of ARF1 by interacting at a distal site of the Switch I loop (Selyunin et al., 2011). Interestingly, this unusual binding architecture is distinct from known endogenous ARF1 substrate interactions, which primarily associate through the Switch II and β2/3 interswitch region (Nie, Hirsch, & Randazzo, 2003). Thus, in addition to locking ARF in the GTP-active state, EspG may drive ARF1-GTP interactions with specific downstream substrates. Structural modeling revealed that EspG has no steric interference with the GAT-domain of GGA1 adaptor protein when associated with ARF1-GTP (Fig. 32a). This GAT-Arf1-EspG complex is striking in its complementarity. In contrast, however, analysis of a recently solved structure of ARF1 in complex with β-COP coat protein (Yu, Breitman, & Goldberg, 2012) revealed a significant clash between EspG and β -COP (Fig. 32b), indicating that EspG would interfere with COPI coat

assembly at the Golgi. These observations suggest that the molecular architecture of EspG stabilizes the GTP-active state of ARF1 and promotes select downstream signaling events. Therefore, we hypothesized that the pathogenic effects of EspG are mediated by hyper-stimulation of ARF1-GTP signaling, and specifically those that regulate microtubule dependent processes.

To test this structural-based hypothesis, we first sought to determine if EspG stabilizes an ARF1/substrate complex on host membranes. As shown in (Fig. 32c), EspG co-localized with p58, implicating Golgi membranes as the primary site of EspG function. Importantly, ARF1 was retained on the p58 positive membranes in the presence of EspG, but was not in cells treated with BFA treatment (Fig. 33a). These data are consistent the biochemical differences between EspG and BFA; EspG locks ARF1 in the GTP active state whereas BFA nucleates an inactive ARF1-GDP/GEF complex in the cytosol. To then determine if EspG association with Golgi membranes requires ARF1-GTP Golgi localization, we assessed the subcellular distribution of fluorescently labeled EspG in either untreated cells, or cells where ARF1 was removed from membranes by BFA treatment. This experiment showed that EspG is cytosolic in the absence of membrane bound ARF1, and thus requires ARF1-GTP for association with Golgi remnants (Fig. 32d).

Next, we sought to determine directly whether membrane-bound GTP-ARF1 could recruit endogenous substrates to membrane bilayers when in complex with EspG. Initially, we reconstituted this system on Golgi-mimetic liposomes using purified recombinant proteins (Fig. 32e). In control experiments, the soluble GAT domain of GGA1, a prototypic ARF1 substrate that binds with high affinity, was selectively pulled down by liposomes carrying GTP-loaded ARF1 (Fig. 32f, lanes 3-6). In agreement with our structural predictions, GGA1(GAT) was

successfully recruited into the EspG/ARF1 complex in an ARF1-GTP dependent manner (Fig. 32f, lanes 7-8). Importantly, EspG blocked the GAP-stimulated release of GGA1(GAT) from liposomes, indicating that EspG effectively induces a constitutively active form of ARF1 on membranes (Fig. 32f, lanes 9-10). In cell-based studies, we also found that GGA1(GAT) was recruited to fragmented Golgi membranes in cells microinjected with EspG, but not in cells where Golgi fragmentation was induced by BFA (Fig. 33b). Taken together, these data strongly support a mechanism whereby EspG selectively maintains specific downstream interactions of membrane bound ARF1-GTP, which combined with inactivation of Rab1, leads to Golgi disassembly and inhibition of the GSP.

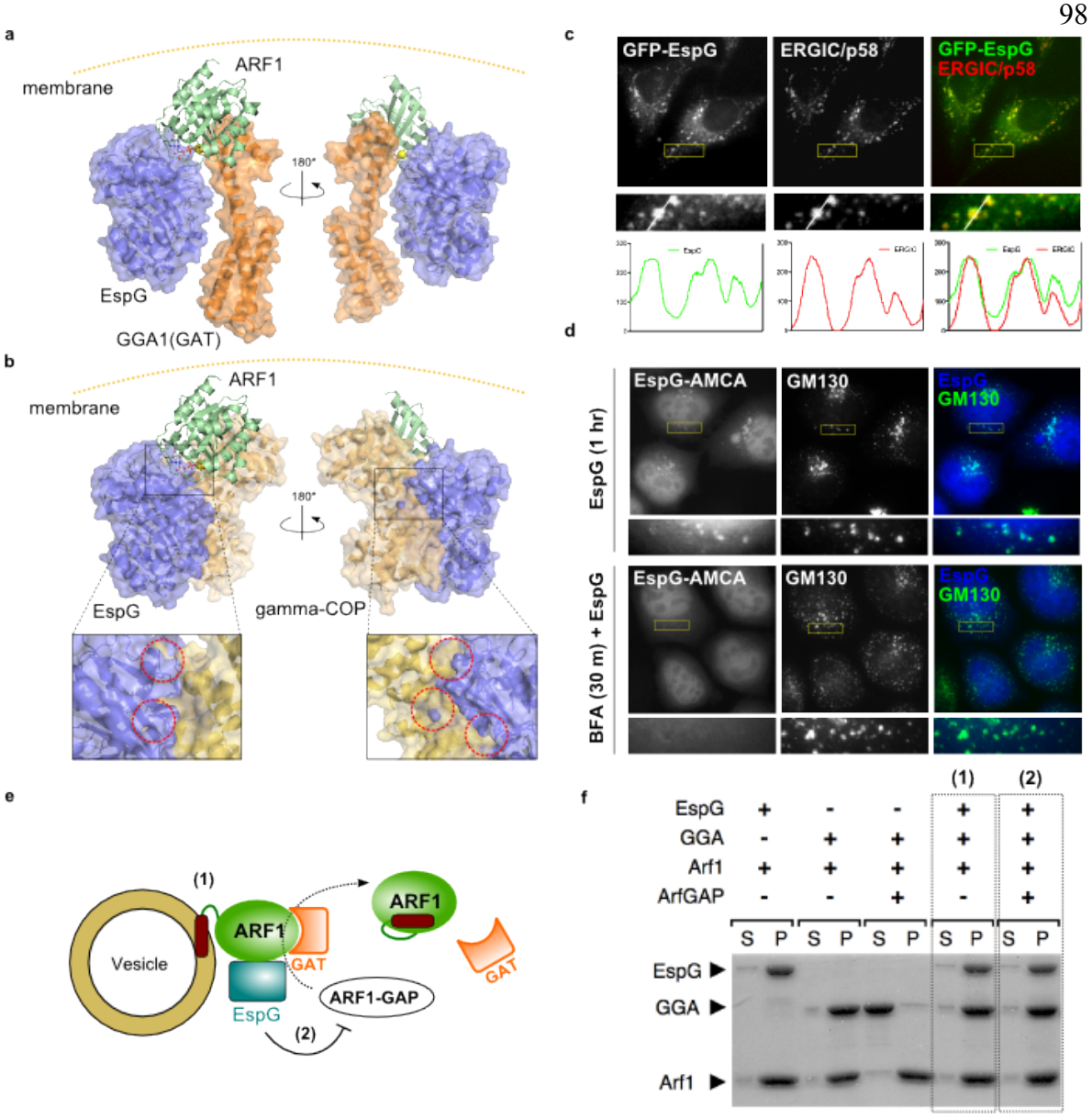

Figure 32. EspG selectively functions through downstream interactions of active ARF1.
a, Structural model of EspG bound to ARF1/GGA1(GAT) complex, based on EspG/ARF1 (1PCR) and ARF1/GGA1(GAT) (1J2J, 1O3X) X-ray structures.
b, Structural model of EspG bound to ARF1/g-COP complex, based on EspG/ARF1 (1PCR) and EspG/g,z-COP (3TJZ) structures. Insets show major steric clashes, highlighted with dotted circles.
c, Fluorescence micrographs show localization of GFP-EspG to p58-positive ERGIC membranes.

d, Membrane association of EspG is dependent on membrane-bound ARF1. Fluorescently-labeled EspG is localized to fragmented endomembranes during microinjection, but is cytosolic when cells are pretreated with BFA.
e, Experimental setup to examine (1) membrane recruitment of downstream effectors by ARF1 and (2) susceptibility of ARF1/effector complex to GAP-mediated inactivation in presence of EspG.
f, Liposome pull-down experiments for the setup described in (D). EspG allows recruitment of ARF1 effector to membranes (1) and prevents its release due to ARF1 inactivation by ArfGAP (2).

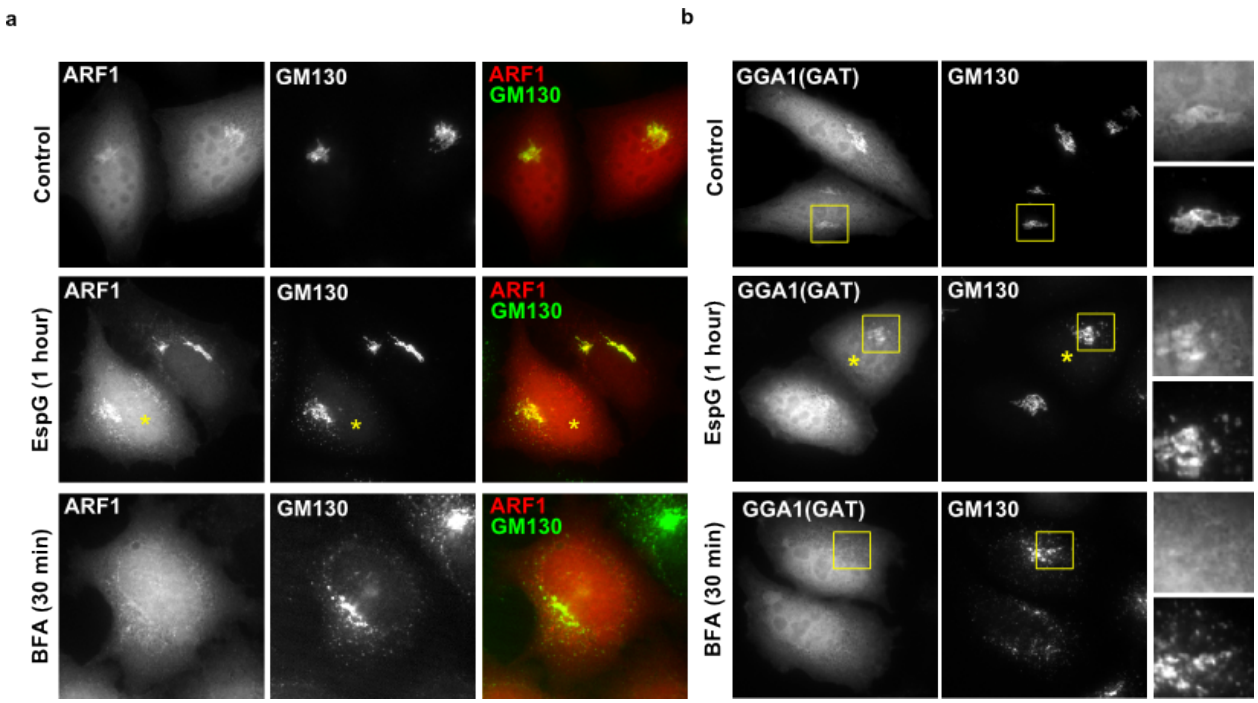

Figure 33. ARF1 remains membrane bound and active during Golgi fragmentation by EspG.
a, ARF1-mCherry is found on fragmented membranes in cells where fragmentation is induced by EspG (asterisks), but not by BFA treatment.
b, ARF1 is capable of recruiting downstream targets (GGA1-GAT) to membranes during Golgi disassembly by EspG.

Identification of downstream ARF1 effectors.

So far, our data indicates that EspG initiates an ARF1 GTPase signaling cascade that is either directly or functionally linked to microtubule dependent membrane transport. Because neither EspG nor ARF1 bind microtubules, the molecular mechanism of EspG must therefore involve a host cellular component that is (1) a specific effector for ARF1, (2) required for Golgi structural maintenance, and (3) capable of inducing Golgi fragmentation without affecting the microtubule network. Through extensive analysis of published observations, we found two proteins, GMAP-210 and Golgin-160, which met these criteria. GMAP-210 is a tubulin binding protein that links small vesicles to organelle membranes via a curvature sensing N-terminal ArfGAP1 Lipid Packing Sensor (ALPS) and a C-terminal GRIP-Related ARF Binding (GRAB) domain that interacts with ARF1-GTP (Drin, Morello, Casella, Gounon, & Antonny, 2008; Rios et al., 2004). Golgin-160, on the other hand, is found primarily on the cis-Golgi and is implicated in membrane transport by connecting ARF1-GTP vesicles to dynein motor (Yadav, Puthenveedu, & Linstedt, 2012). Despite keeping the microtubule network intact, depletion of either GMAP-210 or Golgin-160 disrupts Golgi morphology and results in a dispersed ministack appearance of Golgi when visualized using Transmission Electron Microscopy, similar to the Golgi phenotype following nocodazole treatment (Pernet-Gallay et al., 2002; Rios et al., 2004; Yadav, Puri, & Linstedt, 2009).

Because cellular disruption of GMAP-210 and Golgin-160 result in a well-defined multivesicular Golgi phenotype, we used Correlative Light Electron Microscopy (CLEM) to determine if EspG induced similar Golgi morphology. The cellular membrane fragments that correlated with EGFP-EspG fluorescent signal were organized in clusters of small vesicles (Fig.

34a). These vesicles did not stochastically spread throughout the cell, suggesting that the membranes may be cross-linked through an EspG/ARF1-GTP mediated protein complex. Combining our observations that ARF1-binding by EspG is sufficient to induce Golgi fragmentation and that EspG stabilizes ARF1-GTP on membranes, we hypothesized that EspG most likely blocks vesicular traffic through an ARF1-dependent tether (i.e. GMAP-210 or Golgin-160) (Fig. 34b). Importantly, this mechanism would explain the phenotypic similarity between EspG and nocodazole treatment, as both restrict vesicular movement beyond their budding site (Cole et al., 1996).

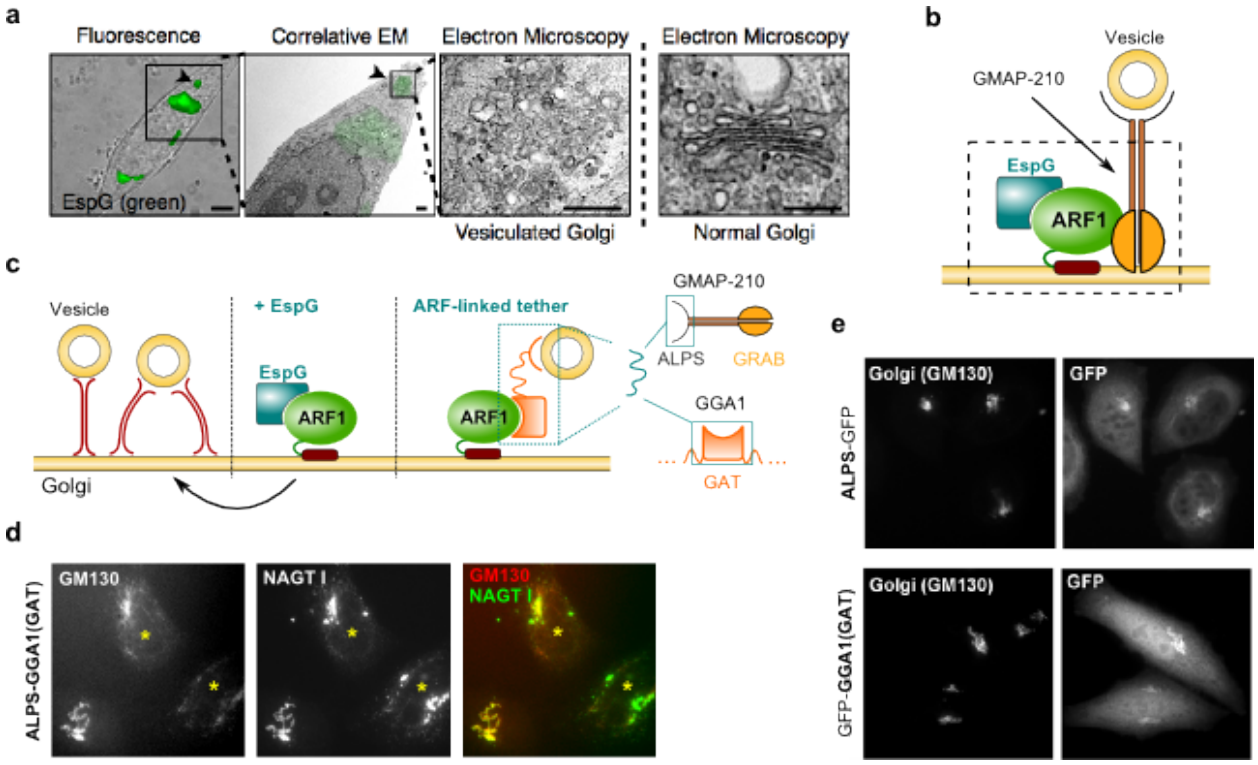

Figure 34. Disruption of Golgi architecture through ARF1-dependent membrane tethering.
a, Correlative Light and Electron Microscopy shows vesicular ultrastructure of Golgi after microinjection with EspG, which remains constrained to areas positive for EspG signal.
b, Identification of golgin GMAP-210 as an ARF1-dependent membrane tether involved in EspG mechanism of Golgi disassembly by linking vesicles to membranes and preventing their transport.
c, Cartoon schematic illustrating the design of an ARF1-dependent membrane-tethering chimera using vesicle-binding motif linked to an ARF1-GTP-binding domain of GGA1. Our model of EspG function predicts vesicle to membrane linkage that is driven by the presence of GTP-ARF1 on membranes.
d, Overexpression of ARF1-dependent membrane tethering chimera is sufficient to disrupt Golgi architecture. Transfected cells are marked with an asterisk.
e, Control experiments show no negative impact on Golgi organization due to overexpression of either vesicle-binding motif or an ARF1-GTP-binding domain alone in absence of direct tether.

The role of GMAP-210 tethering protein in EspG mechanism.

We now propose a model whereby EspG promotes membrane tethering by stabilizing ARF1-GTP on Golgi membranes, in turn effectively increasing the presence of tethering factors such as GMAP-210, and inhibiting vesicle fusion through Rab1-GAP function. This model predicts that excessive expression of GMAP-210 should induce a Golgi phenotype analogous to EspG. To test this assumption, we examined the effects of excess GMAP-210 on Golgi structure and function. Transient overexpression of the tethering protein induced severe Golgi fragmentation and enlarged ERGIC (Fig. 35a), as well as accumulation of Golgi enzymes near p58-positive clusters (Fig. 35b). Similar to EspG, Golgi disassembly by GMAP-210 overexpression was not due to depolymerization of microtubules, which appeared intact (Fig. 35c**).** We then wanted to confirm that inhibition of protein transport due to excessive GMAP-210 tethering occurred in a manner consistent with what we observed during EspG microinjection. Indeed, we found that Golgi-CAD was similarly trapped near p58-positive clusters during an anterograde trafficking assay (Fig. 35d), and that overexpression of GMAP-210 also protected NAGFP from BFA-induced redistribution into the ER (Fig. 35e). Finally, EM analysis of Golgi remnants during overexpression of GMAP-210 shows striking similarity to that observed with EspG overexpression, displaying extensive accumulation of vesicles ((Drin et al., 2008), Fig. 34a).

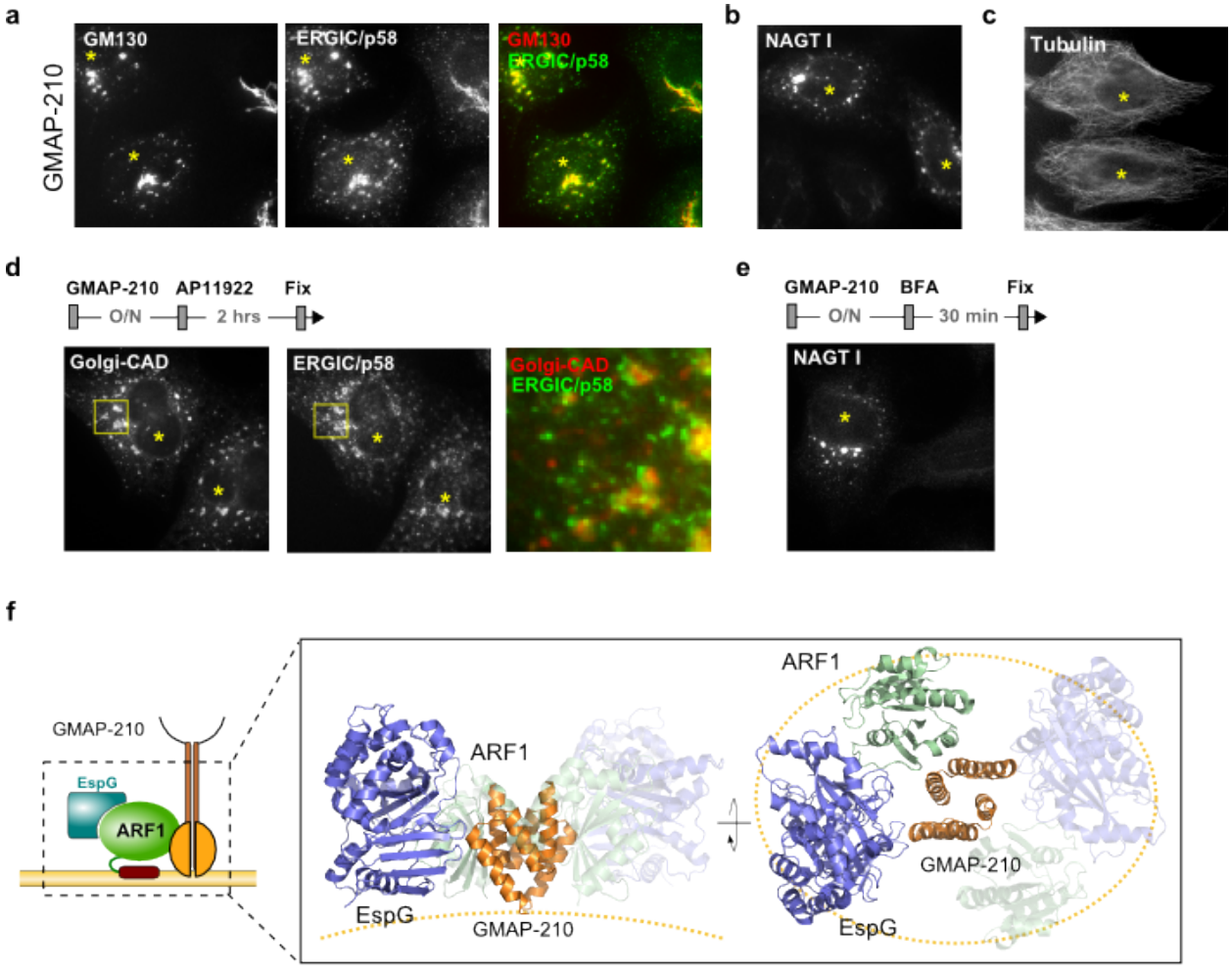

Figure 35. Overexpression of GMAP-210 closely resembles EspG function.
a, Overexpression of GMAP-210 induces fragmentation of Golgi ribbon and enlargement of p58 clusters, similar to EspG.
b,c, Overexpression of GMAP-210 induces accumulation of Golgi enzymes in p58 clusters and does not induce depolymerization of microtubules.
d, Golgi-CAD escapes ER and is arrested near p58 membranes during overexpression of GMAP-210.
e, Overexpression of GMAP-210 protects Golgi enzymes from redistribution into ER during BFA treatment.
f, Structural model of EspG interaction with ARF1/GMAP-210 membrane tethering complex. Published structure of GMAP-210 related Golgin-245 GRIP domain bound to ARL1 (1UPT) was used to model EspG into the complex. EspG is not predicted to clash with ARF1/GMAP-210 assembly.

At the core of our model, EspG protects membrane bound ARF1-GTP from inactivation by ARF GAP, increasing the selective accumulation of downstream ARF1-GTP substrates (i.e. GMAP-210) that promote vesicle tethering and inhibit membrane fusion. This suggests that inhibition of membrane trafficking associated with EspG is due to extensive ARF1-dependent tethering events between membranes and vesicles (Figure 5C). In order to more directly confirm that ARF1 dependent vesicle tethering is sufficient to induce Golgi disassembly, we re-engineered GMAP210 and GGA1-GAT to model the proposed EspG virulence system with a minimum set of interactions. Specifically, we created a synthetic chimera protein (ALPS-GAT) consisting of a GMAP-210 ALPS motif to bind small vesicles, and a soluble GGA1-GAT domain, which associates with membranes only when bound to active ARF1-GTP (Fig. 34c). If our model were correct, then the minimal ALPS-GAT chimera would functionally mimic two aspects of the proposed EspG/ARF1/GMAP210 complex: (1) it would tether vesicles to Golgi membranes in an ARF1-dependent manner, and (2) it would selectively promote tethering while restricting other ARF-GTP signaling events such as COPI vesicle fission. In agreement with our model, cellular expression of ALPS-GAT effectively disrupted Golgi organization and function in a manner similar to EspG (Fig. 34d), but distinct from the phenotype we have reported for BFA. Importantly, expression of either the ALPS motif or GAT domains alone had no effect on Golgi morphology, confirming that disruption was directly dependent on tethering of small vesicles to membrane-bound ARF1-GTP (Fig. 34e).

Because *in vitro* assays to look at direct interaction between GMAP-210 and ARF1 have proved difficult (Gillingham, Tong, Boone, & Munro, 2004), we used structural modeling to assess if EspG could bind to ARF1/GMAP-210 complex on the membrane. Using the structure

of a related GRIP domain of golgin-245 bound to Arl1 (Panic, Perisic, Veprintsev, Williams, & Munro, 2003), we modeled ARF1/GMAP-210 interaction with EspG and did not detect any apparent steric clashes (Fig. 35f). Thus, by preventing ARF1 inactivation, EspG could drive excessive membrane accumulation of specific ARF1 substrates, such as GMAP-210, which consequently would lead to increased tethering of vesicles or allow regulation of additional microtubule dependent processes (Fig. 36).

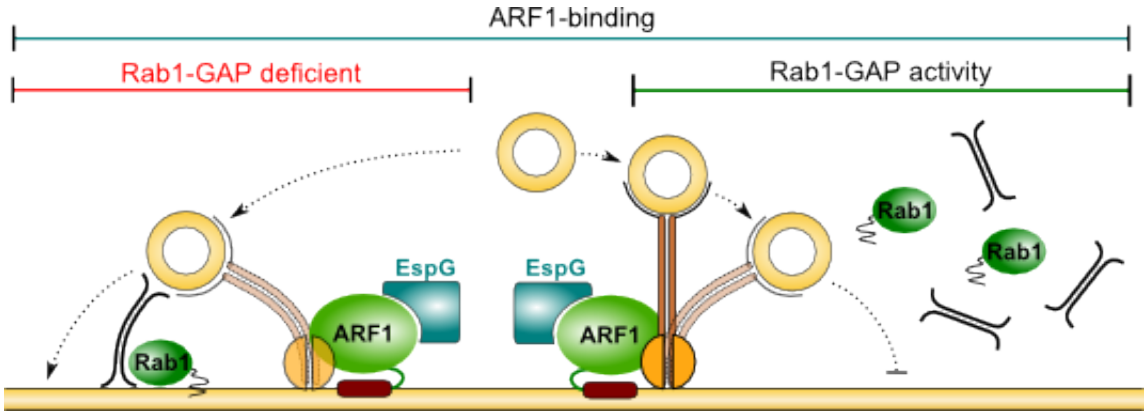

Figure 36. Model for membrane trafficking inhibition by EspG through membrane capture.
Both ARF1-binding and Rab1-GAP activity are required for efficient membrane capture through ARF1-mediated tethering. In absence of Rab1-GAP activity, vesicle fusion can still occur partially via Rab1-dependent machinery (left). Gross accumulation of GMAP-210 on the membrane leads to an increased number of GMAP-210 bound to vesicles, physically restricting membrane fusion and can compensate for defective Rab1-GAP properties (center). Simultaneous ARF1 binding and Rab1-GAP activity of EspG allows stable membrane tethering by locally preventing Rab1-mediated fusion and efficiently inhibits membrane transport (right). By preventing vesicle fusion and capturing vesicle in close proximity to membranes, EspG effectively inhibits membrane transport.

DISCUSSION

In this report, we describe the unique molecular mechanism of a bacterial protein EspG that potently inhibits intracellular vesicular transport and arrests membrane trafficking at ERGIC through cooperative regulation of ARF1 and Rab1 GTPases via its scaffolding architecture. Importantly, EspG induces arrest of membrane transport at pre-Golgi intermediates and does not functionally mimic either disruption of ARF1 cycling by BFA treatment or overexpression of Rab1-GAP, thus suggesting a novel mechanism exclusively dependent on simultaneous regulation of multiple host GTPases. We find that EspG prevents inactivation of ARF1 without interfering with its ability to recruit select downstream targets to membranes, leading to increased membrane tethering mediated by the interaction of ARF1 with GMAP-210 and potentially other tethering factors. This mechanism is exclusively dependent on simultaneous exclusion of Rab1 dependent machinery near EspG/ARF1 complex, which is mediated by direct Rab1-GAP activity of EspG. Thus, our findings uncover a delicate mechanism of multiple host enzyme regulation guided by structural features of the bacterial Type III secreted protein.

In its active state, ARF1 recruits a wide variety of effectors to membranes, including COPI coat proteins, lipid modifying enzymes, and scaffolds for cytoskeletal anchoring (Donaldson & Jackson, 2011). This makes it a prime target for a bacterial protein that has evolved to regulate intracellular trafficking. While restricting GAP access allows EspG to control the activity state of ARF1, maintaining the GTPase in a constitutively active confirmation through allosteric binding alone would be inefficient when compared to molecules mimicking upstream regulatory proteins, such as GEFs. Instead, the binding orientation of EspG suggests that it additionally acts as a selection mechanism that allows interaction of ARF1 with specific,

but not all, downstream substrates. Indeed, some endogenous ArfGEFs have been shown to favor specific downstream signaling by interacting with and preferentially recruiting a set of effectors to ARF1 (Deng, Golinelli-Cohen, Smirnova, & Jackson, 2009). Downstream substrate selectivity combined with protection of ARF1 from GAP inactivation would effectively allow EspG to inhibit some signaling pathways while over stimulating other, thus expanding its function beyond a simple activity modulator. Our proof of concept experiments with Golgi mimetic liposomes support this idea by showing that ARF1 can recruit its effectors to membranes when bound by EspG, and that this complex remains resistant to GAP treatment.

Although structural and functional studies support the ability of EspG to interfere with normal ARF1 nucleotide cycling and Rab1-GAP activity, by developing a robust trafficking assay that allows visualization of ER to Golgi transport we are able to show that EspG neither inhibits ER export nor leads to accumulation of Golgi enzymes in the ER, thus presenting a clear distinction from BFA or Rab1-GAP induced trafficking defects. This finding suggested that simultaneous coupling of GTPase regulation through scaffolding architecture, rather than individual regulatory functions, drives the mechanism of EspG. Targeting multiple host regulatory pathways through a single effector molecule would allow bacteria to more efficiently modulate complex host signaling networks and finely tune a specific environment for their lifestyle. In particular, an EspG homolog from intracellular pathogen *S. flexneri*, VirA, shares potent GAP activity toward Rab1 and induces Golgi disassembly (Burnaevskiy et al., 2013; Dong et al., 2012). In contrast to EspG, however, VirA does not interact with ARF1, perhaps coordinating inactivation of Rab1 with a different signaling pathway and further supporting specific evolutionary adaptation of effector proteins to unique needs of each bacterium. Notably,

Golgi disruption by *S. flexneri* can also be independently induced by the recently characterized IpaJ effector, which demyristoylates and inactivates ARF1 (Burnaevskiy et al., 2013). It is therefore possible that IpaJ and VirA activities complement each other to precisely control a range of trafficking events under different conditions, further underlining the functional need to selectively regulate individual pathways.

Elucidating the exact functional role of an individual bacterial effector molecule in an infection has been difficult due to the large number of proteins secreted by invading bacteria, variable number of bacteria infecting individual cells, and poorly understood order of secretion of effectors, some of which may share host targets or mask activity. All these factors introduce wide variance and make it hard to connect a distinct phenotype to any single molecule. Understanding the molecular mechanism of an effector through focused biochemical studies, such as the one presented here, uncovers its potential function within a host cell and provides direct insight into its role during an infection. Specifically, EspG and VirA have been linked to microtubule cytoskeleton phenotypes in cells infected by EHEC or S. flexneri, respectively (Matsuzawa et al., 2004; Yoshida et al., 2002). Here, we show that a distinct trafficking phenotype appears closely related to that observed during microtubule disruption by nocodazole, and that this connection could be linked to the regulation of ARF and Rab GTPases. In addition, EHEC infection has been shown to inhibit cytokine secretion and decrease trans-epithelial resistance (Dong et al., 2012; Philpott, McKay, Mak, Perdue, & Sherman, 1998). We present evidence that EspG potently inhibits GSP by arresting membrane transport at ERGIC, which in turn inhibits cytokine secretion and delivery of adherence proteins needed to maintain the tight junctions at cell surface in the intestinal lumen.

In summary, we describe a unique mechanism of endomembrane trafficking inhibition at ERGIC by a bacterial protein EspG, whose scaffolding properties allow the regulation of the activity state and downstream signaling of host GTPases ARF1 and Rab1. Although structural studies have shown that EspG can bind ARF1 and Rab1, our study shows for the first time that their activities are functionally linked and require coordination to induce endomembrane phenotype. Simultaneous regulation of select trafficking pathways by secreted proteins may afford bacterial pathogens an ability to avoid immune recognition specific to their lifestyle. Roles of protein and membrane transport in immunity include antigen presentation by MHC Class I molecules, IgM secretion, autophagosome formation, and cytokine secretion, among others. Indeed, EspG has been found responsible for inhibiting IL-8 secretion from HeLa cells during infection (Dong et al., 2012). The arrest of membrane transport by EspG at ERGIC described herein is consistent with the presence of both ARF1 and Rab1 on ERGIC membranes and supports it being the primary site of EspG function. At the same time, bacterial effectors provide researchers with effective tools to better understand the signaling interplay within complex regulatory systems. Taken together, our data expose signaling pathway coupling via small molecular scaffolds as a new regulatory hub of intracellular trafficking and describe an additional level of structural specificity, which may have been previously overlooked.

EXPERIMENTAL PROCEDURES

Plasmids

The *espG* gene from EHEC O157:H7 was PCR cloned in-frame into pEGFP-C2 (Clontech). For bacterial expression, 38 and 41 amino-acid N-terminal deletions (39–398 and

42–398) of EspG were PCR subcloned into pGEX-4T1 (GST-tag) (Amersham), pProEX-HTb (6xHis tag) (Novagen) vectors. EspG mutants were generated with QuickChange site-directed mutagenesis (Stratagene) following manufacturer's instructions. Full length or the GTPase domain of ARF1 (ARF1Δ17) were PCR subcloned into pcDNA3.1-mCherry, or pGEX-4T1 and pProEX-HTb vectors, respectively. The GTPase domain of Rab1 (1-177) was subcloned from Rab1a cDNA (DNASU, Arizona State University) into pGEX-4T3 vector. The GMAP-210 plasmid was a kind gift from Bruno Antonny and Guillaume Drin (Institut de Pharmacologie Moléculaire et Cellulaire, France). All constructs were verified by DNA sequencing.

Protein purification for in vitro assays and microinjection

Recombinant proteins were produced in BL21-DE3 *E. coli* strains. Protein expression was induced with 0.4 mM IPTG for 16 h at 18 °C. Bacterial pellets were lysed in either His buffer (100 mM HEPES, pH 7.5, 300 mM NaCl) or GST buffer (TBS; 50 mM Tris pH 7.5, 150 mM NaCl, 2 mM DTT) supplemented with protease cocktail (Roche). Proteins were purified with nickel agarose (Qiagen) or glutathione Sepharose (Amersham Biosciences) following manufacturer's instructions. Eluted proteins were buffer exchanged into TBS using concentration centrifugal columns (Millipore), glycerol was added to 15% and the proteins were then stored at −80 °C. For microinjection, protein stocks were diluted to concentrations indicated with TBS.

In vitro GST pull-downs

Protein interactions were examined through GST pull-down assays. Unless otherwise stated, 10 μg of recombinant GST proteins immobilized to glutathione Sepharose were incubated with 15 μg of 6xHis- tagged proteins for 1 h at 4 °C. Samples were washed three times in TBS

supplemented with 0.5% Triton X-100. Proteins were eluted from beads with Laemelli sample buffer, separated by SDS–PAGE, and analyzed by Western blot. For nucleotide loading, ARF1Δ17 was incubated in nucleotide loading buffer (40 mM HEPES, 150 mM NaCl, 2 mM EDTA, 10% glycerol) with 10 μM of either GDP or GTP for 30 min at 37 °C, and then $MgCl_2$ was added to 10 mM and the reaction was transferred to ice after 15 min at room temperature (25 °C).

Cell microinjection, transfections and immunofluorescence microscopy

HeLa cells were microinjected with EspG proteins using a semi-automatic InjectMan NI2 micromanipulator (Eppendorf) using a needle concentration of 25 μM unless stated otherwise. Transfections were performed using XtremeGene 9 Transfection Reagent (Roche) following manufacturer's instructions. At 16–18 h post-transfection, cells were fixed with 3.7% formaldehyde and stained with antibodies for immunofluorescence. Expression of NAGT I in NAGFP cells was stimulated by the addition of 5 μM sodium butyrate (Sigma) to the media. AMCA-EspG was produced using an NHS-AMCA labeling kit and 6xHis-tagged EspG (42-398) (Pierce). Brefeldin A and nocodazole treatments were performed at 5 μg ml^{-1} for 30 minutes and 30 μM for 2 hours, respectively. All immunofluorescence images were acquired with a Zeiss LSM 5 Pascal confocal microscope or Zeiss Axiovert 200. Cellular markers were detected using following antibodies: GM130 (BD TransductionLabs), ERGIC-53/p58 (Sigma), TGN46 (abcam), and α-tubulin (Sigma).

Ligand Inducible ER-to-Golgi Trafficking Assay

An inducible trafficking assay was developed by adapting the Conditional Aggregation Domain of FKBP F36M (Rivera et al., 2000) to control the secretory transport of a fluorescent trans-Golgi marker. The signal sequence (residues 1-81) of human b-1,4-galactosyltransferase was fused to mCherry sequence in a modified pcDNA 3.1 plasmid, followed by a furin cleavage site (FCS) and 4x repeats of FKBP F36M CAD domain (see Figure 1A). Cells were transfected with 0.5 μg of plasmid for 16-18 hours. Aggregation of Golgi-CAD in ER was reversed by the addition of AP21998 (2 μM final) to the media, which induced Golgi-CAD trafficking through the general secretory pathway. Final localization of Golgi-CAD was assessed 2 hours later. BFA and nocodazole treatments, as well as EspG microinjection, were performed after transfection and prior to the addition of AP21998, where indicated.

Liposome pull-downs and GAP assays

Golgi mimetic liposomes were generated using lipid ratios reported by Bremser and colleagues (Bremser et al., 1999) and GTP-loading of ARF1, liposome pull down assays, and GAP assays were conducted as previously reported (Selyunin et al., 2011). Briefly, N-terminal His-tagged ARF1 was nucleotide exchanged to GTP and incubated with Golgi mimetic liposomes containing 20 mol% DOGS-NTA (Avanti Polar Lipids), a dioleoyl-lipid with a Ni^{2+}-NTA head group capable of capturing the His-tag of a co-incubated protein. These liposomes were separated from bulk ARF1-GTP via centrifugation and resuspended in liposome binding buffer (20 mM Tris-HCl, pH 7.6, 50 mM NaCl, 10 mM $MgCl_2$). These ARF1-GTP decorated liposomes were then incubated with a combination of EspG, GGA, and ARF1GAP. To test for EspG protection of ARF1 from ARF1GAP, EspG was added 5 min prior to the addition of rat ARF1GAP. Following incubation on ice for 30 min, liposomes were sedimented and samples of

the supernatant and pellet were separated on 12.5% SDS-PAGE. For Rab1 GAP assays, GST-Rab1 (1-177) (5 μM) was loaded with radio labeled GTPgP^{32} in loading buffer (20 mM Tris pH 7.5, 100 mM NaCl, 2 mM EDTA, 0.2 mM DTT) for 15 min at room temperature, and then supplemented with 10 mM $MgCl_2$. Then, it was incubated alone, or with addition of WT or mutant EspG (1 μM) for 15 min at 30°C. Reactions have been stopped with ice-cold buffer and then bound to nitrocellulose membranes. Hydrolysis of GTP was assessed by scintillation counting.

Correlative Light Electron Microscopy

Microinjection and correlative light and electron microscopy was performed similarly to (Reddick & Alto, 2012). Briefly, HeLa cells were cultured on gridded glass coverslips (MatTek Corp., Ashland, MA). EspG was fluorescently labeled using FITC following manufacturer's instructions (Pierce, Rockford, IL). Microinjection needles were pulled with a Sutter instrument model P-97 micropipette puller, and microinjection was performed using an Eppendorf FemtoJet Injectman NI2 Microinjection System. Thirty minutes after microinjection, cells were fixed with 3% formaldehyde in PBS and a confocal Z-stack was acquired on microinjected cells using a Zeiss LSM5 Pascal confocal microscope. Correlative electron microscopy was performed exactly as in (Reddick & Alto, 2012).

CHAPTER SIX

CONCLUSIONS AND PERSPECTIVES

Conclusions

EspG is a multi-domain catalytic scaffold

Bacterial type III secreted effector of EspG from EHEC is a multifunctional protein that directly regulates the activity of ARF GTPases, PAK family kinases, and Rab1. This work for the first time identified ARF GTPases and PAK as its principle host targets, which have been shown to participate in the regulation of membrane trafficking. Molecular structure of EspG in complex with ARF in an active GTP-bound conformation has revealed a unique binding orientation, which prevents inactivation of ARF by interfering with ARFGAP binding. Interestingly, this mode of binding does not disrupt select interactions of ARF with its downstream targets, effectively establishing an active ARF signaling complex without post-translational modifications, a mechanism frequently displayed by other bacterial effectors. The structure of EspG in complex with Ia3-helix of PAK also showed an unusual method of kinase activation, revealing a potential novel regulatory site on PAK.

Importantly, EspG displays scaffolding properties, capable of simultaneously interacting with ARF and PAK. This suggests that EspG nucleates a novel active complex that coordinates two pathways within a single signaling event. Because binding of either substrate does not appear to have a significant effect on EspG activity toward the other, scaffolding properties appear to play a role for spatio-temporal regulation of separate pathways, rather than cooperative. Moreover, binding sites for ARF and PAK share structural elements, consistent with the idea that affinity of EspG for multiple substrates has evolved in parallel.

Recently, Rab1 has been identified as an additional target of EspG. Similar to its function toward ARF1 GTPase, EspG also displays a direct catalytic activity toward Rab1, in this case acting as a GAP. Importantly, the binding interface for Rab1 was also on the surface adjacent to ARF1 site, permitting simultaneous binding of the two GTPases. We have been able to assess the individual contributions of EspG properties toward ARF1 and Rab1, and indeed discovered that both functions play a critical role in its mechanism. These findings highlight that simultaneous recognition of multiple host proteins by a bacterial virulence factor is thus a unique mechanistic strategy, rather than an incidental binding.

One of the key discoveries of this work is that scaffolding properties of EspG appear to be inherently encoded in its molecular architecture. Unlike classical scaffolding proteins that contain linked individual domains responsible for specific protein binding, EspG is a small globular protein whose binding sites for host targets seem to share common structural elements. Therefore, EspG represents a novel class of single domain molecular scaffolds, which harbor direct catalytic properties toward their substrates.

EspG reveals a novel mechanism of PAK activation

The capacity of a eukaryotic cell to survive and function is directly tied to its ability to rapidly adapt cellular processes in response to both external and internal stimuli. One class of proteins in particular, the Rho family GTPases, plays a critical role in signal transduction. Through interaction with downstream effectors, Rho GTPases regulate the assembly and branching of actin filaments at the membrane interface, creating a dynamic structure that is responsible for cell to cell adhesion in tissues, cytokinesis, cell morphology, phagocytosis, and

others (Jaffe & Hall, 2005). In addition, this family of proteins is also capable of modulating the activity of transcriptional regulators both directly and indirectly, exhibiting control over cell cycle progression and survival (Miralles, Posern, Zaromytidou, & Treisman, 2003; Perona et al., 1997). Their significance is especially highlighted by many diseases linked to their absence or dysregulation (Nadif Kasri & Van Aelst, 2008; Pai, Kim, & Williams, 2010).

An analysis of known downstream GTPase effectors revealed a common structural feature known as the Cdc42/Rac Interactive Binding (CRIB) domain for a number of proteins, which include kinases, actin-binding scaffolds, and adaptor proteins (Burbelo, Drechsel, & Hall, 1995). Whereas these CRIB-domain containing proteins are otherwise distinct both structurally and functionally, they are related in that activation is dependent on direct interaction of CRIB with active Cdc42 or Rac GTPases. A simplified model view for effector protein inhibition versus activation can thus be presented by defining the protein through two core domains – an inhibitory CRIB-containing GTPase binding domain (GBD) and an activity-bearing domain (AD).

While the general mechanism of activation includes unfolding and rearrangement of GBD/AD interface due to binding of Cdc42/Rac GTPases to the CRIB domain, EspG targets residues not previously identified in any other interactions of PAK. Through our structural and biochemical studies, we have shown that EspG unfolds a regulatory Ia3 helix in PAK GBD, which leads to displacement of the critical residues involved in maintaining an inhibitory GBD/KD contact. We also discovered that this mechanism of activation may be dependent on conformational changes that autoinhibited PAK dimer may undergo naturally. This comes from observation that while Cdc42 is capable of disrupting GBD/KD interface in an in vitro system

reconstituted with purified GBD and KD domains, consistent with its known mechanism, EspG cannot relieve this inhibition. Despite mechanistic differences, however, EspG is a potent inducer of PAK activity, reaching activation levels equivalent to the endogenous agonist Cdc42.

EspG selectively regulates ARF1 signaling

The molecular structure of EspG in complex with its principle host target EspG has revealed the specificity for an active GTP-bound conformation of ARF GTPases, however the binding residues of ARF1 appear largely conserved among ARF isoforms. This finding suggests that EspG affects a diverse range of signaling processes regulated by this family of GTPases. Indeed, we have confirmed EspG interaction with all three classes of ARFs. Additionally, we have observed phenotypic indications of multiple ARF pathways disruption, i.e. the appearance of endosomes (ARF6-dependnet) and morphology of Golgi (ARF1-dependent).

An important mechanistic insight into the function of EspG toward ARF GTPases came from noting that unlike other interacting partners of ARFs that bind primarily to the Switch regions, EspG sits over the nucleotide-binding pocket. Because ARF GTPases have almost no intrinsic GTPase activity, they require GAP-binding to hydrolyze GTP and switch to an inactive state. This mode of binding sterically hinders access to the nucleotide binding residues of ARFs and as a result prevents ARFGAP-mediated inactivation of ARF signaling. However, it is also unique in that EspG binding does not compete with at least some downstream substrates of ARF1, essentially locking ARF in a GTP-bound state and thus inducing an active signaling complex.

Together, these findings expose two important features driven by the molecular architecture of EspG and critical for its function. First, by maintaining ARF in an active state by an allosteric binding, rather than enzymatically regulating its activity through post-translational modification of acting on its regulatory molecules, EspG function is spatiotemporally restricted locally to a single ARF signaling event. This ensures precise control over signal transduction events affected by EspG due to is targeting of multiple host enzymes, which is particularly relevant in the context its scaffolding properties. Second, by sterically defining the access of host substrates to an active ARF1-GTP membrane complex, EspG can inhibit some interactions while allowing others, thus selectively enhancing specific ARF1 pathways. In agreement with our predictions, we have shown that EspG allows recruitment of select ARF1 substrates to membranes and protects this complex from GAP-induced dissociation and inactivation. At the same time, selective protection of an ARF1 signaling axis enhances recruitment of ARF1-dependnet tethering factors, which contributes to EspG function in inhibiting host endomembrane transport.

Catalytic scaffolding as a strategy for selective regulation of dynamic systems

Endomembrane network is a highly dynamic system that maintains its identity despite constant bidirectional flux of membranes and cargo. Its complex nature requires careful coordination, orchestrated by a variety of proteins and interactions. Identification of the proteins and their functions is generally achieved by assessing defects observed in their absence. Specifically, by introducing dominant negative or constitutively active constructs, silencing by siRNA, or applying specific small molecule inhibitors. While these strategies is very efficient in

highlighting the primary roles of host proteins, they do not have the resolution to dissect the roles of specific interaction cascades that driving specific cellular events. Global targeting of an individual signaling pathway does not differentiate its local function based on interacting partner availability.

Scaffolding molecules are commonly used by cells to enhance signaling, either by establishing a catalytic chain of multiple enzymes or by directing substrate availability through bringing molecules close to their targets, instead of free diffusion. On the reverse side, using substrate availability to determine active signaling location can thus be used to restrict regulatory function to a very specific event. EspG thus defines a new class of catalytic scaffolds, whose functional environment is dependent on the right availability of signaling molecules. Indeed, we show that disassembly of Golgi resulting from bidirectional arrest of membrane trafficking at ERGIC requires simultaneous activity toward both ARF1 and Rab1 GTPases. Because ARF1 and Rab1 are both found on ERGIC, this both determines the primary site of EspG function, but also acts as a safeguard against potential effects on the cell due to disruption of either ARF or Rab signaling at other locations within a host cell.

It is interesting to note how combinatorial approach can thus be used to diversify the type of individual processes that can be targeted by catalytic scaffolds with high specificity. Additional interactions required for the function of a scaffold can be used not only to direct it to a subcellular compartment, but also to define its regulatory properties. EspG has been found to regulate the activity of ARF and Rab GTPases, as well as PAK kinases. Its homolog VirA, however, shares GAP activity toward Rab1, but lacks either ARF or PAK binding, despite similar overall fold. Consistent with the adaptability of small protein scaffolds to unique

functions associated with the lifestyle of a bacterium, VirA is likely to recognize different host targets, which remain to be determined. Further supporting an ongoing adaptation of catalytic scaffold differentiation is our finding that PAK and Rab1 have overlapping binding sites on EspG, suggesting a possibility that EspG may be at a transition step toward acquiring a higher preference toward either enzyme.

Perspectives

Endomembrane transport as a target of pathogenic bacteria

EspG is a potent inhibitor of host endomembrane transport. While we initially have identified it through a screen focused on protein secretion through the General Secretory Pathway, we now have established its role in inhibiting bidirectional membrane transport. While inhibition of protein secretion alone is highly advantageous to a pathogen by preventing secretion of proinflammatory cytokines and chemokines, the additional arrest of vesicular transport it is likely to have a far more reaching consequences.

Like many gut infections, EHEC clinically has a hallmark diarrheal presentation. Accumulation of fluid in stool is attributed to disruption of tight junction barrier within the intestinal epithelium. These junctions are dependent on various proteins that span the membrane and promote lateral adherence of epithelial cells to each other. One such protein is e-cadherin, a calcium dependent cadherin involved in maintaining the trans-epithelial barrier. Its presence on plasma membrane is regulated by the GSP and recycling endosomes, which play roles in the initial delivery and regulation of its membrane levels, respectively. Once at the membrane, it is stabilized by binding to β-catenin. Inhibition of membrane traffic would prevent its transport to

the membrane, while dysregulation of endosomes (an ARF6-regulated process) would in turn affect its availability for tight junction formation. We would thus expect EspG to have an effect on tight junctions, given its role described in this work. Indeed, it has been shown that EspG increases trans-epithelial resistance (TER) in epithelial cells monolayer (Tomson et al., 2005). We have also found an increase in cytosolic staining of β-catenin, which could further lead to a leaky intercellular barrier and accumulation of fluid in the gut due to reduced β-catenin/e-cadherin membrane interaction (Fig. 37).

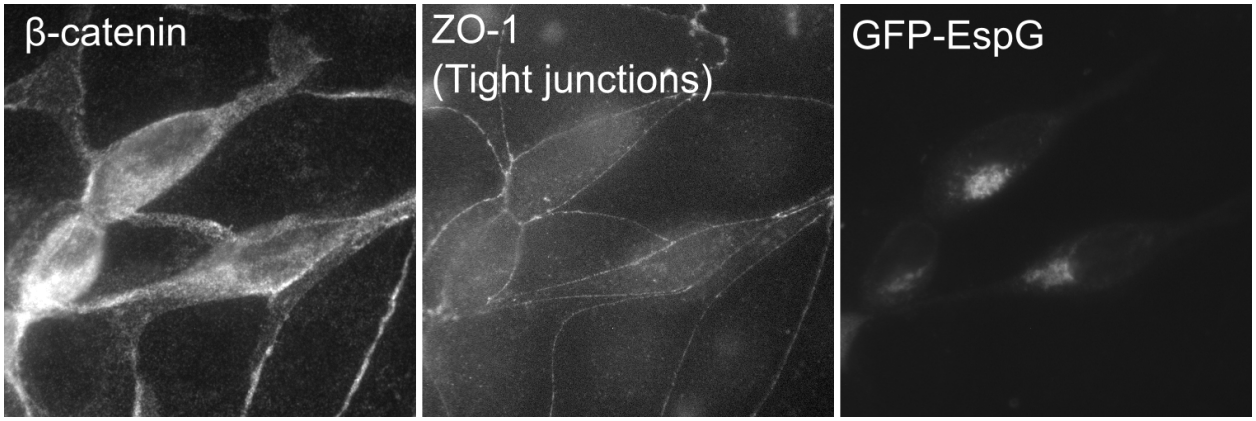

Figure 37. EspG induces b-catenin and tight junction changes.
Fluorescent micrograph showing accumulation of β-catenin in the cytoplasmic portion of the cell. Hazy appearance of tight junction protein Zona Occluden-1 is also visible (middle slide). Cells were transfected with GFP-EspG overnight.

Considering the roles of ARF family of proteins, and potential signaling interplay between ARFs, PAK, and Rab1, it is not surprising that EspG can variably affects many signaling pathways within a host cell. The precise role of its activity toward individual enzyme remains to be investigated further. Here, we focused on characterization of its activity toward ARF1 and Rab1, which we believe to be its primary function as supported both by primary

localization of EspG with fragmented Golgi remnants and the arrest of vesicular transport at ERGIC. How its properties coordinate in context of an infection is the subject of future studies. Potential roles include inhibition of immune signaling pathways, regulation of cell cycle, and secretion of nutrients to support colonization and survival of EHEC.

Evolutionary specialization of bacterial catalytic scaffold proteins

Here we report how scaffolding properties of EspG define its function in regulating the host endomembrane network through direct regulation of host ARF and Rab1 GTPases, and PAK kinase. Importantly, we show that EspG does not mimic phenotypes associated with inhibition of ARF1 cycling or overexpression of Rab1 GAP. Instead, EspG displays a unique cellular phenotype that is exclusively dependent on ARF1 binding and Rab1-GAP activity. This strongly suggests that by scaffolding catalytic function for multiple host proteins, type III secreted effector proteins can carve out a signaling niche within complex regulatory networks.

Indeed, another member of EspG family, VirA from *S. flexneri*, has a similar structural fold and is likely to be a scaffold. While VirA shares Rab1 GAP activity, it lacks structural elements that are found in EspG and allow interaction with ARF and PAK. Taking into account distinct lifestyles of EHEC and Shigella (extracellular vs. intracellular), it is not surprising that the two bacteria would have different goals in the regulation of host signaling pathways. In fact, virulence factors from extracellular pathogens generally displayed less interference with host protein secretion in our screen (see Fig. 6), as opposed to what we observe with EspG. Identification of additional targets of VirA can therefore provide important new insight into the

cooperation of other host pathways in specific cellular events, as well as help define the molecular course of *Shigella* infection.

Structural data presented in this work also provides an interesting perspective to the evolutionary adaptation of proteins toward their function. Although at least three classes of host enzymes are now confirmed as targets of EspG, PAK and Rab1 binding to the same interface adjacent to ARF1 binding site. Whether both ARF/PAK and ARF1/Rab1 complexes play equivalent roles in EspG mechanism, or one is more dominant, remains to be investigated in more detail. Several possibilities exist: both complexes may be active dependent on temporal localization of EspG inside the host cell, or EspG could be transitioning and acquiring preference for either Rab1 or PAK (Fig. 38). Because after translocation through the Type III apparatus EspG travels to perinuclear ERGIC sites, it is easy to imagine that EspG would encounter different substrate availability and ARF/PAK complex indeed may play a role. On the other hand, phylogenetic analysis of bacteria and proteins can be used to trace the course of EspG evolution to determine whether PAK or Rab1 binding has been acquired first.

This study contributes to and builds on an unprecedented level of structure-to-function data of any one protein, which includes structural information of apo-EspG and in complex with three of its host targets, as well as biochemical and cell biological characterization. Data presented here can thus be used to improve our understanding how the molecular architecture is driven by its target substrates.

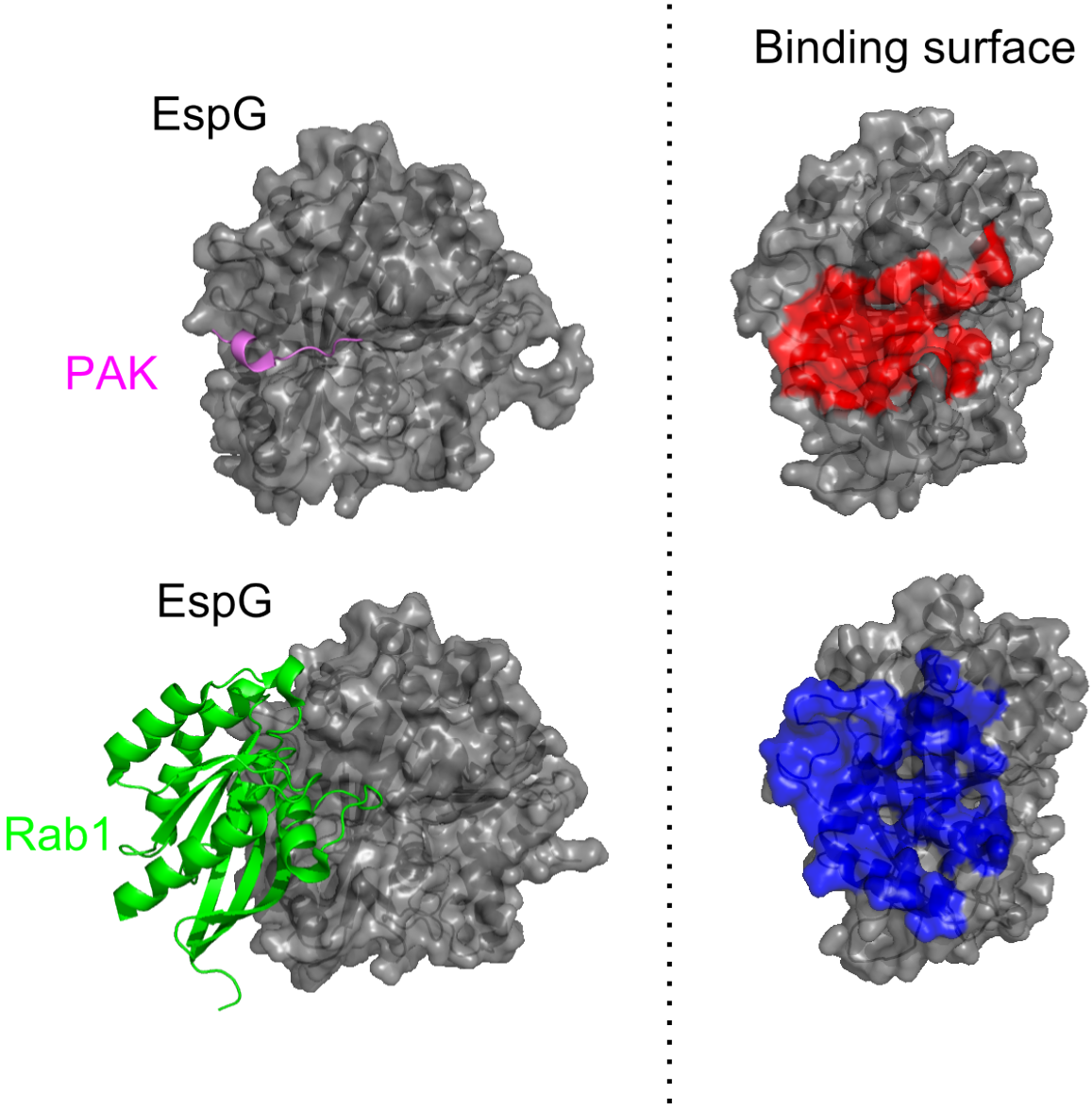

Figure 38. Structural evolution of EspG toward host target specificity.
Crystal structures of EspG in complex with PAK and Rab1are shown, highlighting the similarity in a binding manner and lack of any major conformational differences in EspG; left panel. Surface residues of EspG involved in making direct contact with PAK or Rab1 are shown in red and blue, respectively; right panel.

Secreted bacterial proteins as molecular tools to probe complex regulatory networks

Here, we show an alternative approach to studying complex host regulatory networks, i.e. endomembrane traffic. Specifically, we show bacterial type III secreted proteins can be effectively used to investigate how specific cellular events are controlled by dynamic coordination of signaling enzymes. High efficacy of secreted bacterial virulence factors in hijacking host signaling pathways makes them effective tools to identify key regulatory molecules. At the same time, wide diversity of pathogens with different tropisms, lifestyles, and cellular phenotypes represents an extensive library that is likely to target nearly all aspects of eukaryotic signaling.

Identification and characterization of EspG from EHEC reveals a critical role of ARF1/Rab1 coordination in vesicle tethering and membrane fusion in the early General Secretory Pathway. While EspG induces membrane tethering by selectively protecting and enhancing ARF1 signaling, together with localized inactivation of Rab1-dependent machinery, its function does not mimic phenotypes observed during disruption of ARF1 cycling or inactivation of Rab1 signaling by endogenous Rab1-GAP. Thusly, this finding exposes the significance of membrane budding and fusion events orchestrated by ARF1 and Rab1 on ERGIC membranes vesicle targeting and Golgi maintenance, which would have been difficult to identify using conventional strategies, such as protein overexpression or knockdown. This work provides a proof of concept for how bacterial virulence factors can be used to probe regulatory systems of eukaryotic cells to complement existing methods.

APPENDIX A

Crystallographic Determination Information

Crystallization and X-ray diffraction data collection

Crystals of EspG–ARF6 were grown using the hanging-drop vapor diffusion method from drops containing 2 µl protein (7 mg ml^{-1}) and 1 µl of reservoir solution (0.1M sodium acetate, pH 5.0, 2% PEG4000, 5% 2,3-methylpentanediol (MPD)), and equilibrated over 500µl of reservoir solution. Bipyramid-like crystals appeared after 1 d at 20°C and grew to their maximal extent in 2–3 d. Crystals were relatively large in all three dimensions ($0.3\times0.6\times0.3mm^3$). Cryo-protection was performed by transferring the crystals to a final solution of 37% MPD, 0.1M sodium acetate, pH 5.0, and 2% PEG4000, increasing in 5% steps of MPD over the course of 10 min at 20°C. Crystals were flash-frozen using liquid nitrogen. EspG–ARF6 crystals had the symmetry of space group $P4_32_12$ with unit-cell parameters of $a = b =$ 104.6Å and c = 98.3Å, and contained one molecule each of EspG and ARF6 per asymmetric unit. EspG–ARF6 crystals diffracted isotropically to a d_{min} of 2.50Å when exposed to synchrotron radiation.

Crystals of EspG–PAK2 were grown using the hanging-drop vapor diffusion method from drops containing 1 µl protein (12 mg ml^{-1}) and 1 µl of reservoir solution (0.1 M Tris, pH 8.0, 0.25 M sodium chloride and 20% PEG4000) and equilibrated over 500 µl of reservoir solution. Plate-like crystals appeared after 2 d at 20°C and grew to their maximal extent by 4–5d. Crystals were large in two dimensions ($0.2\times0.5mm^2$) and relatively thin (0.1mm). Cryo-protection was performed by transferring the crystals to a final solution of 15% ethylene glycol, 22% PEG4000, 0.1 M Tris, pH 8.0, and 0.25 M sodium chloride, increasing in 5% steps of

ethylene glycol over the course of 10 min at 20 °C. Crystals were flash-frozen using liquid nitrogen. EspG–PAK crystals had the symmetry of space group $P2_12_12_1$ with unit-cell parameters of a = 86.7 Å, b = 104.6 Å and c = 192.0 Å, and contained four molecules of EspG–PAK per asymmetric unit. EspG–PAK crystals diffracted to a d_{min} of 2.85 Å when exposed to synchrotron radiation. Data were indexed, integrated and scaled using the HKL-3000 program package[31]. Data collection statistics are provided in Table 1.

Phase determination and structure refinement: Phases for the EspG–ARF6 complex were obtained from a three-wavelength anomalous dispersion experiment using selenomethionyl-substituted protein with data to a d_{min} of 2.50 Å. Fifteen selenium sites were located using the program SHELXD[32]; this represented nine single-occupancy selenium sites and six half-occupancy selenium sites per EspG–ARF6 heterodimer. Phases were refined with the program MLPHARE, resulting in an overall figure of merit of 0.41 for data between 32.9 and 2.50 Å. Phases were further improved by density modification with the program DM[33], resulting in a figure of merit of 0.70. An initial model containing 97% of all EspG residues was automatically generated by alternating cycles of the programs RESOLVE[34] and BUCCANEER[35]. Inspection of the electron density map revealed density for the ARF6 molecule, but the automatic model-building programs were unable to build a complete model for this protein. Placement of a model for ARF6 in the cell was performed by means of molecular replacement in the program PHASER[36] using the GTPγS-bound ARF6 (Protein Data Bank ID, 2J5X) as a search model.

Additional residues for EspG were manually modeled in the program O[37]. Refinement was performed with the data collected at the selenium peak wavelength to a resolution of 2.50 Å using the program PHENIX[38] with a random 5% of all data set aside for an R_{free} calculation. The

current model contains one EspG and one ARF6 monomer; included are residues 47–395 of EspG, residues 14–174 of ARF6, one Mg^{2+}-GTP and 138 water molecules. The R_{work} value is 22.5% and the R_{free} value is 32.4%. The higher-than-average R_{free} value is probably due to the relative dearth of lattice contacts for the ARF6 molecule, as evidenced by weak electron density for the portions of ARF6 that are distal to the EspG-binding site. The density for the portions of ARF6 (residues 20–63 and 152–170) that are proximal to EspG and to the Mg^{2+}-GTP is strong and well connected. A Ramachandran plot generated with MOLPROBITY[39] indicated that 99.0% of all protein residues are in allowed regions.

Phases for EspG–PAK were obtained by means of molecular replacement in the program PHASER using the coordinates of EspG from the EspG–ARF6 structure as a search model. Model building and refinement was performed as described above, with the following modification: owing to the lower resolution of the data, restrained non-crystallographic symmetry was implemented during refinement. The current model contains four EspG monomers and four PAK peptides. Included are EspG residues 42–158, 163–318 and 321–397 and PAK residues 122–135, in complex A; EspG residues 43–397 and PAK residues 122–133, in complex B; EspG residues 42–158, 163–316 and 322–395 and PAK residues 123–132, in complex C; and EspG residues 42–158, 163–317 and 320–395 and PAK residues 122–134, in complex D. The R_{work} value is 20.3% and the R_{free} value is 28.6%. A Ramachandran plot generated with MOLPROBITY indicated that 99.4% of all protein residues are in allowed regions. Phasing and model refinement statistics are provided in Table 1.

Table I. Data collection, phasing and refinement statistics

Data collection				
Crystal	EspG-Arf6 Se[a] *peak*	EspG-Arf6 Se[a] *inflection point*	EspG-Arf6 Se[a] *remote*	EspG-PAK
Space group	$P4_32_12$	$P4_32_12$	$P4_32_12$	$P2_12_12_1$
Energy (eV)	12,679.2	12,674.9	12,779.4	12,686.5
Resolution range (Å)	32.9 – 2.50 (2.54 – 2.50)	32.9 – 2.50 (2.54 – 2.50)	32.9 – 2.50 (2.54 – 2.50)	40.5 – 2.85 (2.90 – 2.85)
Unique reflections	35,964 (1,794)	35,993 (1,800)	36,047 (1,818)	42,088 (2,195)
Multiplicity	9.6 (9.9)	9.1 (9.3)	9.6 (9.8)	4.8 (4.8)
Data completeness (%)	99.8 (100.0)	99.8 (100.0)	99.8 (100.0)	99.8 (100.0)
R_{merge} (%)[b]	7.3 (83.6)	6.6 (94.0)	6.1 (90.8)	7.6 (59.5)
I/σ(I)	45.8 (2.3)	44.3 (2.0)	45.4 (2.2)	18.8 (2.2)
Wilson B-value (Å^2)	68.9	70.1	71.0	77.0
Phase determination				
Anomalous scatterers	selenium, 15 out of 12 possible sites[c]			
Figure of merit (32.9 – 2.50 Å)	0.41			
Refinement statistics				
Crystal	EspG-Arf6[d]		EspG-PAK	
Resolution range (Å)	29.0 – 2.50 (2.59 – 2.50)		29.6 – 2.85 (2.95 – 2.85)	
No. of reflections R_{work}/R_{free}	34,977/1,804 (2,620/152)		41,480/2,052 (3,862/235)	
Data completeness (%)	97.4 (78.0)		99.9 (100.0)	
Atoms (non-H protein/solvent)	4,023/138		11,254/0	
R_{work} (%)	22.3 (30.5)		20.3 (32.4)	
R_{free} (%)	32.4 (40.1)		28.6 (42.5)	
R.m.s.d. bond length (Å)	0.015		0.008	
R.m.s.d. bond angle (°)	1.27		1.14	
Mean B-value (Å^2) (protein/nucleotide/solvent/peptide)	65.0/51.2/35.7/NA		76.7/NA/NA/99.3	
Ramachandran plot (%) (favored/additional/disallowed)[e]	89.3/9.7/1.0		93.6/5.8/0.6	
Maximum likelihood coordinate error	0.44		0.46	
Missing residues, by chain	A: 42-46, 396-398. B: None.		A: 159-162, 319-320, 398. B: 42, 398. C: 159-162, 317-321, 396-398. D: 159-162, 318-319, 396-398. E: 121, 136. F: 121, 134-136. G: 121-122, 133-136. H: 121, 135-136.	

Data for the outermost shell are given in parentheses.

[a]Bijvoet-pairs were kept separate for data processing

[b]$R_{merge} = 100\ \Sigma_h\Sigma_i|I_{h,i} - \langle I_h\rangle|/\Sigma_h\Sigma_i I_{h,i}$, where the outer sum (h) is over the unique reflections and the inner sum (i) is over the set of independent observations of each unique reflection.

[c]Three methionine residues that were present in two conformations were located in *SHELXD* and refined in *MLPHARE*.
[d]The Se peak dataset was used for refinement of the EspG-Arf6 structure.
[e]As defined by the validation suite MolProbity (Davis, I.W., Leaver-Fay, A., Chen, V.B., Block, J.N., Kapral, G.J., Wang, X., Murray, L.W., Arendall, W.B., Snoeyink, J., Richardson, J.S. and Richardson, D.C. (2007) MolProbity: all-atom contacts and structure validation for proteins and nucleic acids. Nucleic Acids Res. **35**, W375-W383.).

BIBLIOGRAPHY

Abdul-Manan, N., Aghazadeh, B., Liu, G. A., Majumdar, A., Ouerfelli, O., Siminovitch, K. A., & Rosen, M. K. (1999). Structure of Cdc42 in complex with the GTPase-binding domain of the 'Wiskott-Aldrich syndrome' protein. *Nature, 399*(6734), 379-383. doi: 10.1038/20726

Akeda, Y., & Galan, J. E. (2005). Chaperone release and unfolding of substrates in type III secretion. *Nature, 437*(7060), 911-915. doi: 10.1038/nature03992

Aktories, K., Schmidt, G., & Just, I. (2000). Rho GTPases as Targets of Bacterial Protein Toxins. *Biological Chemistry, 381*(5-6), 421-426. doi: 10.1515/bc.2000.054

Alto, N. M., & Orth, K. (2012). Subversion of cell signaling by pathogens. *Cold Spring Harb Perspect Biol, 4*(9), a006114. doi: 10.1101/cshperspect.a006114

Alto, N. M., Weflen, A. W., Rardin, M. J., Yarar, D., Lazar, C. S., Tonikian, R., . . . Dixon, J. E. (2007). The type III effector EspF coordinates membrane trafficking by the spatiotemporal activation of two eukaryotic signaling pathways. *J Cell Biol, 178*(7), 1265-1278.

Appenzeller-Herzog, C., & Hauri, H. P. (2006). The ER-Golgi intermediate compartment (ERGIC): in search of its identity and function. *J Cell Sci, 119*(Pt 11), 2173-2183. doi: 10.1242/jcs.03019

Barlowe, C. K., & Miller, E. A. (2013). Secretory protein biogenesis and traffic in the early secretory pathway. *Genetics, 193*(2), 383-410. doi: 10.1534/genetics.112.142810

Baxt, L. A., Garza-Mayers, A. C., & Goldberg, M. B. (2013). Bacterial subversion of host innate immune pathways. *Science, 340*(6133), 697-701. doi: 10.1126/science.1235771

Bokoch, G. M. (2003). Biology of the p21-activated kinases. *Annu Rev Biochem, 72*, 743-781.

Borthakur, A., Gill, R. K., Hodges, K., Ramaswamy, K., Hecht, G., & Dudeja, P. K. (2006). Enteropathogenic Escherichia coli inhibits butyrate uptake in Caco-2 cells by altering the apical membrane MCT1 level. *Am J Physiol Gastrointest Liver Physiol, 290*(1), G30-35.

Brandizzi, F., & Barlowe, C. (2013). Organization of the ER-Golgi interface for membrane traffic control. *Nat Rev Mol Cell Biol, 14*(6), 382-392. doi: 10.1038/nrm3588

Bremser, M., Nickel, W., Schweikert, M., Ravazzola, M., Amherdt, M., Hughes, C. A., . . . Wieland, F. T. (1999). Coupling of coat assembly and vesicle budding to packaging of putative cargo receptors. *Cell, 96*(4), 495-506.

Burbelo, P. D., Drechsel, D., & Hall, A. (1995). A conserved binding motif defines numerous candidate target proteins for both Cdc42 and Rac GTPases. *J Biol Chem, 270*(49), 29071-29074.

Burnaevskiy, N., Fox, T. G., Plymire, D. A., Ertelt, J. M., Weigele, B. A., Selyunin, A. S., . . . Alto, N. M. (2013). Proteolytic elimination of N-myristoyl modifications by the Shigella virulence factor IpaJ. *Nature, 496*(7443), 106-109. doi: 10.1038/nature12004

Chardin, P., & McCormick, F. (1999). Brefeldin A: the advantage of being uncompetitive. *Cell, 97*(2), 153-155.

Cherfils, J., & Zeghouf, M. (2013). Regulation of small GTPases by GEFs, GAPs, and GDIs. *Physiol Rev, 93*(1), 269-309. doi: 10.1152/physrev.00003.2012

Clements, A., Smollett, K., Lee, S. F., Hartland, E. L., Lowe, M., & Frankel, G. (2011). EspG of enteropathogenic and enterohemorrhagic E. coli binds the Golgi matrix protein GM130 and disrupts the Golgi structure and function. *Cell Microbiol, 13*(9), 1429-1439. doi: 10.1111/j.1462-5822.2011.01631.x

Cole, N. B., Sciaky, N., Marotta, A., Song, J., & Lippincott-Schwartz, J. (1996). Golgi dispersal during microtubule disruption: regeneration of Golgi stacks at peripheral endoplasmic reticulum exit sites. *Mol Biol Cell, 7*(4), 631-650.

Collins, B. M., Watson, P. J., & Owen, D. J. (2003). The structure of the GGA1-GAT domain reveals the molecular basis for ARF binding and membrane association of GGAs. *Dev Cell, 4*(3), 321-332.

D'Souza-Schorey, C., & Chavrier, P. (2006). ARF proteins: roles in membrane traffic and beyond. *Nat Rev Mol Cell Biol, 7*(5), 347-358.

Davis, J., Wang, J., Tropea, J. E., Zhang, D., Dauter, Z., Waugh, D. S., & Wlodawer, A. (2008). Novel fold of VirA, a type III secretion system effector protein from Shigella flexneri. *Protein Sci*.

Deacon, S. W., Beeser, A., Fukui, J. A., Rennefahrt, U. E., Myers, C., Chernoff, J., & Peterson, J. R. (2008). An isoform-selective, small-molecule inhibitor targets the autoregulatory mechanism of p21-activated kinase. *Chem Biol, 15*(4), 322-331.

Deng, Y., Golinelli-Cohen, M. P., Smirnova, E., & Jackson, C. L. (2009). A COPI coat subunit interacts directly with an early-Golgi localized Arf exchange factor. *EMBO Rep, 10*(1), 58-64. doi: 10.1038/embor.2008.221

Donaldson, J. G., & Honda, A. (2005). Localization and function of Arf family GTPases. *Biochem Soc Trans, 33*(Pt 4), 639-642. doi: 10.1042/BST0330639

Donaldson, J. G., Honda, A., & Weigert, R. (2005). Multiple activities for Arf1 at the Golgi complex. *Biochim Biophys Acta, 1744*(3), 364-373. doi: 10.1016/j.bbamcr.2005.03.001

Donaldson, J. G., & Jackson, C. L. (2011). ARF family G proteins and their regulators: roles in membrane transport, development and disease. *Nat Rev Mol Cell Biol, 12*(6), 362-375. doi: 10.1038/nrm3117

Dong, N., Zhu, Y., Lu, Q., Hu, L., Zheng, Y., & Shao, F. (2012). Structurally distinct bacterial TBC-like GAPs link Arf GTPase to Rab1 inactivation to counteract host defenses. *Cell, 150*(5), 1029-1041. doi: 10.1016/j.cell.2012.06.050

Drin, G., Morello, V., Casella, J. F., Gounon, P., & Antonny, B. (2008). Asymmetric tethering of flat and curved lipid membranes by a golgin. *Science, 320*(5876), 670-673. doi: 10.1126/science.1155821

Duesbery, N. S., Webb, C. P., Leppla, S. H., Gordon, V. M., Klimpel, K. R., Copeland, T. D., . . . Vande Woude, G. F. (1998). Proteolytic inactivation of MAP-kinase-kinase by anthrax lethal factor. *Science, 280*(5364), 734-737.

Elliott, S. J., Krejany, E. O., Mellies, J. L., Robins-Browne, R. M., Sasakawa, C., & Kaper, J. B. (2001). EspG, a novel type III system-secreted protein from enteropathogenic Escherichia coli with similarities to VirA of Shigella flexneri. *Infect Immun, 69*(6), 4027-4033.

Espinosa, A., & Alfano, J. R. (2004). Disabling surveillance: bacterial type III secretion system effectors that suppress innate immunity. *Cell Microbiol, 6*(11), 1027-1040. doi: 10.1111/j.1462-5822.2004.00452.x

Galan, J. E., & Collmer, A. (1999). Type III secretion machines: bacterial devices for protein delivery into host cells. *Science, 284*(5418), 1322-1328.

Galan, J. E., & Wolf-Watz, H. (2006). Protein delivery into eukaryotic cells by type III secretion machines. *Nature, 444*(7119), 567-573.

Germane, K. L., Ohi, R., Goldberg, M. B., & Spiller, B. W. (2008). Structural and functional studies indicate that Shigella VirA is not a protease and does not directly destabilize microtubules. *Biochemistry, 47*(39), 10241-10243. doi: 10.1021/bi801533k

Gillingham, A. K., Tong, A. H., Boone, C., & Munro, S. (2004). The GTPase Arf1p and the ER to Golgi cargo receptor Erv14p cooperate to recruit the golgin Rud3p to the cis-Golgi. *J Cell Biol, 167*(2), 281-292. doi: 10.1083/jcb.200407088

Guttman, J. A., Samji, F. N., Li, Y., Deng, W., Lin, A., & Finlay, B. B. (2007). Aquaporins contribute to diarrhoea caused by attaching and effacing bacterial pathogens. *Cell Microbiol, 9*(1), 131-141.

Haas, A. K., Yoshimura, S., Stephens, D. J., Preisinger, C., Fuchs, E., & Barr, F. A. (2007). Analysis of GTPase-activating proteins: Rab1 and Rab43 are key Rabs required to maintain a functional Golgi complex in human cells. *J Cell Sci, 120*(Pt 17), 2997-3010. doi: 10.1242/jcs.014225

Ham, H., & Orth, K. (2012). The role of type III secretion system 2 in Vibrio parahaemolyticus pathogenicity. *J Microbiol, 50*(5), 719-725. doi: 10.1007/s12275-012-2550-2

Hanzal-Bayer, M., Renault, L., Roversi, P., Wittinghofer, A., & Hillig, R. C. (2002). The complex of Arl2-GTP and PDE delta: from structure to function. *Embo J, 21*(9), 2095-2106.

Harrison, R. E., Brumell, J. H., Khandani, A., Bucci, C., Scott, C. C., Jiang, X., . . . Grinstein, S. (2004). Salmonella impairs RILP recruitment to Rab7 during maturation of invasion vacuoles. *Mol Biol Cell, 15*(7), 3146-3154. doi: 10.1091/mbc.E04-02-0092

Horgan, C. P., & McCaffrey, M. W. (2011). Rab GTPases and microtubule motors. *Biochem Soc Trans, 39*(5), 1202-1206. doi: 10.1042/BST0391202

Hutagalung, A. H., & Novick, P. J. (2011). Role of Rab GTPases in membrane traffic and cell physiology. *Physiol Rev, 91*(1), 119-149. doi: 10.1152/physrev.00059.2009

Isabet, T., Montagnac, G., Regazzoni, K., Raynal, B., El Khadali, F., England, P., . . . Menetrey, J. (2009). The structural basis of Arf effector specificity: the crystal structure of ARF6 in a complex with JIP4. *Embo J, 28*(18), 2835-2845.

Jaffe, A. B., & Hall, A. (2005). Rho GTPases: biochemistry and biology. *Annu Rev Cell Dev Biol, 21*, 247-269.

Kahn, R. A. (2009). Toward a model for Arf GTPases as regulators of traffic at the Golgi. *FEBS Lett, 583*(23), 3872-3879.

Kahn, R. A., & Gilman, A. G. (1984). Purification of a protein cofactor required for ADP-ribosylation of the stimulatory regulatory component of adenylate cyclase by cholera toxin. *J Biol Chem, 259*(10), 6228-6234.

Kim, A. S., Kakalis, L. T., Abdul-Manan, N., Liu, G. A., & Rosen, M. K. (2000). Autoinhibition and activation mechanisms of the Wiskott-Aldrich syndrome protein. *Nature, 404*(6774), 151-158. doi: 10.1038/35004513

Kim, J., Thanabalasuriar, A., Chaworth-Musters, T., Fromme, J. C., Frey, E. A., Lario, P. I., . . . Gruenheid, S. (2007). The bacterial virulence factor NleA inhibits cellular protein secretion by disrupting mammalian COPII function. *Cell Host Microbe, 2*(3), 160-171.

Klausner, R. D., Donaldson, J. G., & Lippincott-Schwartz, J. (1992). Brefeldin A: insights into the control of membrane traffic and organelle structure. *J Cell Biol, 116*(5), 1071-1080.

Lei, M., Lu, W., Meng, W., Parrini, M. C., Eck, M. J., Mayer, B. J., & Harrison, S. C. (2000). Structure of PAK1 in an autoinhibited conformation reveals a multistage activation switch. *Cell, 102*(3), 387-397.

Li, H., Xu, H., Zhou, Y., Zhang, J., Long, C., Li, S., . . . Shao, F. (2007). The phosphothreonine lyase activity of a bacterial type III effector family. *Science, 315*(5814), 1000-1003.

Lippincott-Schwartz, J., Yuan, L. C., Bonifacino, J. S., & Klausner, R. D. (1989). Rapid redistribution of Golgi proteins into the ER in cells treated with brefeldin A: evidence for membrane cycling from Golgi to ER. *Cell, 56*(5), 801-813.

Matsuzawa, T., Kuwae, A., Yoshida, S., Sasakawa, C., & Abe, A. (2004). Enteropathogenic Escherichia coli activates the RhoA signaling pathway via the stimulation of GEF-H1. *EMBO J, 23*(17), 3570-3582. doi: 10.1038/sj.emboj.7600359

Miralles, F., Posern, G., Zaromytidou, A. I., & Treisman, R. (2003). Actin dynamics control SRF activity by regulation of its coactivator MAL. *Cell, 113*(3), 329-342. doi: S0092867403002782 [pii]

Mossessova, E., Corpina, R. A., & Goldberg, J. (2003). Crystal structure of ARF1*Sec7 complexed with Brefeldin A and its implications for the guanine nucleotide exchange mechanism. *Mol Cell, 12*(6), 1403-1411.

Nadif Kasri, N., & Van Aelst, L. (2008). Rho-linked genes and neurological disorders. *Pflugers Arch, 455*(5), 787-797. doi: 10.1007/s00424-007-0385-1

Nagai, H., Kagan, J. C., Zhu, X., Kahn, R. A., & Roy, C. R. (2002). A bacterial guanine nucleotide exchange factor activates ARF on Legionella phagosomes. *Science, 295*(5555), 679-682.

Nie, Z., Hirsch, D. S., & Randazzo, P. A. (2003). Arf and its many interactors. *Curr Opin Cell Biol, 15*(4), 396-404.

O'Neal, C. J., Jobling, M. G., Holmes, R. K., & Hol, W. G. (2005). Structural basis for the activation of cholera toxin by human ARF6-GTP. *Science, 309*(5737), 1093-1096.

Olkkonen, V. M., & Stenmark, H. (1997). Role of Rab GTPases in membrane traffic. *Int Rev Cytol, 176*, 1-85.

Padrick, S. B., Cheng, H. C., Ismail, A. M., Panchal, S. C., Doolittle, L. K., Kim, S., . . . Rosen, M. K. (2008). Hierarchical regulation of WASP/WAVE proteins. *Mol Cell, 32*(3), 426-438. doi: S1097-2765(08)00726-0 [pii]
10.1016/j.molcel.2008.10.012

Padrick, S. B., & Rosen, M. K. (2010). Physical mechanisms of signal integration by WASP family proteins. *Annu Rev Biochem, 79*, 707-735. doi: 10.1146/annurev.biochem.77.060407.135452

Pai, S. Y., Kim, C., & Williams, D. A. (2010). Rac GTPases in human diseases. *Dis Markers, 29*(3-4), 177-187. doi: 9221636233027803 [pii]
10.3233/DMA-2010-0738

Panic, B., Perisic, O., Veprintsev, D. B., Williams, R. L., & Munro, S. (2003). Structural basis for Arl1-dependent targeting of homodimeric GRIP domains to the Golgi apparatus. *Mol Cell, 12*(4), 863-874.

Pasqualato, S., Menetrey, J., Franco, M., & Cherfils, J. (2001). The structural GDP/GTP cycle of human Arf6. *EMBO Rep, 2*(3), 234-238.

Pernet-Gallay, K., Antony, C., Johannes, L., Bornens, M., Goud, B., & Rios, R. M. (2002). The overexpression of GMAP-210 blocks anterograde and retrograde transport between the ER and the Golgi apparatus. *Traffic, 3*(11), 822-832.

Perona, R., Montaner, S., Saniger, L., Sanchez-Perez, I., Bravo, R., & Lacal, J. C. (1997). Activation of the nuclear factor-kappaB by Rho, CDC42, and Rac-1 proteins. *Genes Dev, 11*(4), 463-475.

Philpott, D. J., McKay, D. M., Mak, W., Perdue, M. H., & Sherman, P. M. (1998). Signal transduction pathways involved in enterohemorrhagic Escherichia coli-induced alterations in T84 epithelial permeability. *Infect Immun, 66*(4), 1680-1687.

Popoff, V., Adolf, F., Brugger, B., & Wieland, F. (2011). COPI budding within the Golgi stack. *Cold Spring Harb Perspect Biol, 3*(11), a005231. doi: 10.1101/cshperspect.a005231

Presley, J. F., Cole, N. B., Schroer, T. A., Hirschberg, K., Zaal, K. J., & Lippincott-Schwartz, J. (1997). ER-to-Golgi transport visualized in living cells. *Nature, 389*(6646), 81-85. doi: 10.1038/38001

Puertollano, R., Randazzo, P. A., Presley, J. F., Hartnell, L. M., & Bonifacino, J. S. (2001). The GGAs promote ARF-dependent recruitment of clathrin to the TGN. *Cell, 105*(1), 93-102.

Reddick, L. E., & Alto, N. M. (2012). Correlative light and electron microscopy (CLEM) as a tool to visualize microinjected molecules and their eukaryotic sub-cellular targets. *J Vis Exp*(63), e3650. doi: 10.3791/3650

Rios, R. M., Sanchis, A., Tassin, A. M., Fedriani, C., & Bornens, M. (2004). GMAP-210 recruits gamma-tubulin complexes to cis-Golgi membranes and is required for Golgi ribbon formation. *Cell, 118*(3), 323-335. doi: 10.1016/j.cell.2004.07.012

Rivera, V. M., Wang, X., Wardwell, S., Courage, N. L., Volchuk, A., Keenan, T., . . . Clackson, T. (2000). Regulation of protein secretion through controlled aggregation in the endoplasmic reticulum. *Science, 287*(5454), 826-830.

Sallee, N. A., Rivera, G. M., Dueber, J. E., Vasilescu, D., Mullins, R. D., Mayer, B. J., & Lim, W. A. (2008). The pathogen protein EspF(U) hijacks actin polymerization using mimicry and multivalency. *Nature, 454*(7207), 1005-1008.

Schmidt, G., Sehr, P., Wilm, M., Selzer, J., Mann, M., & Aktories, K. (1997). Gln 63 of Rho is deamidated by Escherichia coli cytotoxic necrotizing factor-1. *Nature, 387*(6634), 725-729.

Schwartz, S. L., Cao, C., Pylypenko, O., Rak, A., & Wandinger-Ness, A. (2007). Rab GTPases at a glance. *J Cell Sci, 120*(Pt 22), 3905-3910. doi: 10.1242/jcs.015909

Sciaky, N., Presley, J., Smith, C., Zaal, K. J., Cole, N., Moreira, J. E., . . . Lippincott-Schwartz, J. (1997). Golgi tubule traffic and the effects of brefeldin A visualized in living cells. *J Cell Biol, 139*(5), 1137-1155.

Selyunin, A. S., Sutton, S. E., Weigele, B. A., Reddick, L. E., Orchard, R. C., Bresson, S. M., . . . Alto, N. M. (2011). The assembly of a GTPase-kinase signalling complex by a bacterial catalytic scaffold. *Nature, 469*(7328), 107-111. doi: nature09593 [pii]
10.1038/nature09593

Shaw, R. K., Smollett, K., Cleary, J., Garmendia, J., Straatman-Iwanowska, A., Frankel, G., & Knutton, S. (2005). Enteropathogenic Escherichia coli type III effectors EspG and EspG2 disrupt the microtubule network of intestinal epithelial cells. *Infect Immun, 73*(7), 4385-4390.

Shiba, T., Kawasaki, M., Takatsu, H., Nogi, T., Matsugaki, N., Igarashi, N., . . . Wakatsuki, S. (2003). Molecular mechanism of membrane recruitment of GGA by ARF in lysosomal protein transport. *Nat Struct Biol, 10*(5), 386-393.

Short, B., Haas, A., & Barr, F. A. (2005). Golgins and GTPases, giving identity and structure to the Golgi apparatus. *Biochim Biophys Acta, 1744*(3), 383-395. doi: 10.1016/j.bbamcr.2005.02.001

Sinka, R., Gillingham, A. K., Kondylis, V., & Munro, S. (2008). Golgi coiled-coil proteins contain multiple binding sites for Rab family G proteins. *J Cell Biol, 183*(4), 607-615. doi: 10.1083/jcb.200808018

Stenmark, H. (2009). Rab GTPases as coordinators of vesicle traffic. *Nat Rev Mol Cell Biol, 10*(8), 513-525. doi: 10.1038/nrm2728

Sutterlin, C., Hsu, P., Mallabiabarrena, A., & Malhotra, V. (2002). Fragmentation and dispersal of the pericentriolar Golgi complex is required for entry into mitosis in mammalian cells. *Cell, 109*(3), 359-369.

Takeuchi, O., & Akira, S. (2010). Pattern recognition receptors and inflammation. *Cell, 140*(6), 805-820. doi: 10.1016/j.cell.2010.01.022

Terebiznik, M. R., Vazquez, C. L., Torbicki, K., Banks, D., Wang, T., Hong, W., . . . Jones, N. L. (2006). Helicobacter pylori VacA toxin promotes bacterial intracellular survival in gastric epithelial cells. *Infect Immun, 74*(12), 6599-6614. doi: 10.1128/IAI.01085-06

Tomson, F. L., Viswanathan, V. K., Kanack, K. J., Kanteti, R. P., Straub, K. V., Menet, M., . . . Hecht, G. (2005). Enteropathogenic Escherichia coli EspG disrupts microtubules and in conjunction with Orf3 enhances perturbation of the tight junction barrier. *Mol Microbiol, 56*(2), 447-464.

Viaud, J., & Peterson, J. R. (2009). An allosteric kinase inhibitor binds the p21-activated kinase autoregulatory domain covalently. *Mol Cancer Ther, 8*(9), 2559-2565.

Vingadassalom, D., Kazlauskas, A., Skehan, B., Cheng, H. C., Magoun, L., Robbins, D., . . . Leong, J. M. (2009). Insulin receptor tyrosine kinase substrate links the E. coli O157:H7 actin assembly effectors Tir and EspF(U) during pedestal formation. *Proc Natl Acad Sci U S A, 106*(16), 6754-6759.

Visvikis, O., Maddugoda, M. P., & Lemichez, E. (2010). Direct modifications of Rho proteins: deconstructing GTPase regulation. *Biol Cell, 102*(7), 377-389. doi: BC20090151 [pii]
10.1042/BC20090151

Winnen, B., Schlumberger, M. C., Sturm, A., Schupbach, K., Siebenmann, S., Jenny, P., & Hardt, W. D. (2008). Hierarchical effector protein transport by the Salmonella Typhimurium SPI-1 type III secretion system. *PLoS One, 3*(5), e2178.

Yadav, S., Puri, S., & Linstedt, A. D. (2009). A primary role for Golgi positioning in directed secretion, cell polarity, and wound healing. *Mol Biol Cell, 20*(6), 1728-1736. doi: 10.1091/mbc.E08-10-1077

Yadav, S., Puthenveedu, M. A., & Linstedt, A. D. (2012). Golgin160 recruits the dynein motor to position the Golgi apparatus. *Dev Cell, 23*(1), 153-165. doi: 10.1016/j.devcel.2012.05.023

Yarbrough, M. L., Li, Y., Kinch, L. N., Grishin, N. V., Ball, H. L., & Orth, K. (2009). AMPylation of Rho GTPases by Vibrio VopS disrupts effector binding and downstream signaling. *Science, 323*(5911), 269-272.

Yoshida, S., Handa, Y., Suzuki, T., Ogawa, M., Suzuki, M., Tamai, A., . . . Sasakawa, C. (2006). Microtubule-severing activity of Shigella is pivotal for intercellular spreading. *Science, 314*(5801), 985-989.

Yoshida, S., Katayama, E., Kuwae, A., Mimuro, H., Suzuki, T., & Sasakawa, C. (2002). Shigella deliver an effector protein to trigger host microtubule destabilization, which promotes Rac1 activity and efficient bacterial internalization. *EMBO J, 21*(12), 2923-2935. doi: 10.1093/emboj/cdf319

Yu, X., Breitman, M., & Goldberg, J. (2012). A structure-based mechanism for Arf1-dependent recruitment of coatomer to membranes. *Cell, 148*(3), 530-542. doi: 10.1016/j.cell.2012.01.015

Zhao, L., Helms, J. B., Brugger, B., Harter, C., Martoglio, B., Graf, R., . . . Wieland, F. T. (1997). Direct and GTP-dependent interaction of ADP ribosylation factor 1 with coatomer subunit beta. *Proc Natl Acad Sci U S A, 94*(9), 4418-4423.